applied sciences

MDPI

Review

A Review of Recent Developments and Advances in Eco-Friendly Geopolymer Concrete

Lahiba Imtiaz [1], Sardar Kashif Ur Rehman [1,*], Shazim Ali Memon [2,*], Muhammad Khizar Khan [1,3] and Muhammad Faisal Javed [1]

1 Department of Civil Engineering, COMSATS University Islamabad, Abbottabad Campus, Abbottabad 22060, Pakistan; laibaimtiaz01@gmail.com (L.I.); MuhammadKhizar.Khan@UGent.be (M.K.K.); arbabfaisal@cuiatd.edu.pk (M.F.J.)
2 Department of Civil and Environmental Engineering, School of Engineering and Digital Sciences, Nazarbayev University, Nur-Sultan 010000, Kazakhstan
3 Department of Civil Engineering, Ghent University, B-9052 Gent, Belgium
* Correspondence: skashif@cuiatd.edu.pk (S.K.U.R.); shazim.memon@nu.edu.kz (S.A.M.)

Received: 25 August 2020; Accepted: 23 October 2020; Published: 5 November 2020

check for updates

Abstract: The emission of CO_2 and energy requirement in the production of Ordinary Portland Cement (OPC) causes the continuous depletion of ozone layer and global warming. The introduction of geopolymer concrete (GPC) technology in the construction industry leads to sustainable development and cleaner environment by reducing environmental pollution. In this article, constituents of GPC and their influence on properties of GPC has been reviewed critically. Fresh and hardened properties of GPC as well as the factors influencing these properties are discussed in detail. Flow charts have been proposed to show which factors have higher/lower impact on the fresh and hardened properties of GPC. A comprehensive review on the mix design of GPC, nanomaterial-based GPC, 3D printing using GPC, reinforced GPC and Global warming potential (GWP) assessment was conducted. Finally, the practical applications of GPC in the construction industry are provided.

Keywords: aluminosilicates; activators geopolymer concrete (GPC); geopolymer OPC concrete; Global warming potential (GWP); mix design; reinforced geopolymer concrete; graphene-based GPC; 3D printing

1. Introduction

Portland concrete is the most consumed product in the world because of its availability, versatility, low cost, and high structural performance [1]. Ordinary Portland Cement (OPC) production in the cement industry devours about 5% of industrial energy with a 7% release of CO_2 worldwide [2–4]. It is well known that the emission of CO_2 in the atmosphere contributes about 65% of global warming [5]. Moreover, it is found that OPC production increases annually at the rate of about 3%, and the manufacturing of 1-ton of OPC releases 1 ton of CO_2 [5]. Furthermore, global average carbon dioxide volume mixing ratio is increasing and reached 146% of the preindustrial level. It is mainly attributed to deforestation, cement production, and fossil fuel combustion [6]. According to the recent research, it was reported that CO_2 reached to its highest record of 417.1 ppm and this year's value is 2.4 ppm higher than last year value. This value creates an alarming situation as increase in CO_2 level impacts the environmental conditions like an increment in atmospheric temperature and pressure. This increment can affect the CO_2 adsorption on amorphous silica surfaces and can change the amorphous nature of materials to crystallization phases. That is why the production of cement is considered unsustainable due to the high emission of greenhouse gases [6]. Hence, sustainable building materials' production and construction is the primary focus in the construction industry and the global housing, which encourages the researchers to develop alternative supplementary cementitious materials that partially or fully replace the cement. One such alternative emerging technology in the construction industry is geopolymer concrete (GPC). The introduction to GPC technology leads to sustainable development by reducing the global emission of CO_2 and provides a cleaner environment in the long term. It can reduce CO_2 emission by up to 80% as compared to OPC by using aluminosilicate as a full replacement of OPC [1]. GPC is gaining acceptance due to its numerous benefits such as sustainable construction, longer service life, low carbon emission, recycled industrial waste, durable properties, and high strength [7] but, it has limited structural application, due to lack of standard design codes and reliable data, high construction cost, high shrinkage, and rapid setting [8,9].

In literature, a lot of appreciable investigations and reviews are available on GPC. Therefore, it is important to compare and critically analyze the previously published research works with this study. For instant, Zhang et al. [10] reviewed only the mechanical properties (fresh, hardened, and durability) of GPM. Connie et al. [11] studied the mechanical strength and microstructural properties of geopolymer paste, GPM and GPC. Likewise, the mechanical properties of only Fly Ash (FA)/slag-based GPC were reviewed by Zhang et al. [12]. Hassan et al. [7] also reviewed the fresh, hardened, and durability properties of GPC along with some applications of GPC. Based on published literature, it was also found that the effect on GPC properties were assessed with respect to addition of superplasticizers and additives. For example, Jindal [13] studied the change in mechanical and microstructural characteristics of GPC in the presence of different minerals additives. Reddy et al. [14] reviewed the effect of different oxides compositions of binder on compressive strength of GPC. Furthermore, the comprehensive and in-depth analysis of normal and foamed GPC [1], structural and material performance [9], FA-based GPC [15], Rice Husk Ash (RHA)-based GPC [16], and ambient cured GPC [17] were reviewed by researchers for providing solution to sustainable development.

In addition to this, Ning et al. [18] investigated the different mix design proportion of FA and slag-based GPC in which 3 mix design categories were identified such as target strength, statistical-based, and performance-based methods. However, until now, no review paper is available, which has discussed in detailed mix proportion of different types of GPC. This paper presents the inclusive investigation of GPC and GPM along with providing critical review on different mix design procedures used for any binder-based GPC with highlighted input and output variables considered for mix design procedure. Moreover, this paper focusses on recently published research on the mechanical, durable, and microstructural properties of GPC and GPM. Figure 1 shows the papers analyzed in this review paper published in the different time regimes. On the basis of critical review, this study proposed the factors having the highest and lowest impacts on both fresh and hardened properties of GPC. In addition, as per authors knowledge, for the first time, the nanomaterial-based GPC, 3D printing using GPC, reinforced GPC and Global warming potential (GWP) assessment of GPC are reviewed critically.

In this article, a comprehensive review on current investigation of GPC is presented (Figure 1). A detailed explanation of GPC, including its constituents, activators, aluminosilicate precursor, mix design, and the geopolymerization process is presented in Section 2. In Sections 3 and 4, fresh and hardened properties of GPC as well as the factors influencing these properties are discussed in detail. Flow charts have been proposed to show which factors have higher/lower impact on the fresh and hardened properties of GPC. In Section 5, factors affecting properties of GPC are discussed and their respective flow charts are proposed that represents the effect of properties on mechanical behavior of GPC from fresh to hardened state. The effect of the addition of OPC in GPC is elaborated in Section 6. A critical review on reinforced GPC and application of GPC are presented in Sections 7 and 8, respectively. The recent advances in geopolymer technology such as 3D printing, GWP assessment and nanoparticle-based GPC are added in Section 9. Finally, the conclusions and research gaps in GPC are highlighted in Section 10.

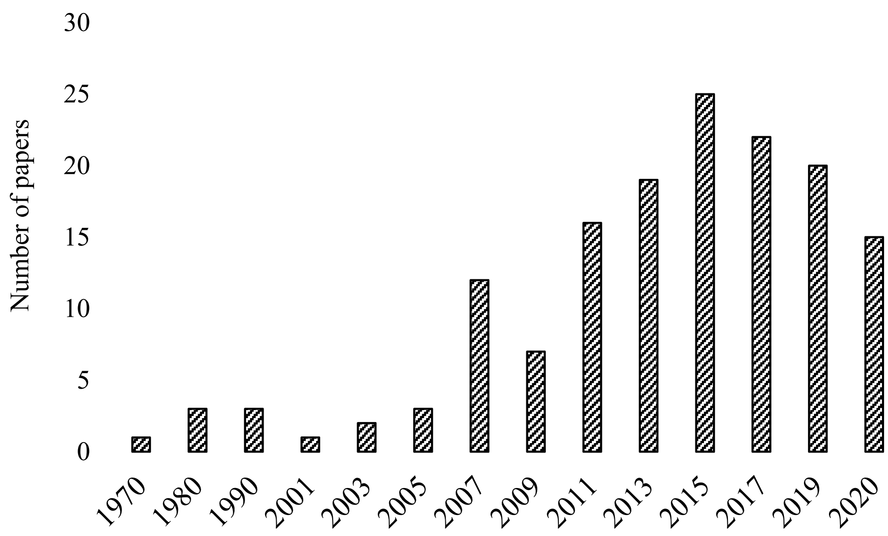

Figure 1. Papers analyzed critically in this review paper published in the different time regimes.

2. Geopolymer Concrete (GPC)

GPC is an inorganic polymer produced by utilizing the agricultural and industrial by-products with high silica and alumina content that are disposed-of openly. The GPC is the combination of silica and alumina provided by thermally activated natural materials like kaolinite and bentonite or industrial by-products like fly ash (FA), rice husk ash (RHA), wheat straw ash (WSA), and alkaline activating solutions which polymerizes these materials into molecular chains and network to create a hardened binder.

In general, GPC is often called alkali-activated materials (AAMs) but both systems have different chemistry. The activation in AAM is not the long-term process forming unstable monomers, while geopolymerization forms a 3-D stable polymer structure. The AAMs have high strength but have poor durability when compared to GPC [19].

GPC may be one-part or two-part depending on the procedure of adding activator source. In one-part GPC, also known as "Just Add Water", the activators are used in solid form rather than liquid and dry mixture is required with the addition of water. The dry mixture is the combination of solid aluminosilicates along with solid alkaline activators [20]. In two-part GPC, also called conventional GPC, the activators are added in liquid form with water in solid aluminosilicate precursor [21].

2.1. Constituents of GPC

Generally, GPC consists of a combination of activators and different sources of aluminosilicates with or without the inclusion of OPC [7]. The aluminosilicates are obtained from the usage of pozzolanic materials containing ample amount of silica and alumina. The pozzolans may be industrial or agricultural wastes such as bagasse ash (BA), rice husk ash (RHA), fly ash (FA), palm oil fuel ash (POFA), ground granulated blast furnace slag (GGBFS) that are used to reduce the pollution and natural resources consumption [22]. These agricultural and industrial wastes are used individually or in combination as the aluminosilicate source in geopolymers for sustainable construction.

Alkaline activators are the second crucial component of GPC needed to liberate silica and alumina contents of aluminosilicate. The most commonly used alkaline activators are sodium silicate (Na_2SiO_3) and sodium hydroxide (NaOH) [23]; however, any hydroxide or silicate source such as potassium hydroxide and potassium silicate can be used as activator. The geopolymerization process occurs at a high rate if the alkaline liquid contains soluble silicates in addition to hydroxides as compared to the use of only hydroxides [23]. The constituents of GPC are presented in Figure 2 [24].

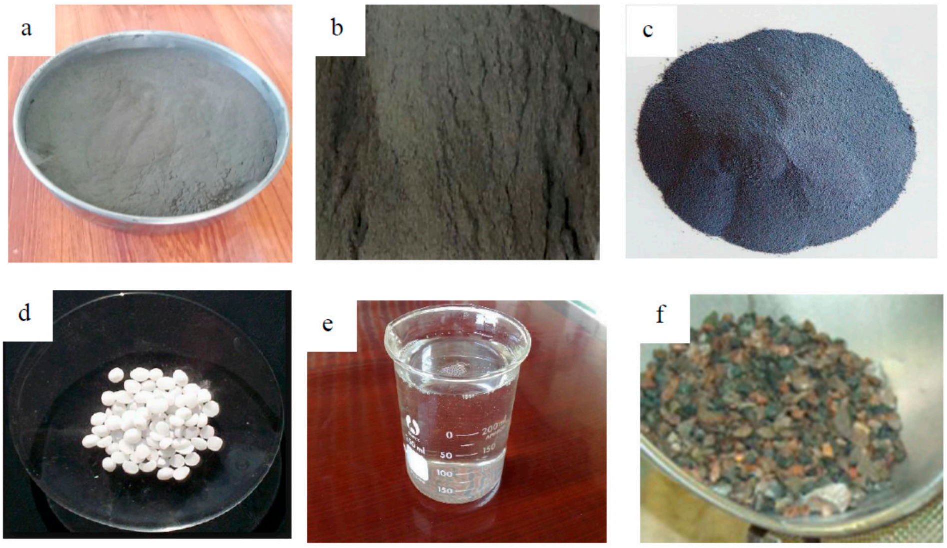

Figure 2. Constituents of geopolymer concrete (GPC): (**a**) Ordinary Portland Cement (OPC), (**b**) fly ash (FA), (**c**) silica fume (SF), (**d**) NaOH pellets, (**e**) Na_2SiO_3, (**f**) GPC aggregate.

2.1.1. Aluminosilicates

The aluminosilicates used in GPC are a natural and industrial by-product which contains amorphous silica and alumina. These are various mineral admixtures including SF, GGBFS, BA, WSA, FA [25,26], and chemicals in particular like calcium silicate and sodium aluminate [27] which have been used as aluminosilicates [28]. In developing countries, the industrial and agro-waste materials containing amorphous silica and alumina are commonly used for energy generation [29]. The resulting ash disposal problem of these wastes is resolved by using them in the cement-based materials and in the production of geopolymer technology.

Mostly six groups of aluminosilicates sources are used in GPC. These are FA-based, MK-based, SG-based, RHA-based, HCWA-based, and a combination of either two of the earlier mentioned aluminosilicates [9]. However, different GPCs show different performances depending on the content of alumina and silica in the aluminosilicates used in geopolymer. The various types of aluminosilicates, along with their sources and chemical composition are tabulated in Table 1. It is shown that different aluminosilicates have different ions concentrations. However, the performance of an aluminosilicate depends mostly on optimum percentage of silica and alumina available in the chain reaction of the geopolymerization process.

Table 1. X-ray fluorescence (XRF) analysis of different aluminosilicates modified from [30].

Chemical Composition	FA	POFA	MK	Dolomite	Kaolin
Sources from raw Materials	From coal mining	From oil palm industry	Natural Resources	Natural Resources	Natural Resources
SiO_2	52.11	51.18	55.90	15.37	52.00
Al_2O_3	23.59	4.61	37.20	1.69	35.00
Fe_2O_3	7.39	3.42	1.70	0.51	1.00
TiO_2	0.88	-	2.40	0.015	0.90
CaO	2.61	6.93	0.11	23.00	<0.05
MgO	0.78	4.02	0.24	17.20	0.70
K_2O	0.80	5.52	0.18	0.195	2.00
Na_2O	0.42	0.06	0.27	0.013	0.05
SO_3	0.49	-	0.02	-	-
P_2O_5	1.31	-	0.17	0.019	-
Loss in ignition	-	21.6	0.80	-	-

The most commonly used aluminosilicate binder is fly ash (obtained from coal combustion stations), which has been found to improve (or substantially improve) the mechanical and durability properties of GPC [9]. It is actually the physical, chemical, and microstructural properties of FA, which are responsible and improve the mechanical properties in GPC. The particle shape and fineness of FA in GPC plays an important role as the particle size distribution and fineness of FA, significantly affect the reactivity of precursor and, thus, to the geopolymerization process [31]. As a result of the higher surface area, the silica and alumina leached down quickly on the FA surface before condensation that will result in a higher geopolymerization rate [32]. Increasing the fineness of FA results in the lessening of porosity and thus provides superior resistance against aggressive environments [33]. It is known that both silica and alumina content are the main constituents in the geopolymerization reaction. The fast dissolution of reactive silica and alumina helps in the synthesis of aluminosilicate gel, which in turn, enhances the mechanical strength of GPC [32]. Generally, the presence of silica and alumina oxides in GPC is usually expressed by silica to alumina ratio. According to Kamhangrittirong et al. [34], with the increase in silica to alumina ratio, the compressive strength of FA-based GPC increases.

The second most widely used aluminosilicate is slag. The use of slag as an aluminosilicate in GPC has been found to perform better both in temperature and ambient curing conditions. It was found that slag-based geopolymer concrete at ambient curing exhibits high compressive strength at early age and it can be used practically in road construction [35]. Slag-based GPC promotes to sustainable concreting technique and can provide green concrete production when used at ambient curing conditions [36]. However, this production requires the effective selection of type and concentration of activators along with consideration of other dominant ratios [37]. It is pertinent to mention here that slag can be used along with other aluminosilicates in GPC to enhance both the mechanical and structural properties [38,39].

2.1.2. Activators

Alkaline activators in GPC are used for polymerizing the aluminosilicates. These are strong alkaline solutions such as sodium hydroxide (NaOH), potassium hydroxide (KOH), sodium silicate (Na_2SiO_3), potassium silicate (K_2SiO_3), or combination of these hydroxides and silicates for dissolving Al and Si atoms [40]. The geopolymerization process depends on the reactivity and concentration of alkaline activator. The alkali-enrichment in GPC increases shrinkage and pore structure development of the cementitious system, which considerably affects the sample with less water to binder ratio. Furthermore, the increase in alkalinity results in the degradation of mechanical strength [41,42]. Therefore, the quantity of alkaline activators needs to be considered wisely while designing the GPC mix. The list of different alkaline activators used by several researchers is given in Table 2.

Table 2. List of alkaline activators with various dependent parameters.

Reference	Activator Used	Molarity of Hydroxide	Activator to Binder Ratio	Silicate to Hydroxide Ratio
[43]	Na_2SiO_3 + NaOH	10 M	0.6	2
[44]	Na_2SiO_3 + NaOH	13 M	0.4	-
[45]	Na_2SiO_3 + NaOH	14 M	0.45	0.25
[46]	Na_2SiO_3 + NaOH	10 M	-	2.5
[47]	Na_2SiO_3 + NaOH	10 M	0.43	-
[48]	Na_2SiO_3 + NaOH	10 M	0.7	-
[49]	Na_2SiO_3 +NaOH	8 M + 10 M	-	0.5–2.5
[50]	Na_2SiO_3 + NaOH	12 M	0.5	2.5
[51]	Na_2SiO_3 + NaOH	10 M +20 M		0.67–1.0
[52]	Na_2SiO_3 + NaOH	10 M	-	0.2
[53]	Na_2SiO_3 + NaOH	14 M	-	1.5–2.5
[54]	NaOH	6 M	0.35	-
[55]	Na_2SiO_3 +NaOH	14 M	-	1.5–2.5
[56]	Na_2SiO_3 + NaOH	12 M	0.4	1:2.5
[57]	Na_2SiO_3 + NaOH		0.35	
[58]	Na_2SiO_3 + KOH	7 M	0.3	-

Several researchers [39,59–61] have concluded that the composition and type of activator is the major factor responsible for the strength development of GPC. According to these studies, the effect of ratios of activator/binder and silicate to hydroxide plays an important role in geopolymerization process and hence, a critical step in preparing the GPC/GPM. Generally, the most commonly used activators in GPC are Na_2SiO_3 and NaOH. The GPC sample prepared with Na_2SiO_3 and NaOH showed better mechanical, durable, and microstructural properties [62]. The GPC, containing only hydroxides as an activator, results in poor mechanical properties, contains pores and shrinkage cracks because it only helps in the dissolution of Si and Al ions of precursor. However, inclusion of silicate source as an activator in combination with hydroxide source results in the promotion of the condensation process of GPC [63–65]. According to Reddy et al. [66], the excess use of silicates in GPC inhibits the geopolymerization while the excess of hydroxides led to early and vigorous precipitation of aluminosilicate precursors hindering the further formation of geopolymeric gel [66]. It has been found by Deb et al. [55], with the decrease in silicate to hydroxide ratio, the workability and compressive strength of GPC have been found to increase.

2.2. Mix Design

The development of appropriate and rational mix design is required to achieve the desired strength and workable GPC. Mix design of GPC is a complex process because of the influence of numerous variables like alkaline content [67], curing time and temperature [68], water to solid ratio [69], pH and molarity of activators [70], aluminosilicate composition and type [71], aluminates to silicate ratio [72], and silicate to hydroxide ratio [73] involved in the geopolymerization process [69].

Different researchers used different types of mix design for GPC based on the parameters considered in their studies. They adopted mix design calculations that were based on the hit and trial method [74], strength considerations [66], activator to binder ratio [66], or binder to sand ratio. The different factors involved in different approaches of mix design calculations are discussed in the following sections.

2.2.1. Hit and Trial Method of Mix Design

There are different hit and trial mix design studies followed by researchers [75,76]. Generally, the hit and trial method is dependent on mechanical and rheological properties such as strength and flow parameters. Mallikarjuna Rao et al. [74] studied the mix design based on the strength of GPC in which alkaline to binder ratio was taken on a trial. The first step was to determine the required target strength, given in Equation (1), and set the slump value. Then after the selection of alkaline/binder and aggregate/binder ratio, the aggregate and alkaline content were determined. This mix design procedure is more clearly presented by flow chart given in Figure 3. Furthermore, some studies of mix design procedures are based on hit and trial method [77].

$$f_t = f_{ck} + 1.65\, S_d, \tag{1}$$

where,

F_t = target average compressive strength of GPC at 28 days,

F_{ck} = characteristic compressive strength at 28 days,

S_d = standard deviation.

Taguchi's method is also one of the hit and trial methods for mix design of GPC that is feasible to determine the number of factors and their interaction [78]. The factors that need to be considered are the activator to binder ratio, silicates to hydroxide ratio, binder content, activator concentration, and molarity [79]. The main objective of this method is to design a high strength GPC while considering different influential parameters. In this method, the number of trial mixes are prepared based on different values of influential parameters, and the optimum mix is selected by calculating the response index. Here, the response index is calculated by taking the average compressive strength of 7 days of different trial mixes [79]. However, the response index might be calculated at later age strength due to the dense microstructure of GPC.

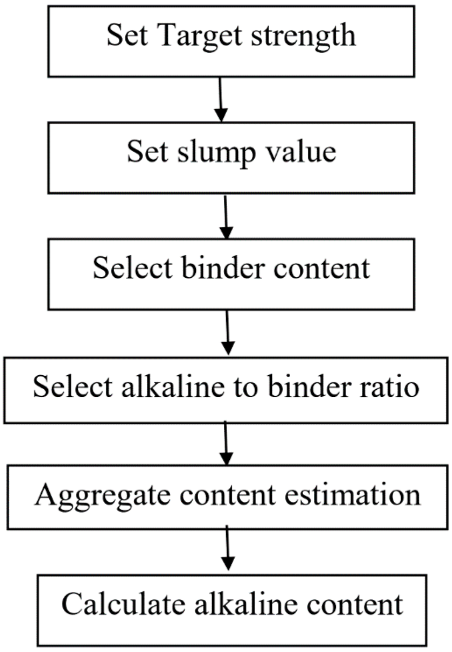

Figure 3. Flow chart by hit and trial method modified from [77], Springer, 2012.

2.2.2. Strength-Based Mix Design

There are several key factors that need to be considered in the strength-based mix design. Junaid et al. [80] determined the strength-based mix design of GPC by acknowledging the crucial factors, for example, water to binder and activator to binder ratios. In addition, another mix design procedure was proposed while establishing graphs obtained from experimental data of strength and workability, called G-Graphs, in which the parameters such as the water to binder, activator to binder, and silicates to hydroxides ratios, the molarity of activators, silicate composition, aggregate types, aggregate grading, curing temperature, and curing time were taken into considerations [80]. However, the novel mix design approaches were developed by using a different designing tools based on the strength parameters. One such tool used was Multivariate Adaptive Regression Spline (MARS) model, where mix design was developed by using a contour plot based on four parameters i.e., water to binder, activator to binder, silicates to hydroxides ratio, and molarity of activator [81]. Moreover, the strength-based mix design was proposed based on ACI standard (ACI 211.4R-93) [82] with some modifications. This procedure depends on activator to binder ratio, activator concentration, and aggregate gradation [83], as given in Figure 4.

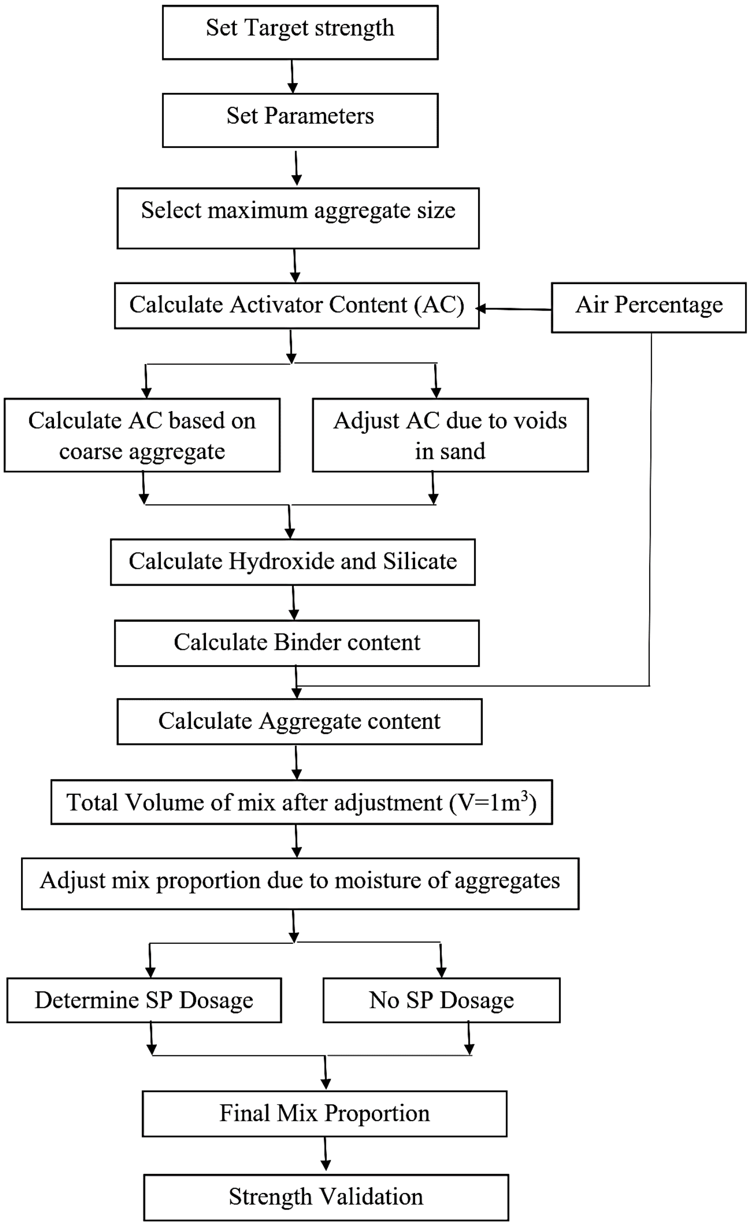

Figure 4. Flow chart based on strength of GPC modified from [83], Elsevier, 2018.

2.2.3. Activator to Binder Ratio-Based Mix Design

The activator to binder ratio is the most crucial parameter for the determination of mix design proportion. Reddy et al. [66] proposed a rational mix design using two different approaches by considering alkaline to binder ratio and strength characteristics. In both the approaches, they fixed the activator content to 200 kg/m^3, enough to maintain the required workability. The parameters like molarity of hydroxide, silicate to hydroxide ratio, and total activator content are predetermined using literature in both methods. The next step is to determine the strength or activator to binder content by the experimental curve. The factors to be considered in this rational approach are the evaluation of binder content, water content, superplasticizer content, aggregate content, and its grading. The respective equations for determining factors are given in Equations (2)–(6). In short, mix design based on strength and activator to binder approach is presented in Figure 5.

$$\text{Binder Content } (BS_c) = AAC/BS, \tag{2}$$

$$\text{Hydroxide weight } (W_h) = Wa/(X + 1), \quad (3)$$

$$\text{Silicate weight } (W_s) = W_a - W_h, \quad (4)$$

$$\text{Water content in silicate} = W_s\,(1 - SP_s), \quad (5)$$

$$\text{Water content in hydroxide} = W_h\,(1 - SP_h), \quad (6)$$

where,

AAC = alkali activator content,
hydroxide weight (W_h),
silicate weight (W_s),
BS = binder solids,
W_a = total weight of AAC,
SP_s = solid percentage in silicates,
SP_h = solid percentage in hydroxide.

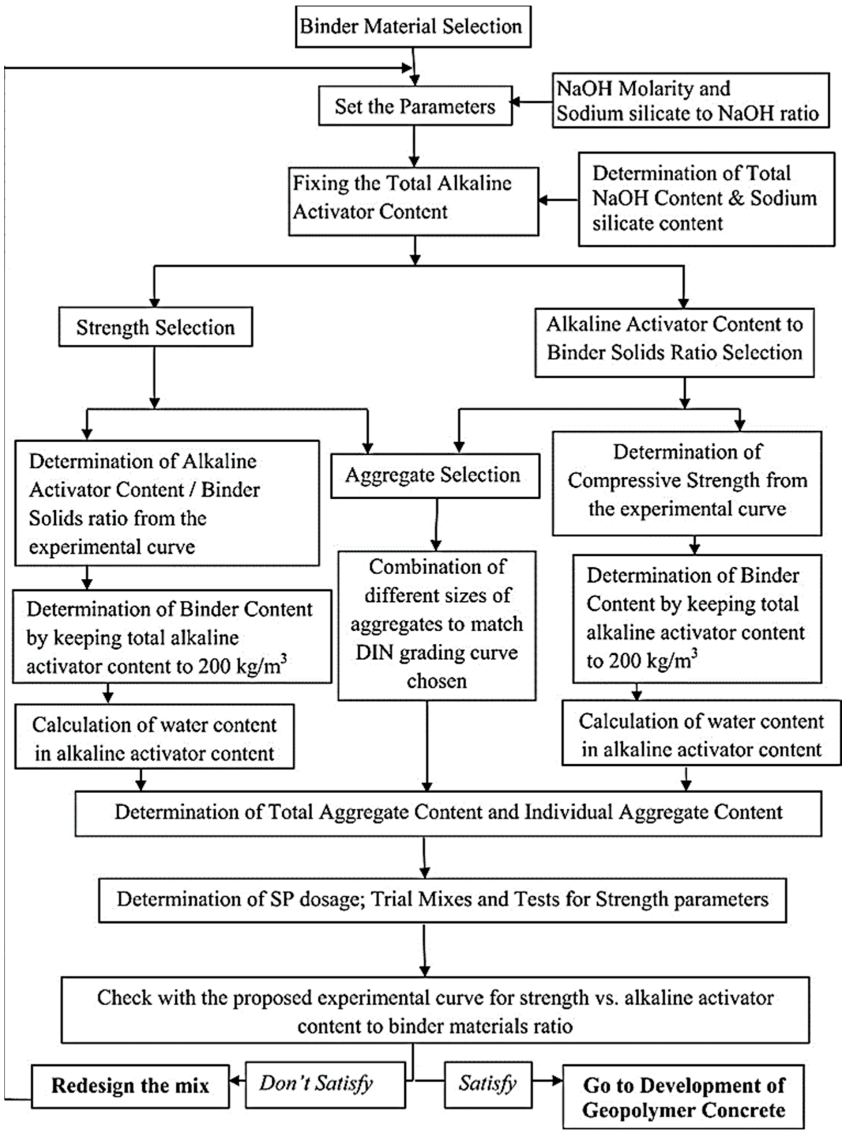

Figure 5. Flow chart representing mix design based on strength and activator to binder approach [66].

2.2.4. Binder to Sand Ratio-Based Mix Design

Researchers also determined the mix design of GPC based on the binder to sand ratio because of its considerable influence on the mechanical, rheological, and microstructural properties of GPC. Kim et al. [84] determined the mix design based on the precursor to sand ratio and found the factors influencing the mix design are the concentration of activators, activator to binder ratio, water to binder ratio, silicates to hydroxide ratio, and temperature characteristics. In this mix design, the optimum binder to sand ratio is obtained. Then, the hydroxide concentration and optimum silicate to hydroxide ratio is determined. After establishing the activator molarity and ratios, the activator to binder and water to binder ratios are considered as dependent parameters. The flow chart of the respective mix design is illustrated in Figure 6. Moreover, different key factors considered in mix design by various researchers is provided in Table 3.

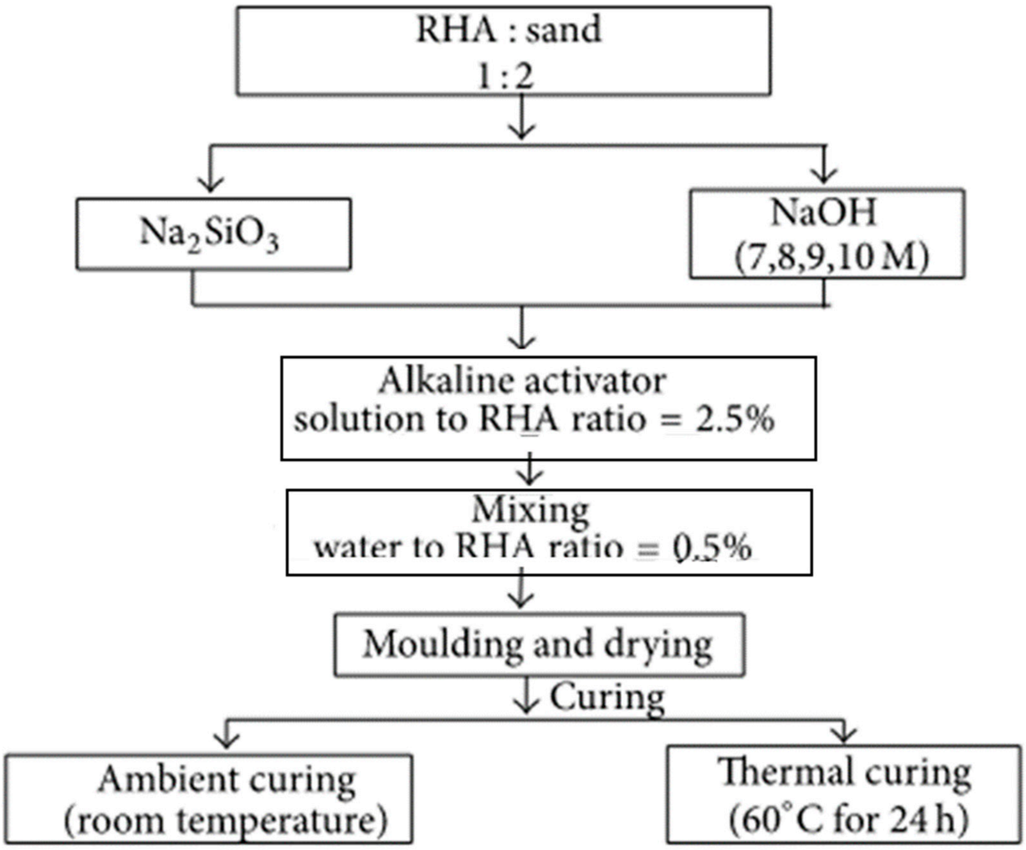

Figure 6. Mix design of GPC based on binder to sand ratio [84].

Table 3. Factors to be considered in mix design of different studies.

Reference	Water to Binder Ratio	Activator to Binder Ratio	Silicate to Hydroxide Ratio	Binder to Sand Ratio	Aggregate Content and Grading	Superplasticizer Consideration
[85]	0.27	-	-	1	-	0.8% of binder
[86]	-	0.42–0.49	-	-	-	-
[87]	0.16–0.24	0.3–0.45	2.0–2.5	-	✓	1.5–4% of binder
[80]	0.23–0.29	0.37–0.5	2.5	-	✓	-
[88]	-	0.5	2.5	-	-	2–6% of binder
[81]	0.25	0.5	3	-	✓	-

Based on the literature review, it is concluded that while determining mix design of GPC, all key factors contributing to strength and durability properties such as molarity of activator, aluminosilicate type, silica/alumina ratio, silicates/hydroxides ratio, activator/binder ratio, curing condition, binder/sand ratio, aggregate behavior, and addition of admixtures should be addressed. The summary of mix designs of GPC is presented in Table 4.

Table 4. Summary of mix designs of GPC.

Name of Method	Parameters Considered as an Input	Constants	Variables	Output	Remarks
Hit and trial method	Slump value and target strength	Target Strength	Activator/Binder Ratio	Alkaline Content	Designed for high strength GPC. In addition, specific gravity of raw materials is not considered and aggregate content is fixed on weight basis [66].
Strength -based Mix design	Target strength, Silicate/Hydroxide ratio, Molarity of activator, Aggregate size	Target strength, Silicate/Hydroxide ratio, Molarity of activator, Aggregate size	-	Mix proportion	Aggregate grading, specific gravity, superplasticizer are considered in it [66]. Based on modification of ACI standard (ACI 211.4R-93)
Activator/Binder-based mix design	Activator content, Silicate/Hydroxide ratio, Molarity of activator	Activator Content	-	Mix proportion including Binder content, Water content, Superplasticizer content, aggregate Content	Specific gravity of raw materials is incorporated in it. Based on strength and activator to binder ratio
Binder/Sand ratio-based mix design	Binder/Sand ratio	Concentration of activators, Activator/Binder ratio, Silicates/Hydroxide ratio	Water/binder ratio	Mix proportion	Based on binder/sand ratio along with determining the curing conditions. Water to binder ratio governs the ultimate strength [66].

2.3. *Geopolymerization Process*

Geopolymers are alkali-activated cement manufactured by polymerizing aluminosilicates with alkaline activators [21]. The polymerization process involves the quick reaction of silica and alumina under an alkaline environment that results in a three-dimensional polymeric aluminosilicate network [89]. Generally, the dissolution of silica and alumina species takes place in alkaline solution followed by an orientation of these species to convert into a three-dimensional chain of silica aluminate polymeric structure [90]. Depending on the composition of aluminosilicates, various geopolymer types are obtained. As far as geopolymer OPC concrete (geopolymer concrete with the inclusion of OPC) is concerned, it develops its mechanical properties based on both calcium silicate hydrate (CSH) bonding and polymerization process [91].

The research studies on GPC and alkali activation emerged in the 1950s. Glukhovsky model [92] has widely been used for alkali activation of aluminosilicates materials [93]. Later on, researchers have conducted experimental investigations and extended the Glukhovsky's theory on the geopolymerization process involved in GPC [94]. The research of GPC has shown an increasing trend in recent years, as shown in Figure 7. The data presented are from the year 2001 onwards.

In GPC, when aluminosilicates fully replace the cement, the polymerization process is involved in the activation of aluminosilicates [95]. The geopolymerization process is an exothermic process that involved the dissolution of aluminosilicate into aluminosilicate oxides under highly alkaline conditions. These oxides are taken up into aqueous phase in which they are dissolved by high pH solution and led to the formation of gel as oligomers species consisting of polymeric bonds of Si-O-Si and Si-O-Al or both that then form the geopolymeric framework. This 3-D framework hardened into the final polymeric structure by the bonding of filler materials and un-reacted solid particles [96,97]. Davidovits et al. [98] found that when aluminosilicates completely replace cement in geopolymer concrete, the poly-condensation of silica and alumina species occurred rather than the formation of C-S-H gel, as in the case of OPC. The process of geopolymerization is elaborated in Figure 8.

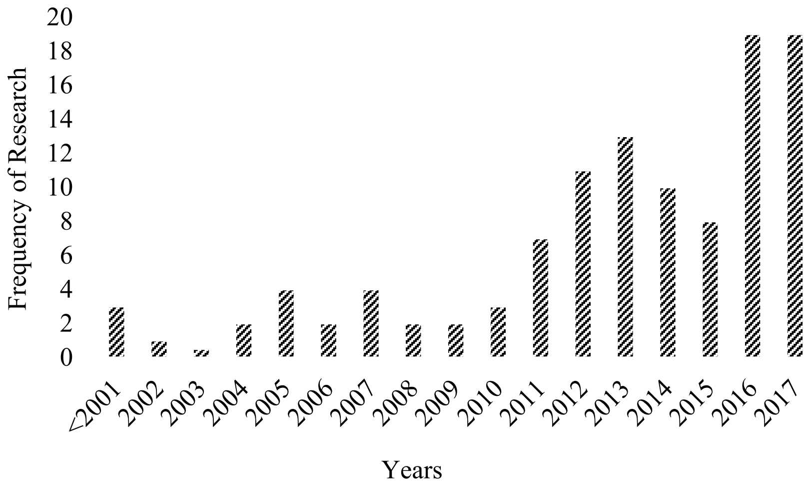

Figure 7. Research trend of GPC modified from [9]; Elsevier, 2018.

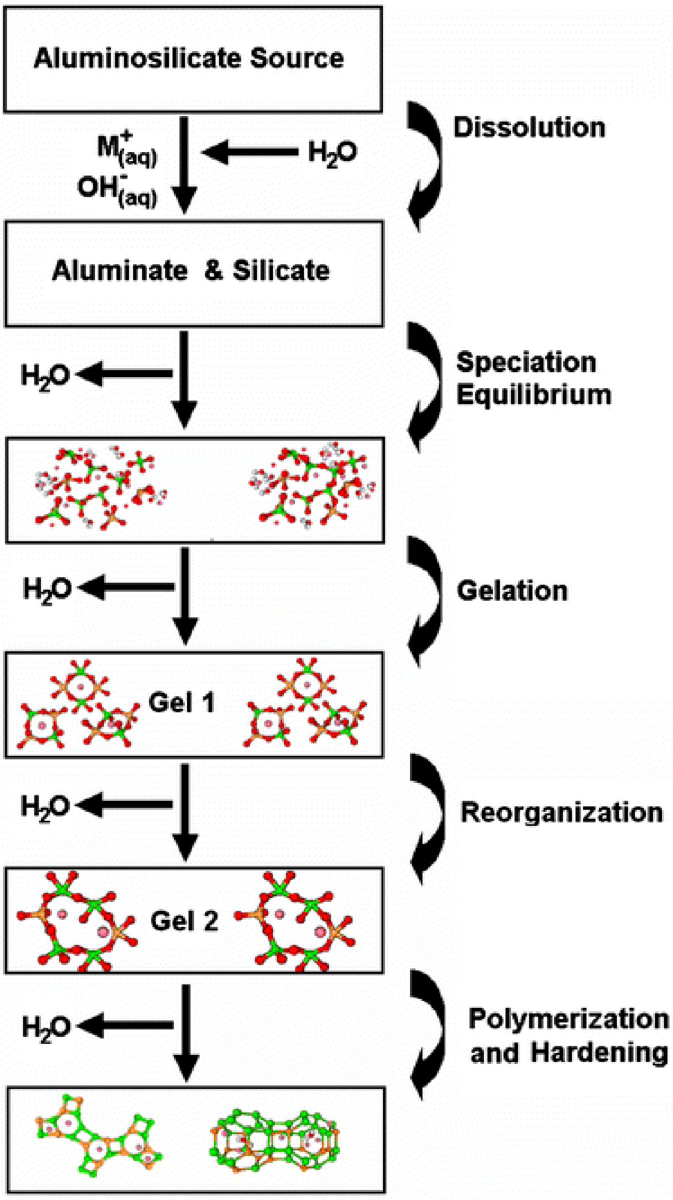

Figure 8. Geopolymerization process [98].

3. Fresh and Hardened Properties of GPC

Several researchers have investigated the fresh and hardened properties of GPC. Table 5 summarizes the fresh and hardened properties of GPC as reported in literature.

3.1. Workability

Generally, the workability of geopolymer mortar is controlled by flowability. Depending on the concentration of activators and their respective ratios, the workable flow ranges from 110 ± 5% (mm) to 135 ± 5% (mm). The workability of GPC influences its hardened properties [51]. Jumrat et al. [105] found that the flowability further depends on the fly ash/alkaline solution ratio and Na_2SiO_3/NaOH ratio. The increase of the mentioned ratios results in more water demand to produce workable mix due to the higher viscosity of Na_2SiO_z. It is reported that workability decreases with an increase in the molarity of NaOH [81,106,107]. Malkawi et al. [108] studied the effect of the alkaline solution on HCWA geopolymer mortars and observed that by increasing Na_2SiO_3/NaOH ratio or NaOH molarity, the workability decreases owing to a substantial influence of NaOH concentration on the flowability of geopolymer mortar. Ismail et al. [109] concluded while studying the type of activator, Ca/Si ratio, and temperature effect on geopolymer mortar that the addition of Na_2SiO_3 with no percentages of NaOH reduces the workability due to its higher viscosity. Musaddiq Laskar and Talukdar [110] noticed that GPC with NaOH as an activator exhibits significant improvement in workability than the mixes containing the blend of NaOH and Na_2SiO_3 [110]. According to Mehta and Siddique [111], the workability depends on the fineness of the aluminosilicate particle and SiO_2/Al_2O_3 ratio [111] present in GPC. The more value of fineness, the higher the slump value of GPC and vice versa [83].

Several researchers studied the effect of superplasticizers and nanoparticles on the workability of geopolymer pastes. Rangan et al. [112] found that with the use of naphthalene-based superplasticizer, the workability of FA-based geopolymer increases. However, the use of water significantly improved the workability than that of naphthalene-based superplasticizer but with a small reduction in strength [113]. According to Majidi et al. [114], the flowability of geopolymer mortar is reduced with the use of high content of GGBFS due to the increase of non-spherical particles in FA. Deb et al. [115] investigated that the use of silica nanoparticles decreases the slump value due to accelerated reaction and high demand of nanoparticles. Figure 9 shows the effect of activator concentration and water to ash ratio on the flow of geopolymer samples. It is clear that with the increase of water to ash ratio, the workability increases while with a rise of NaOH concentration the workability decreases, due to an increase of viscosity. In addition, a strong relationship can also be visualized between flow and water/ash ratio with the coefficient of determination (R^2) of 0.96. It is also observed that with the increase in silicates to hydroxide ratio, flow decreases, and the decrease drops with the rise in hydroxide concentration. The linear dependence exists between flow and hydroxide molarity with R^2 of 0.91 and 0.87 in case of higher and lower silicate/hydroxide ratio, respectively.

From Table 5, it is observed that GPC has the highest workability when retarder is added. According to Umniati et al. [52], also retarder affects the initial and final setting time along with an insignificant change in strength development of GPC. Nath and Sarkar [53] reported that increasing alkaline content increased the workability and the flow value. However, the GPC mix containing OPC reduces workability and setting time and thus enhances compressive strength [53]. According to Reddy et al. [66], the aggregate grading, type, and packing influence the workability of GPC. The authors also found that GPC exhibits segregation when the coarse aggregate to sand ratio becomes higher, while it exhibits excessive bleeding when the ratio becomes lower. To achieve good workable concrete free from bleeding and segregation, combined grading is recommended.

Table 5. Fresh and hardened properties of GPC.

Reference	Precursor	Activator	Curing Condition	Workability (mm)	Setting Time (Min)	Compressive Strength (MPa)	Tensile Strength (TS) and Flexural Strength (FS) (MPa)
[50]	FA	NaOH + Na_2SiO_3	Heat curing at 60–90 °C	710	-	47.54–53.99	-
[51]	FA	NaOH + Na_2SiO_3	75 °C	110 ± 5%–135 ± 5%	-	10–65	-
[52]	FA	NaOH + Na_2SiO_3	-	240	IST [1] = 405 FST [2] = 570	47.21	-
[53]	FA	NaOH + Na_2SiO_3	Ambient curing		IST = 66–112 FST = 160–245	40	-
[99]	FA	NaOH + Na_2SiO_3	80 °C	-	-	48	-
[100]	FA	NaOH + Na_2SiO_3	Ambient curing	-	-	11.8–29.2	-
[55]	FA +GGBFS	NaOH + Na_2SiO_3	-	195–250	-	20% slag strength = +17% of 10% slag strength	20% slag strength = +55% of slag TS
[56]	FA+GGBFS+POFA	NaOH + Na_2SiO_3	65 °C	-	-	66	-
[101]	FA+GGBFS+HCWA	NaOH + Na_2SiO_3	-	145–160	IST = 20–280 FST = 90–360	36.56	FS = 7.7
[102]	GGBFS+FA+OPC+CH Where, CH=Calcium hydroxide	NaOH + Na_2SiO_3	Ambient curing	-	IST = 110–607	26–58	-
[103]	FA+GGBFS+NS	NaOH + Na_2SiO_3	Ambient curing	-	-	40.28–56.7	-
[104]	FA+GGBFS	NaOH + Na_2SiO_3	Ambient curing	-	-	30.5–80.5	TS = 8.35 FS = 17.95
[4]	FA	NaOH + KOH + Na_2SiO_3	-	-	-	24.96–30.11	TS = 3.72–4.95 FS = 5.22–6.03

[1] IST = initial setting time; [2] FST = final setting time.

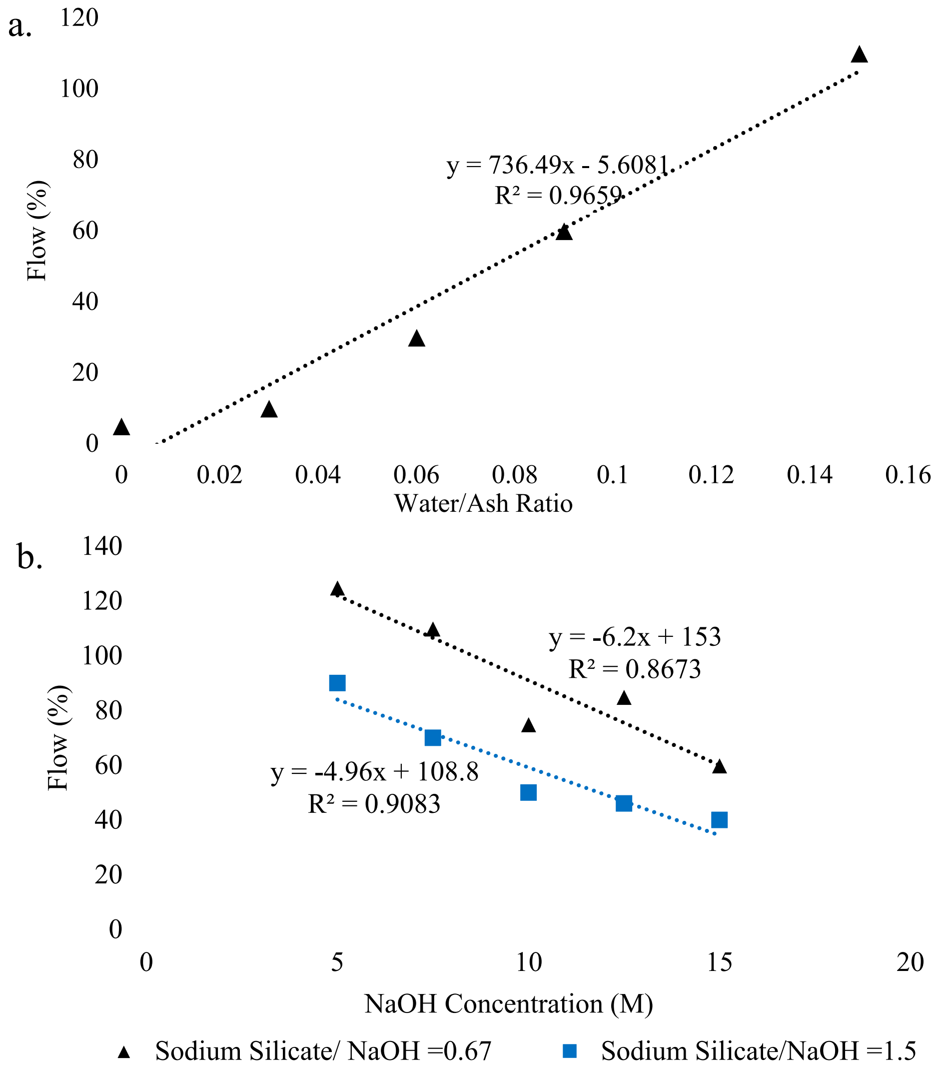

Figure 9. Factors effecting workability. (**a**) Effect of water to ash ratio on flow. (**b**) Effect of NaOH concentration on flow, adopted from [113]; Elsevier, 2009.

3.2. Setting Time

Several researchers investigated the effect of molarity, silicates/hydroxide ratio, binder content, and superplasticizer content on setting time. The setting time of geopolymer decreases with an increase in molarity of NaOH from 10M to 16M due to the faster dissolution rate of aluminosilicates that enhances the geopolymerization process. Elyamani et al. [116] observed the setting time behavior of FA-based geopolymer with 100% FA, Fly Ash-Silica fume (FAS) mixed geopolymer with 50% FA and 50% silica fume, and the Fly Ash-Silica fume-Furnace Slag (FASS)-based geopolymer containing 50% FA, 35% GGBFS, and 15% silica fume. It was found that with rise in NaOH molarity, the final setting time of both FAS and FASS geopolymer mix linearly increases (Figure 10). Contrarily, the FA mix showed linear decline with the rise in molarity in the initial setting time, while remain constant in the case of final setting time. The increase in setting time might be due to effect of composition of silica fume added or because of slower rate of geopolymerization process [117–119]. Several researchers [105,120] have concluded that activator to FA ratio and Na_2SiO_3 /NaOH ratio have no significant impact on the setting time of FA-based geopolymer mortar. However, it is clear that the setting time of FA-based geopolymer mortar decreases with increasing molarity [120,121]. While studying the effect of superplasticizer on workability, Talukdar et al. [110] investigated the setting time effect of ultrafine slag-based GPC with superplasticizers having both NaOH activator and blend of NaOH and Na_2SiO_3. It has been confirmed that the NaOH activator considerably delays the setting time as compared to the geopolymer containing a blend of both NaOH and Na_2SiO_3. This might be due to the instability of superplasticizers in a high alkaline environment. In addition, the effect of micro-encapsulated phase change materials (MPCM) on setting time of FA and slag GPC was studied by Pilehvar et al. [122]. It was found that the initial setting time increases and final setting time decreases with decreasing concentration of MPCM and depends on samples viscosities, the absorption capacity of microcapsules and the latent heat. The behavior of setting time on GGBFS content was studied by Nath et al. [102]. It was found that with the increase in the GGBFS content, the initial and final setting time decreases due to an increase in viscosity. In addition, the inclusion of additives in GPC accelerates the setting time depending on the type of additive added.

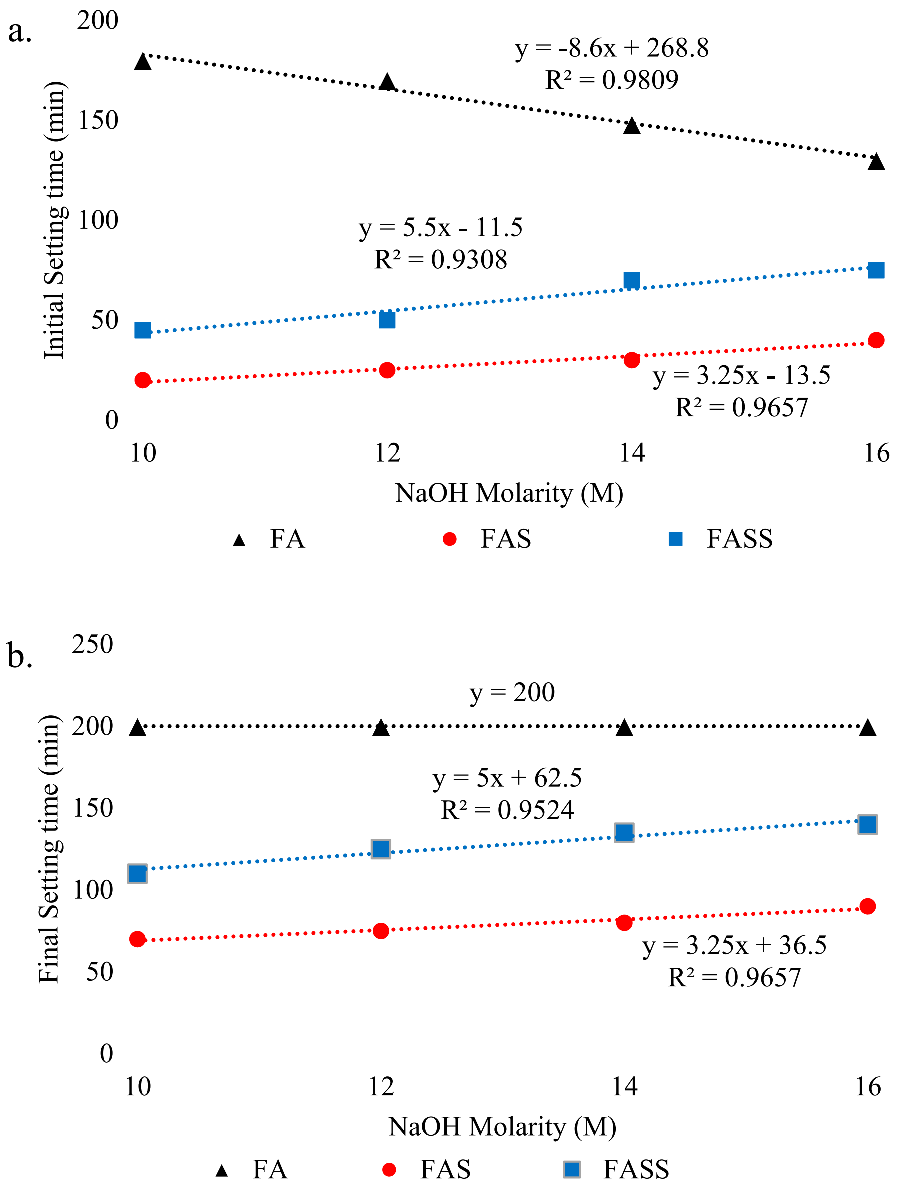

Figure 10. Effect of NaOH molarity on setting time of FA, FAS, and FASS-based geopolymer. (**a**) Effect on initial setting time, (**b**) effect on final setting time, adopted from [116]; Elsevier, 2018.

From above discussion, it is determined that, in general, the setting time decreases with an increase in molarity. However, the inclusion of superplasticizers in GPC reduces the workability which in turn causes an increment in setting time (Figure 11). This increment could provide an economical solution during formwork when GPC is used practically.

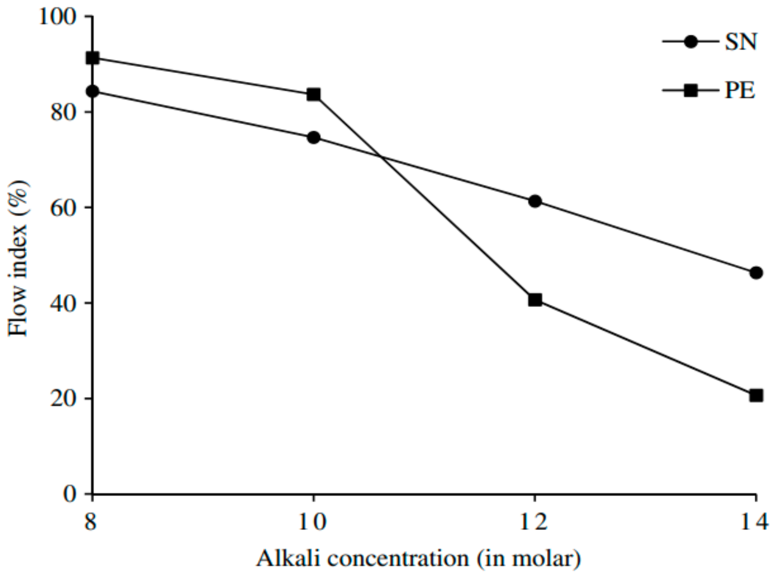

Figure 11. Effect of alkaline concentration on setting time [110].

3.3. Heat of Hydration

The heat of hydration of GPC is higher than that of OPC concrete due to the vigorous geopolymerization process of aluminosilicates activated with alkaline activators [123,124]. Singh et al. [125] investigated the effect of alkaline activator on strength properties of FA/slag geopolymer concrete. The authors found that the heat release was not substantially affected during paste formation beyond optimum dosage of 14M activator concentration. Rangan et al. [112] concluded that metakaolin-based geopolymer exhibits a direct relationship between compressive strength and exothermic reaction while FA-based geopolymer at ambient temperature does not exhibit an exothermic reaction during the first 25 h due to the difference in geopolymerization process of FA-based and metakaolin-based GPC. Figure 12 shows the effect of sodium silicate to FA ratio and hydroxide to FA ratio on the temperature of FA-based geopolymer [126]. It was found that with an increase in Na_2SiO_3/fly ash and NaOH/fly ash ratio, the temperature increases which might be due to the vigorous exothermic reaction with an increase in alkali content. The increase of temperature was enormous in the case of hydroxide activators as shown by a slope of 26.8 compared to 7.6. However, temperature rose linearly in the case of both the activators. In short, the type of activator used has direct effect on the temperature of FA-based geopolymer.

3.4. Structural Changes over Time

Geopolymers have a wide range of microstructural changes due to its various types of raw sources, exposure conditions, and type of activators. As discussed earlier, both the early and later age strength of GPC/GPM depends on the composition of aluminosilicates and activator which are involved in geopolymerization reaction. This reaction is a complicated process and mainly depends on input sources and their compositions along with temperature conditions.

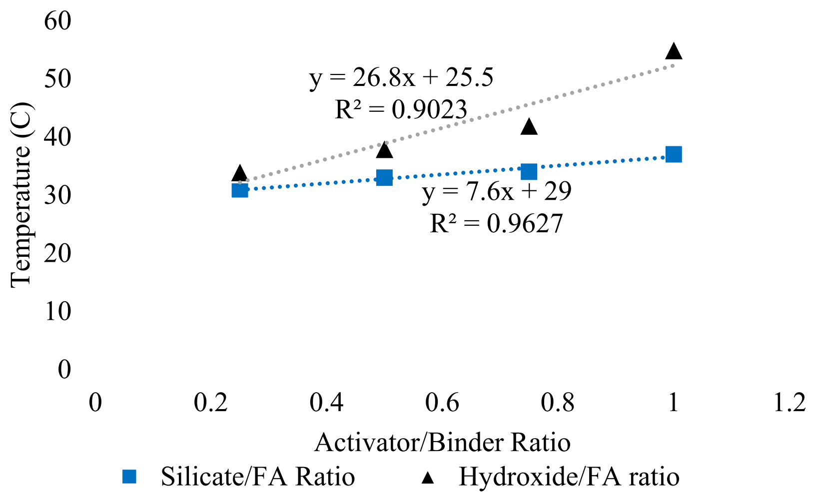

Figure 12. Effect of sodium silicate/FA ratio and hydroxide/FA ratio on the temperature, adopted from [126]; SciELO, 2014.

The composition and amount of silicate/hydroxide, activator/binder, Si/Al and Na_2O/SiO_2 ratios mainly influence the polymeric chains in the geopolymerization reaction. It was reported that the GPC containing Na_2O in polymerization process has greater impact on microstructural and durability properties [127]. Hongen et al. [128] investigated the long term strength of FA-based GPC at 480 days and found that to some extent, the concentration of NaOH affect the Si/Al ratio in polymerization reaction that directly influence the microstructure and hence, mechanical and durability properties. Further, the later age strength increase with increment of Na_2O/SiO_2 ratio was due to a better binding mechanism involved in alkali activation process.

Apart from the composition, the temperature condition also influences the mechanical behavior of GPC. The samples cured at ambient temperature have less early age strength than temperature cured samples but have greater later age strength. According to Mo et al. [129], the temperature cured samples exhibit fast evaporation along with vigorous geopolymeric reactions that provide higher strength at early stage but with time, the dissolution of silica and alumina disturbs, that in turn, increases problems of shrinkage and porosity [129].

3.5. Compressive Strength

The compressive strength of FA-based geopolymer is directly affected by source material and its particle size distribution [130]. Islam et al. [56] studied the compressive strength of GGBFS and POFA-based geopolymers and found the maximum compressive strength of approximately 66 MPa at the binder composition of 70% GGBFS and 30% POFA, respectively. Ranjbar et al. [131] determined that while increasing the dosage of POFA, the SiO_2/Al_2O_3 ratio increases, and this result reduced compressive strength due to delayed geopolymerization process. According to the authors, it can be explained by the reaction of alumina at the early stages and thus there exists a scarcity of Al_2O_3 at the later reaction stage. Compressive strength also depends on the sand type and binder to sand ratio. The effect of limestone sand on compressive strength of geopolymer was studied by Aguilar [132] and it was observed that compressive strength of geopolymer mortar decreased with the inclusion of limestone sand; however, by using limestone sand with sand/binder ratio of 7:1, the green construction material can be produced. In addition, Wazien et al. [133] inspected the strength and density of ambient cured geopolymer samples and found that with the rise in the binder to sand ratio from 0.25 to 0.5, the compressive strength increased while it decreased when this ratio was above 0.5. Iswarya et al. [134] studied the effect of fly ash/slag ratio on the compressive strength of GPC and found that the strength was higher at fly ash/slag ratio of 2:1 when compared to 4:1 and 3:1. This increase was due to the denser microstructure.

Several researchers [63,135] have found that the compressive strength of FA-based GPC increases with the increase in the molarity due to improved polycondensation process. Vora et al. [135] further considered the effect of curing temperature Na_2SiO_3/NaOH and alkaline liquid/FA ratio on the compressive strength of GPC. While increasing curing temperature, the 7th day's compressive strength increases; conversely, with a rise of Na_2SiO_3/NaOH ratio, the compressive strength decreases. However, the alkaline liquid/FA ratio has shown no significant effect on compressive strength, as shown in Figure 13.

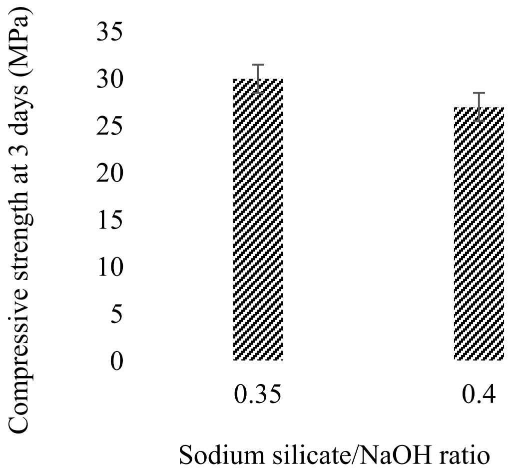

(**a**)

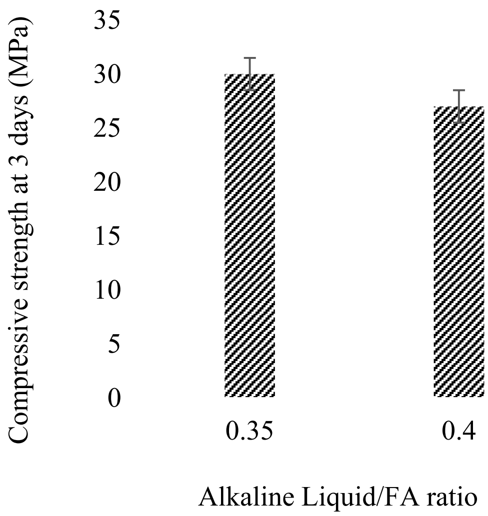

(**b**)

Figure 13. *Cont.*

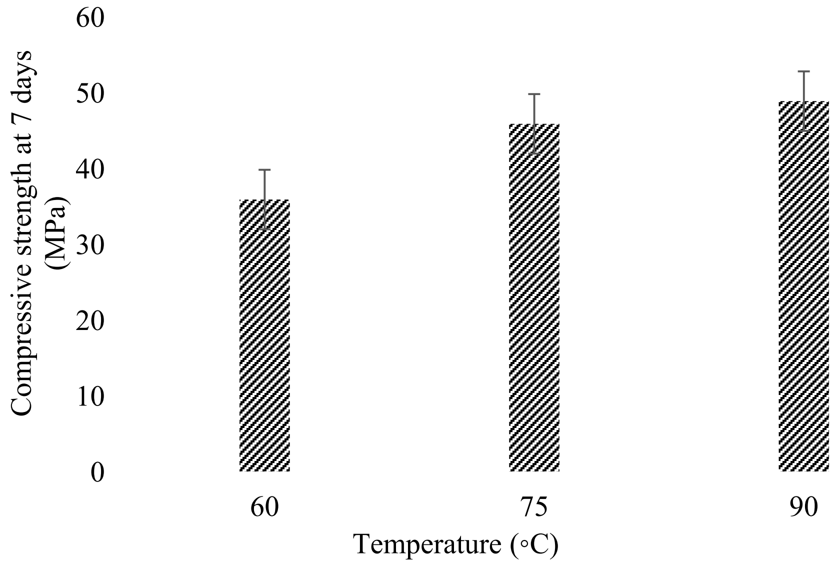

(c)

Figure 13. Effect of early compressive strength on: (**a**) Na_2SiO_3/NaOH ratio, (**b**) alkaline liquid/FA ratio, (**c**) curing temperature, modified from [135]; Springer, 2019.

Aliabdo et al. [2] summarized the different factors that affect the compressive strength of GPC. The authors defined the distinct factor levels as 0, 1, and 2 while determining the compressive strength as presented in Table 6. The effect on the compressive strength of different factor levels is displayed in Figure 14. It can be seen that with an increase in NaOH molarity and Na_2SiO_3/NaOH ratio, the compressive strength of alkali-activated slag increases while an increase in alkaline solution to slag ratio results in a decrease in compressive strength. However, heat curing is not recommended for slag-based GPC because the increment in dry curing temperature leads to more water evaporation, which negatively affects the amount of CSH formation. In addition, the increase in alkali content from 35–45% of the total binder decreases the compressive strength of samples [53]. Likewise, the inclusion of nanoparticles enhances the compressive strength of geopolymer mortar at different curing age [136].

Table 6. Factor description [2].

Factor Level	Factor Description				
	A (Molarity) Moles	B (AL/Slag) by Weight	C (Curing Temp) °C	D (Curing Time) Days	E (NaOH:Na_2SiO_3)
0	10	0.40	30	1	1:1.75
1	12	0.45	60	2	1:2.5
2	14	0.50	90	3	1:3.25

From Table 5, it is concluded that the strength development of FA-based GPC at ambient temperature enhanced due to the addition of external agents like superplasticizers or additives. The addition of calcium hydroxide improved the dissolution process of FA in alkaline activator media due to precipitation of CSH or CASH phases [100]. Further, the incorporation of additives in GPC up to optimum content enhanced the strength, flow, and other mechanical properties. The 70% GGBFS content or 30% POFA content increases the compressive strength (up to 66 MPa), while further increase in content did not yield desired results [56].

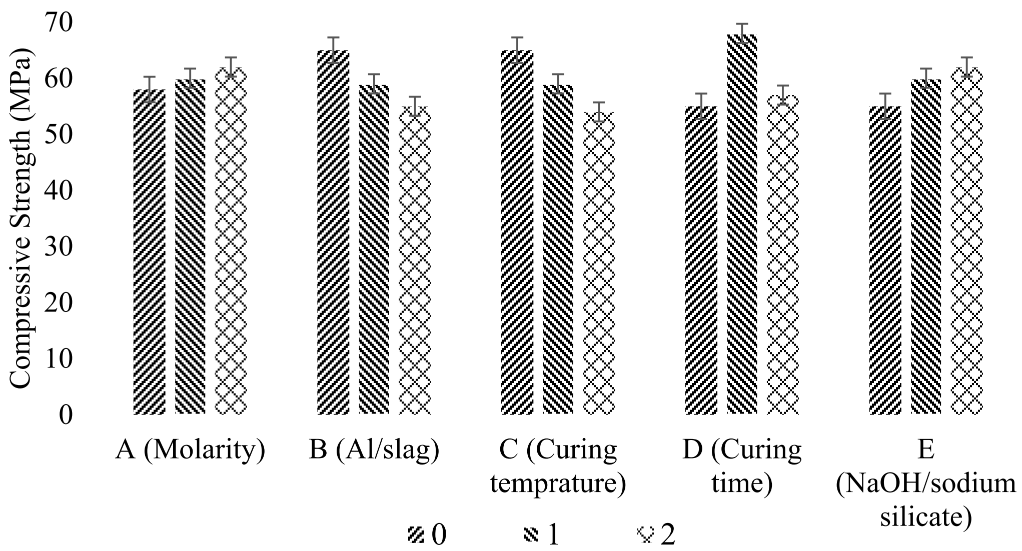

Figure 14. Factors affecting compressive strength after 28 days, modified from [2]; Elsevier, 2019.

3.6. Tensile and Flexure Strength

Tensile strength, an imperative mechanical property used in design facets of concrete structure is determined by direct tension, splitting tension (ASTM C496) [137], and flexural tension (ASTM C78) [138]. According to Deb et al. [55], tensile strength of GPC has a direct relation with compressive strength. Hence, the effect of different variables on tensile strength was the same as in case of the compressive strength. Kolli et al. [139] concluded that the spilt tensile strength of heat-cured GPC is similar to the corresponding strength of OPC concrete, and its relation with the compressive strength of GPC was also well comparable to that of ACI-318-99 for Ordinary concrete as expressed by regression analysis. Sarkar et al. [140] recognized the effect of nano-silica (NS) on strength and durability characteristics of GPC and concluded that the tensile strength of GPC at normal curing enhanced with the inclusion of 56% nano-silica. In addition, while increasing slag content, the tensile strength increases [114]. It was reported that under ambient curing conditions, the mechanical strengths such as compressive, tensile, and flexural strength increases with the addition of 6% nano-silica [140] (Figures 15 and 16). Lee et al. [141] evaluated the effect of sand/FA ratio on FA-based GPC and found that with an increase in the sand/FA ratio, the tensile strength at 7, 14, and 28 days decreased.

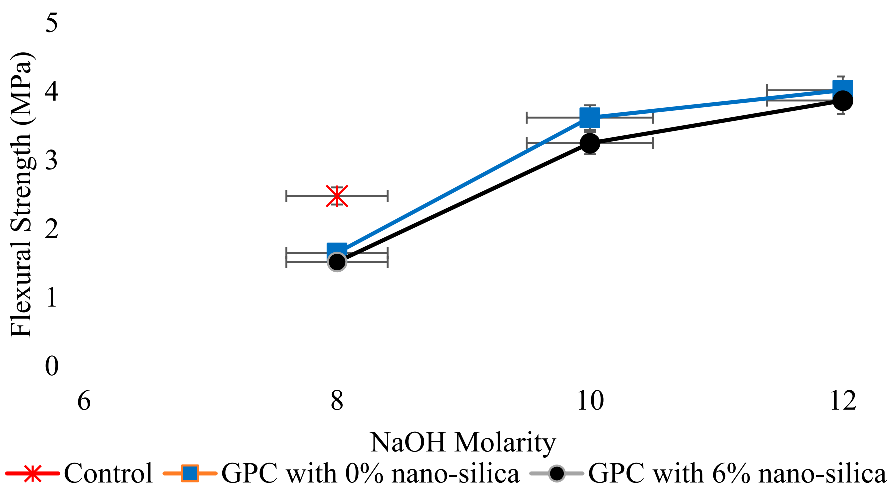

Figure 15. Relation of flexural strength with molar concentration, modified from [140]; Elsevier, 2014.

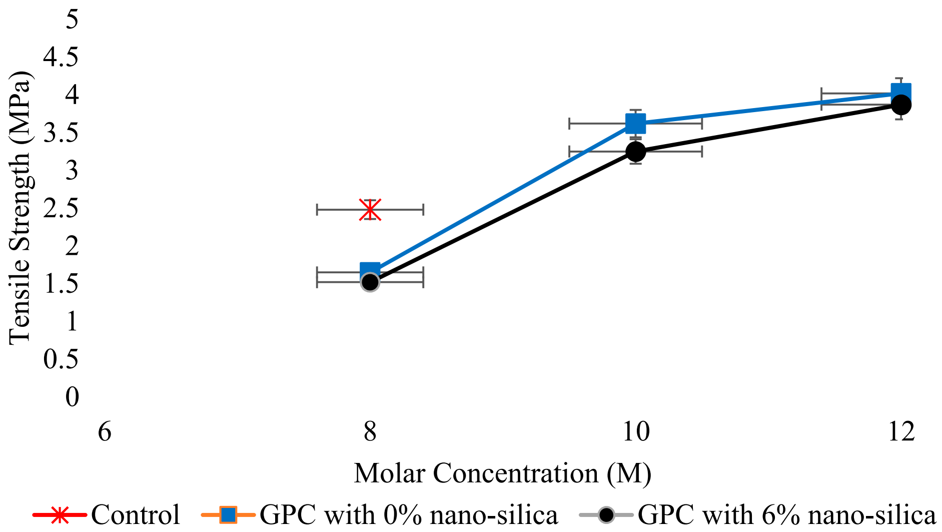

Figure 16. Relation of tensile strength with molar concentration, modified from [140]; Elsevier, 2014.

As far as the flexural strength of geopolymer mortar is concerned, Elyamany et al. [116], found that it increases with the enhancement of compressive strength (Figure 17). The figure summarizes the relationship between the square root of compressive strength and flexural strength of different mixes.

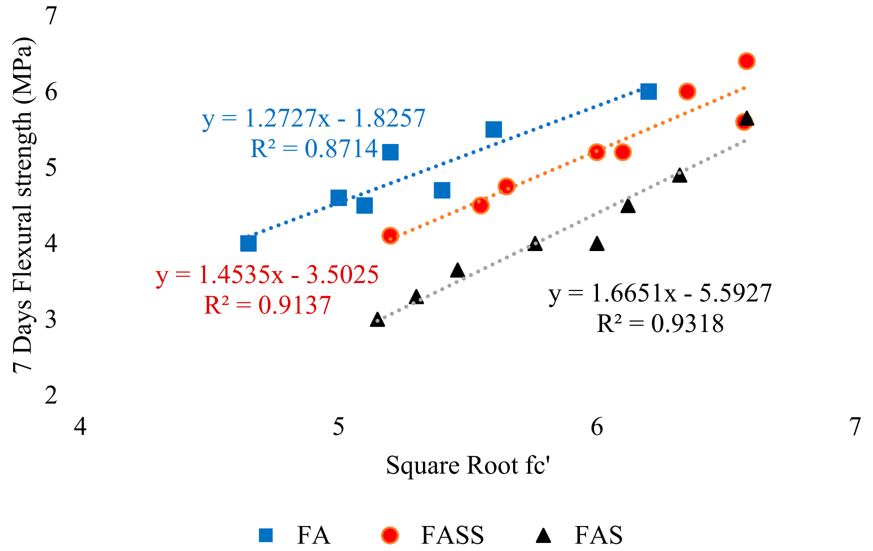

Figure 17. Relationship between square root of compressive strength and flexural strength of different mixes, adopted from [116]; Elsevier, 2018.

Table 6, which summarizes the fresh and hardened properties of GPC, shows that the geopolymer mix having lower flexural strength is due to the absence of calcium oxide amount that enables the CSH and CASH formation in geopolymer process [101]. The increase in additive content enhances the tensile and flexural strengths [56].

3.7. Elastic Modulus of GPC

Elastic modulus is a significant mechanical property that determines the material stiffness of concrete and is measured according to ASTM standard C469M-14 [142]. For the prediction of modulus of elasticity, the aggregate behavior, curing temperature, binder type, and curing time plays an important role [143]. Literature shows that for given compressive strength, the GPC has a lower modulus of elasticity than OPC concrete [144–146], This might be due to the effect of aluminosilicate composition, and other processes involved in the geopolymerization process. Haq et al. [147] concluded that with the enrichment of NaOH content, the elastic modulus of bottom ash-based GPC increases and the increase is linear with R^2 value of 0.96 depicting strong relation between the NaOH and elastic modulus, as shown in Figure 18. Contrarily, Ban et al. [148], found that with the enhancement of HCWA in GPC at different curing times, the elastic modulus of FA-based GPC decreases.

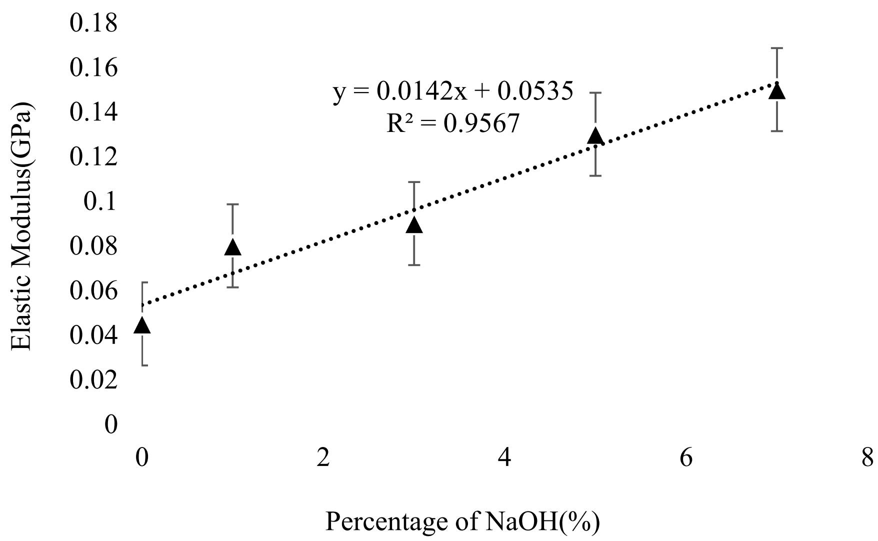

Figure 18. Effect of NaOH content on elastic modulus, adopted from [147]; Elsevier, 2016.

3.8. Shrinkage

Drying shrinkage has a significant role in the development of the cracks of hardened GPC [149]. Several researchers have found that GPC exhibits higher shrinkage than OPC concrete. Lee et al. [150] studied the shrinkage characteristics of alkali-activated FA-slag (AFS) GPC and showed that AFS paste shows higher drying shrinkage than OPC due to presence of large mesopore volume in AFS paste as compared to OPC paste. Moreover, the alkali-activated binder has two times more shrinkage than OPC (Figure 19); however, this shrinkage can be reduced to OPC level with the usage of additives [149]. In addition, cracks in both types of pastes are visually presented in Figure 20 [149].

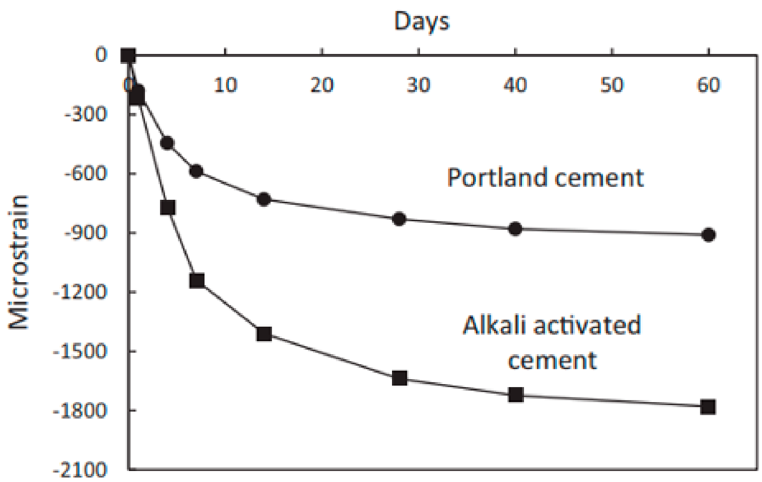

Figure 19. Shrinkage with respect to time of both OPC and alkali activator binder [149].

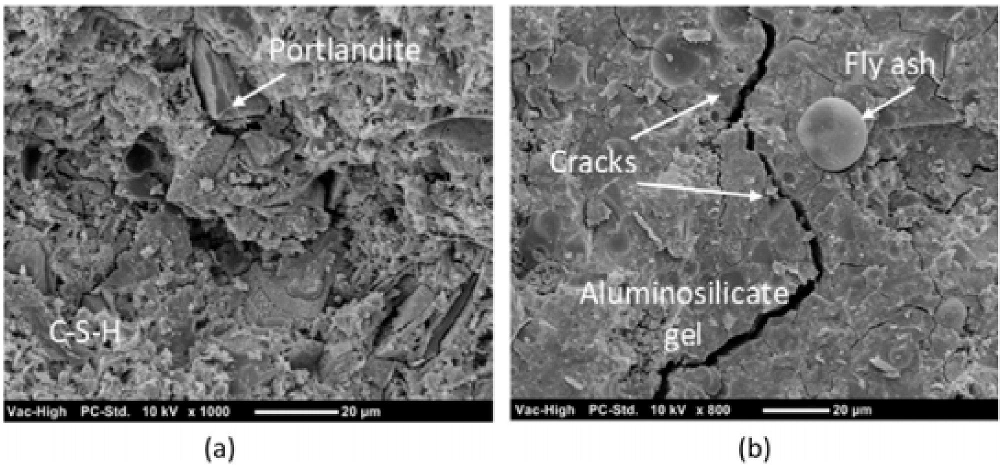

Figure 20. SEM image of (**a**) OPC paste and (**b**) alkali activated binder paste [149].

Hojati et al. [151] determined the effect of FA and GGBFS proportions on strength and shrinkage characteristics of geopolymer pastes. It was found that the inclusion of slag decreases the setting time and enhances the compressive strength and bulk modulus, but also results in higher autogenous shrinkage. Furthermore, Sumesh et al. [152] studied the effect of different content of MK/GGBFS ratios on shrinkage of GPC. They appraised that GPC after 28 days exhibits lowest drying shrinkage with 25–30% MK content and 70–75% GGBFS content. Hence, it is concluded that the shrinkage of GPC can be reduced by addition of optimum content of aluminosilicate and admixture.

At the end of Section 3, Figures 21 and 22 are proposed to highlight the several parameters which significantly alter the fresh and hardened properties of GPC. Molarity of activators was found to significantly contribute towards both fresh and hardened properties. Figure 21 shows the factors influencing the compressive strength, tensile strength, workability, and setting time of GPC, while Figure 22 represents factors contributing to elastic modulus and drying shrinkage of GPC properties from top to bottom on different parameters. The highly desirable factor is represented by red color to the least desirable factor with a light orange color. Moreover, the fresh and hardened properties of GPC in term of its different influential parameters are summarized in Table 7. This table critically analyzes and concludes the crucial considerations taken for development of both fresh and hardened properties.

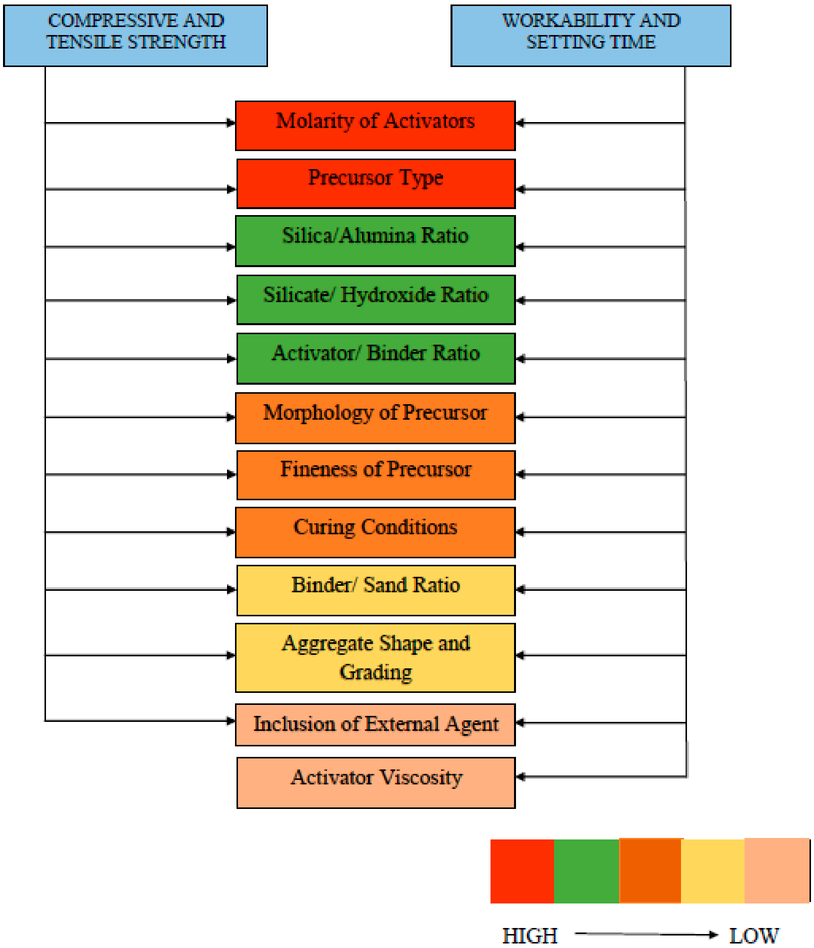

Figure 21. Contributing factors to strength and workability of GPC.

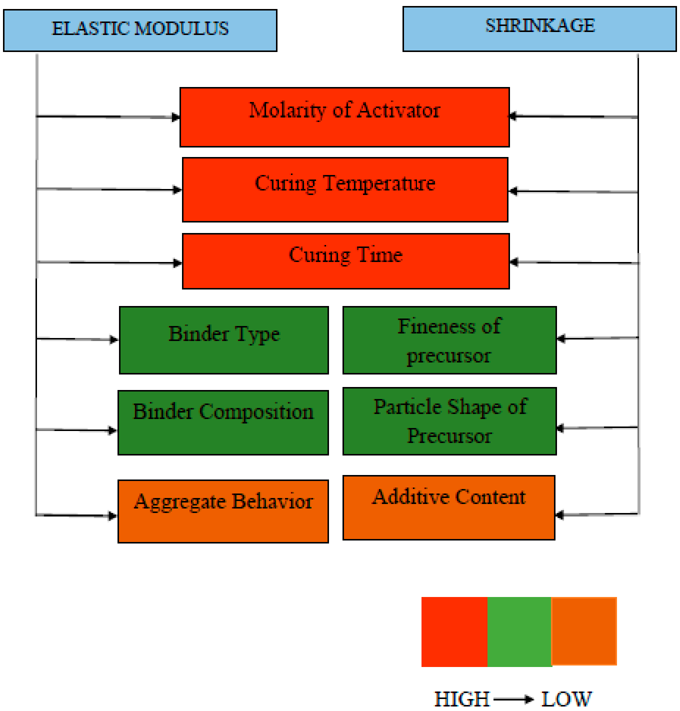

Figure 22. Contributing factors to elastic modulus and shrinkage.

Table 7. Overview on fresh and hardened properties on GPC.

Property	Test Methods	Reference Code *	Used For	Dependent Parameters	Remarks
Workability	Slump test/Compaction factor test	*ASTM C143*	Flow and compaction properties of GPC	Activator molarity, precursor type, its fineness and morphology, silica/alumina ratio, silicate/hydroxide ratio, activator/binder ratio, binder/sand ratio, addition of superplasticizer	Increase in molarity of hydroxides in GPC results in lower workability. Further, increase in water/binder ratio the workability increases. However, the effect of addition of superplasticizer depends on type of precursor and activator source in GPC
Setting time	Vicat needle setting	*ASTM-C191*	Determines the setting time properties in field applications	Activator molarity, precursor type, its fineness and morphology, silica/alumina ratio, silicate/hydroxide ratio, activator/binder ratio, binder/sand ratio, aggregate grading, and type	Increase in molarity of activator decreases the setting time. However, the setting time could be increased by controlling the water/binder ratio, binder content, or superplasticizer content.
Sorptivity	Sorptivity test	*ASTM C1585-20*	Determines the micro-pores and immersed water absorption of GPC	Activator molarity, silica/alumina ratio, silicate/hydroxide ratio, activator/binder ratio, curing temperature, curing time	The increase in molarity of hydroxides and curing temperature results in vigorous exothermic reactions in geopolymeric process that results in micro and macro pores, which further caused the higher sorptivity rate.
Water absorption	Water absorption test	ASTM C1585-13	Determines the pores structure, shrinkage, and absorption capacity of GPC	Activator molarity, silica/alumina ratio, silicate/hydroxide ratio, activator/binder ratio, curing temperature, curing time, heat of hydration, superplasticizer addition.	Greater heat of hydration due to higher molarity or curing temperature cause the shrinkage in GPC samples that results in higher absorption rates.
Compressive Strength	Compressive Strength test	ASTM C39	Primary indicator for strength development and mechanical properties	Activator molarity, precursor type, its fineness and morphology, silica/alumina ratio, silicate/hydroxide ratio, activator/binder ratio, binder/Sand ratio, curing temperature, curing time, heat of hydration, superplasticizer addition.	Increase in molarity of activator up to its optimum amount increases the compressive strength of GPC. Higher percentages of activator/binder ratio or silicate/hydroxide ratio results in reduction of compressive strength. Hence, these ratios should be controlled to their optimum amounts by taking consideration of precursor and activator type. Further, increase in curing temperature results in higher early age strength but lower later age strength.
Tensile and Flexural strength	Flexural strength test	ASTM C496/ASTM C78	Determines the strength behavior of GPC in terms of bending	Activator molarity, precursor type, its fineness and morphology, silica/alumina ratio, silicate/hydroxide ratio, activator/binder ratio, binder/sand ratio, curing temperature, curing time, heat of hydration, superplasticizer addition.	Tensile and flexural strength has direct relation with compressive strength.
Durability	Volume of permeable voids (VPV) test/Rapid Chloride permeability test (RCPT)/Acid Attack test/	ASTM C642/ASTM C1202/ASTM C267	Determines the resistivity and protection against aggressive environments	Precursor type, its fineness and morphology, activator molarity, activator/binder ratio, curing temperature, curing time, heat of hydration, weight loss, microstructure, porosity.	Reduction in micro pores and shrinkage of GPC would results in durable geopolymer concrete. Hence, it is important to control activator content, silicate/hydroxide ratio, activator/binder ratio and curing conditions.

* The reference code is used for normal concrete and can be used for GPC.

4. Durability Properties of GPC

Durability of any structural component is its ability to resist weathering action, chemical attack, abrasion, or any process of deterioration. It is considered as an important component for structural performance in aggressive environments. The durability of GPC can be determined by the properties like sorptivity, immersed absorption, water absorption, apparent volume of permeable voids (AVPV), chloride ingress, sulphate, or other acid attack [153]. In general, GPC has significant higher durability compared to ordinary OPC [154–157]. The summary of properties that are used to determine the durability of GPC is presented in Table 8. The impact of each properties is analyzed and scaled from 'very strong' to 'strong' and 'average'.

Kurtoglu et al. [158] compared GPC prepared with FA and slag and found that slag-based GPC exhibit better durability performance than FA-based GPC due to stable geopolymeric structure. However, FA-based GPC showed better performance than ordinary concrete that might be due to the presence of chemical activity of Na^+ and K^+ ions when exposed to acidic environment. Likewise, inclusion of both slag and black rise husk ash (BRHA) improves the microstructural properties. Venkatesan et al. [159] found that the increase in BRHA content improved the durability of GPC because of reduced chloride ingress and sorptivity. The durability performance of GPC replaced with recycled coarse aggregate were studied by Koushkbaghi et al. and Shaikh [61,160]. It was reported that ordinary concrete deteriorates more when exposed to an aggressive acidic environment than recycled aggregate GPC. It was found that with an increase in silicate/hydroxide ratio, the microstructural and durability performance of MK-based GPC increases because of strong interfacial transition zone (ITZ) between recycled aggregates and binder [61]. Hence, it is concluded that durability performance of GPC compared to OPC concrete is higher due to the presence of a complex geopolymeric structure that enables the GPC to resist the acid attacks.

Table 8. Properties effecting the durability of GPC.

Durability Parameters	Relationship with Durability	Impact on Durability	Remarks
Sorptivity	Inverse relation	Strong	Higher rate of sorptivity results in greater capillary rise of water in micro and macro pores of GPC mixture.
Water Absorption	Inverse relation	Very strong	Higher the water absorption lower will be the durability of GPC mixture. Higher water absorption rate will reveal the transport mechanism for water in GPC.
Weight loss	Inverse relation	Strong	Higher amount of weight loss in specimen will result in deterioration and decrease in durability specially when specimens immersed in sulphuric acid solutions, sodium chloride and sodium sulphate + magnesium sulphate solutions. Initially, when these chemical penetrate in concrete the weight of GPC increased. It also cause expansion in concrete volume which will form the micro-cracks inside GPC [161]. The expansion mechanism will have a detrimental impact on durability.
AVPV	Inverse relation	Strong	Same effect as water absorption and sorptivity of GPC. Increase in AVPC will expose the GPC for environmental impacts and deterioration.
Discontinuous pores and voids	Direct relation	Strong	Discontinuous entrained air voids will enhance the workability and durability in GPC especially exposed to extreme environmental conditions.
Shrinkage cracks	Inverse relation	Average	Greater shrinkage cracks will make it susceptible for deterioration.
Strength degradation	Inverse relation	Strong	Degradation in compressive, flexural and splitting tensile strength of the GPC specimens exposed to different chemical solutions will indicate the compactness of the GPC.
Chloride ingress	Inverse relation	Strong	Chloride ingress in GPC depends both on physical and chemical conditions on which the GPC samples are exposed. Greater chloride ingress in GPC results from greater micro and macro cracks that will further impacts the durability of GPC.

Table 8. *Cont.*

Durability Parameters	Relationship with Durability	Impact on Durability	Remarks
Wetting-drying cycles	Inverse relation	Strong	The wetting–drying and heating–cooling cycles will influence the compressive strength and internal microstructure of GPC. Higher weight loss in these cycles will result in poor durability condition of GPC.
Acid attack	Inverse relation	Strong	Any type of acid attack depends on the exposure conditions of GPC samples. The acid attack in GPC is dependent on both the physical condition of GPC sample and chemical composition of geopolymeric mixture.

5. Factor Affecting the Properties of GPC

5.1. Molarity of Activators

It is the most crucial step in preparing the geopolymer concrete because its type concentration, and amount significantly affect both fresh and hardened properties of GPC. Different types of activators along with varying molarities were studied in literature [49,55,57,125,126,134]. In addition, type and concentration of numerous activators were also suggested for the different type of aluminosilicates-based GPC. Aliabdo et al. [2] investigated the factors that affect the mechanical properties of GGBFS-based GPC. They found that with the increase of NaOH molarity, the compressive strength of alkali-activated slag increases due to a rise in alkalinity that results in the formation of a high amount of hydration products. Elyamany et al. [116] evaluated the 7-day strength and setting time of GPC comprising of various binders. The authors found ascending trend in the compressive strength and decline in workability of fly ash-based geopolymer when molarity increased from 10M to 16M. The increase showed strong correlation as shown in the Figure 23. According to the authors [116], this increase is due to the improvement of dissolution rate of aluminosilicates that improve poly-condensation process and geopolymeric structure (Figure 23). Conversely, Nath et al. [38] evaluated the effect of different alkaline activator solutions having activator content of 35% (A35), 40% (A40), and 45% (A45) of total binder weight on the fresh and hardened characteristics of GPC. It was noticed that increasing activator content from 35–45% reduces the strength of both GPC and mortar (Figure 24), which might be due to precipitation of aluminosilicate gel at higher alkali content. In addition, the reduction increases with the age of the mortar upto more than 60% after 60 days in the case of A45. In addition, algorithmic increase was found with respect to age (Figure 24).

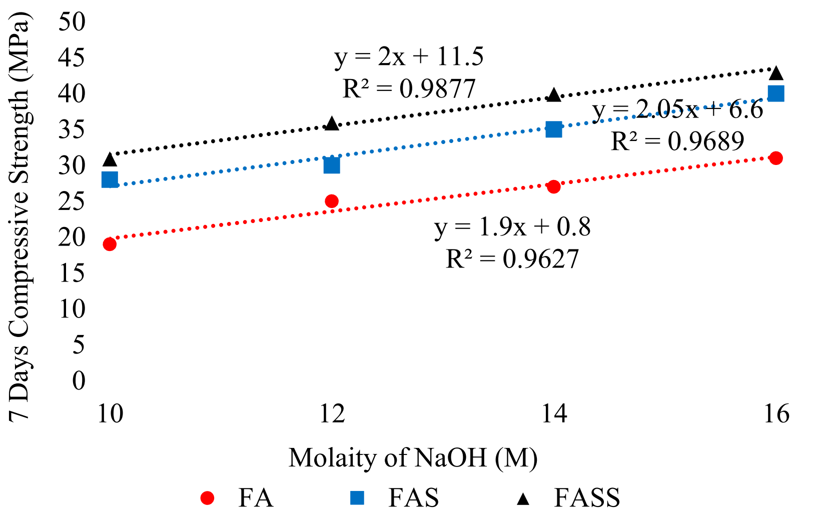

Figure 23. Relationship between molarity and compressive strength, modified from [116]; Elsevier 2018.

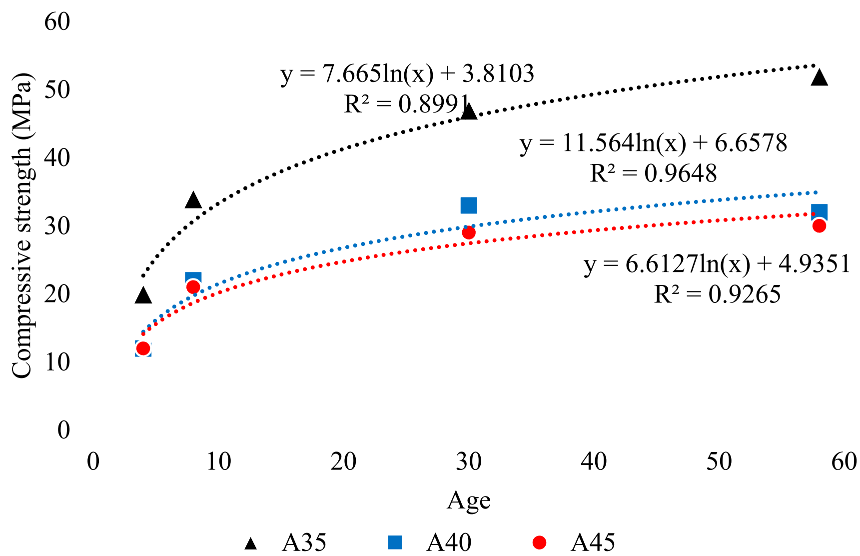

Figure 24. Effect of activator content on compressive strength, adopted from [38]; Elsevier, 2014.

Palomo et al. [162] concluded that the alkaline liquids containing soluble silicates showed the vigorous rate of reaction when compared to the hydroxides. Sharayu et al. [163] investigated the strength effect of FA-based concrete with the use of different alkaline activators such as NaOH + Na_2SiO_3, NaOH + K_2SiO_3, and KOH + Na_2SiO_3 of different molarity at 90 °C. The alkaline activator consisting of a combination of KOH and Na_2SiO_3 showed higher compressive strength when compared to the other two mixtures, as displayed in Figure 25. Hence, it is concluded that the type and concentration of molarity effects the compressive strength of GPC. In addition, with increase in molarity, the compressive strength of GPC increases.

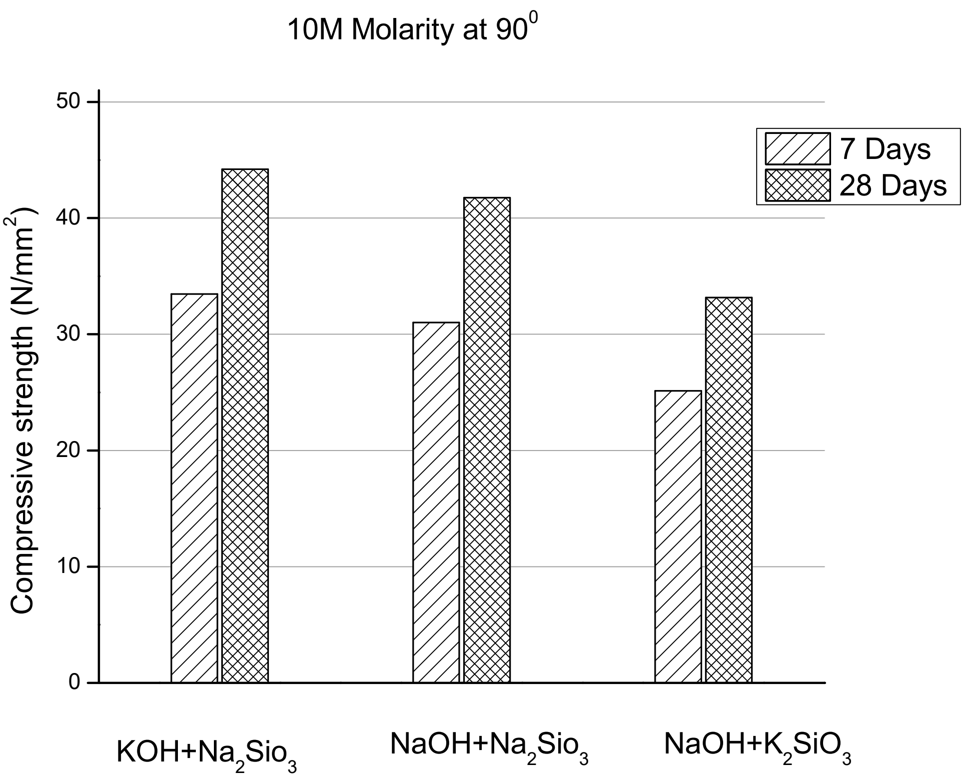

Figure 25. Comparison of compressive strength of different activator combinations for 10M at 90 °C, modified from [163], Morse Florse, 2016.

5.2. Curing Temperature

Curing temperature results in high early strength but causes a porous geopolymer mix, which reduces the strength at later age. The reduction in strength at later ages and at higher temperatures is due to early and fast evaporation of water, which not only disturbs the geopolymerization process and hinders the dissolution of Silica (SiO_2) and Alumina (Al_2O_3), but also increases porosity [129].

Singh et al. [134] studied the effect of temperature curing (80 °C) and ambient curing (25 °C) of a fly ash/slag aluminosilicates mix on the strength development. It was found that temperature cured samples showed higher compressive strength than the samples cured at room temperature after 7 days due to heat release during both alkali activation and temperature curing process. At 28 days, the samples cured at room temperature possessed higher compressive strength than samples temperature cured at 80 °C due to formation of CSH or CASH. According to the authors, this behavior is expected to be due to the inhomogeneity of microstructure and the increase of cumulative pore volume of GPC at high temperature curing. The authors also investigated the microstructure of both temperature cured and ambient cured samples and found that the temperature cured samples had rough microstructures with voids distributed throughout the surface (Figure 26a). In contrast, the ambient cured samples exhibited smooth, compact, and soft microstructure with low void content which could be responsible for their superior strength at 28 days, as shown in Figure 26b.

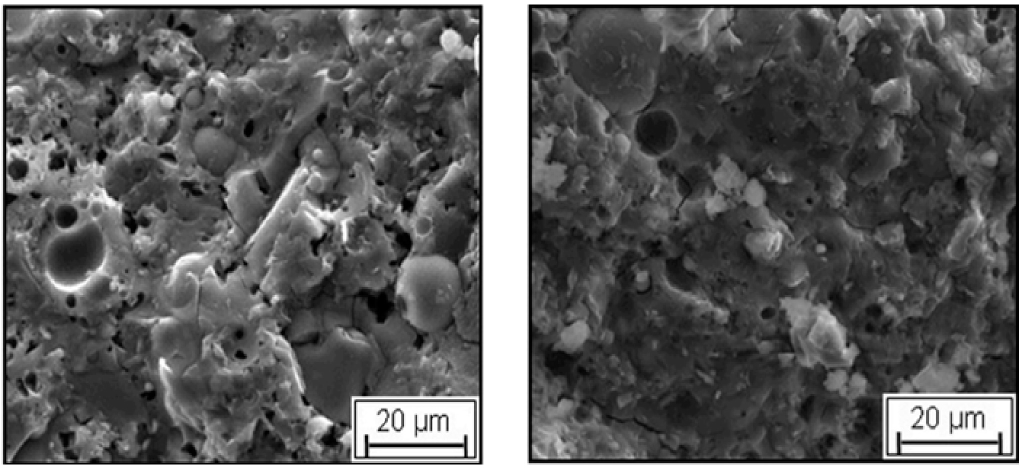

Figure 26. SEM analysis. (**a**) Temperature cured sample; (**b**) ambient temperature cured samples [134].

Aliabdo et al. [2] also did not recommend heat curing for alkali-activated slag concrete because the formation of C-S-H is affected by an increase of temperature as the rise in dry curing temperature leads to more water evaporation. Likewise, Memon et al. [50] investigated that with an increase in curing temperature of 10 °C from 60 °C to 70 °C, the compressive strength of SCGC increases, but beyond 70 °C, the strength decreases. Unlikely, it was found that for FA-based geopolymer concrete curing temperature accelerates the polymerization and significantly affects the mechanical strength as presented in Figure 27 [162,164,165]. This might be due to different composition of fly ash and slag aluminosilicates.

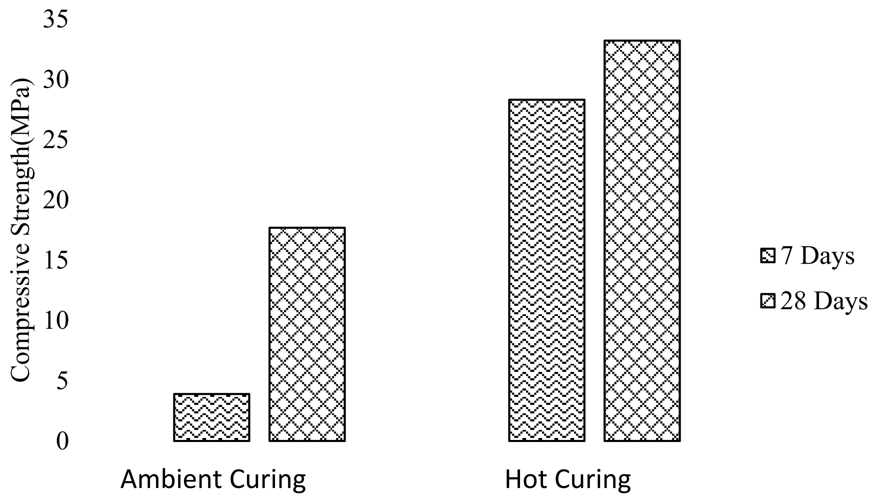

Figure 27. Effect of curing age and curing temperature on compressive strength of FA-based GPC, modified from [165], Academic journals, 2010.

5.3. Activator to Binder Ratio (A/B)

The activator to binder ratio is inversely related to strength parameters. The compressive strength of GGBFS-based GPC diminishes with increase in alkaline solution to slag ratio [2]. Ishwarya et al. [134] studied the rheology and strength characteristics of fly ash/slag geopolymer pastes and concluded that the compressive strength of fly ash-based GPC decreased with the increase of activator to binder ratio. At lower activator to binder ratio, the mix was not workable, resulting from insufficient wetting of particles, while at a higher ratio, the hydroxylation of particles of fly ash was affected due to less Al and Si species in the aqueous phase, that in turn, resulted in lower compressive strength. This trend is shown in Figure 28. Xie et al. [166] studied the behavior of FA and bottom ash-based GPC. It was found that better workability can be maintained with greater FA/ bottom ash and liquid/binder ratios.

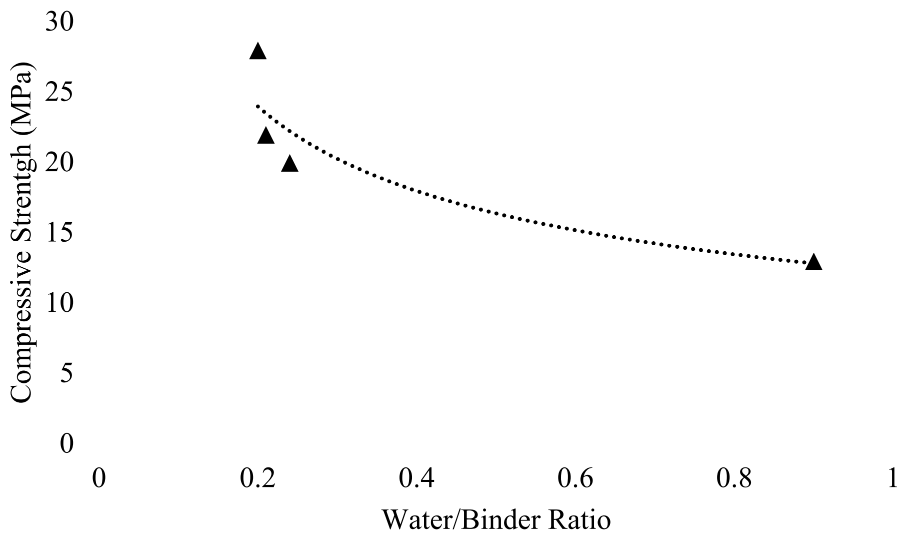

Figure 28. Relation between activator to binder (A/B) ratio and compressive strength at 2:1 fly ash/slag ratio, modified from [134], Elsevier, 2019.

The flow charts presented in Figures 29–31 are proposed which summarize the properties to be considered while determining the notable factors such as molarity, curing temperature, curing time, silicate to hydroxide ratio, and activator to binder ratio. Fresh properties of GPC significantly depend silica to alumina ratio, activator content and its molarity. However, curing temperature affects the hardened properties, strength development, and crack generation. Moreover, each influential parameter effecting the GPC properties are presented in Table 9 with its advantages and disadvantages. The pros and cons of each influential parameter are highlighted that help in determining the different ratios in the mix design of GPC.

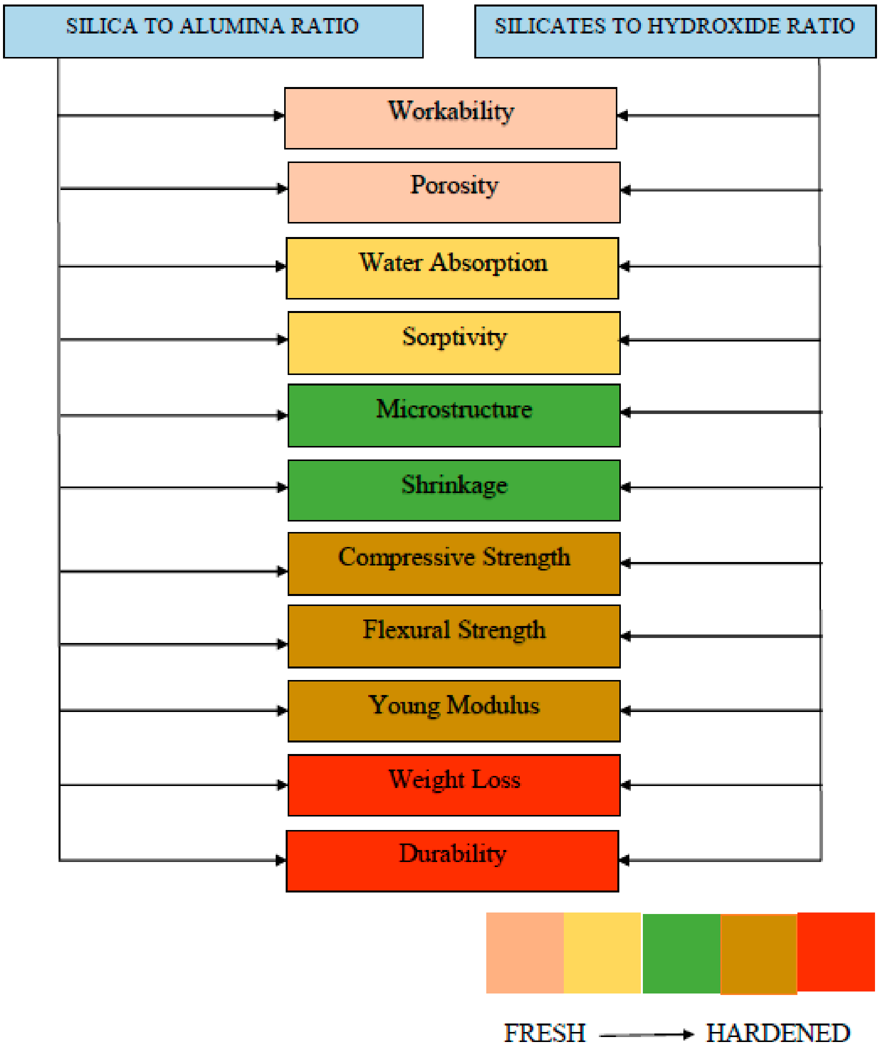

Figure 29. Fresh and hardened properties considered while determining the ratios of GPC.

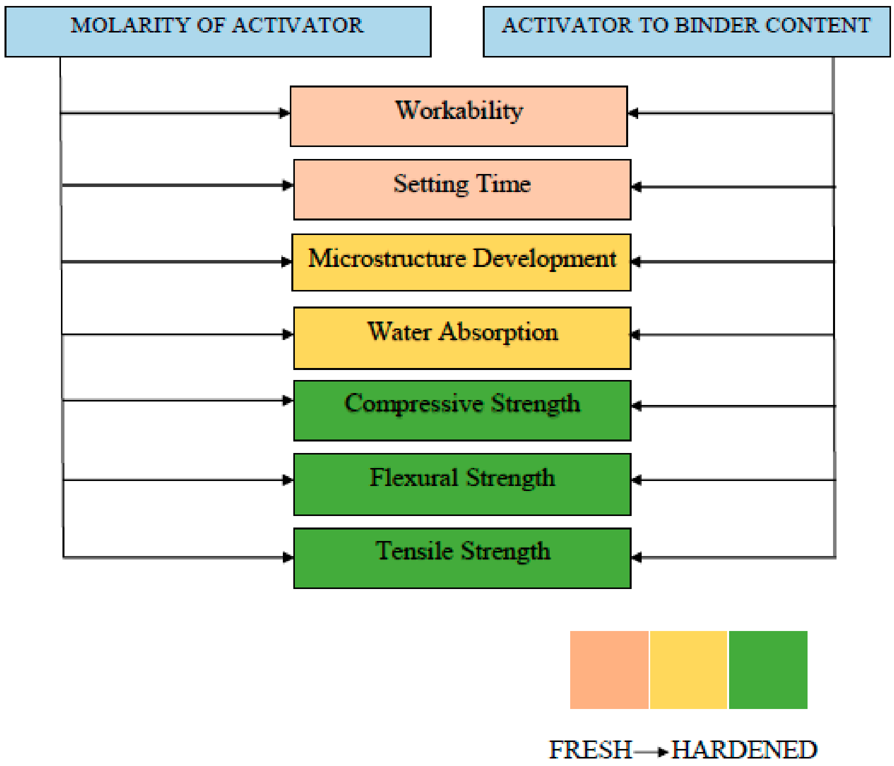

Figure 30. Fresh and hardened properties considered while determining activator to binder content and molarity.

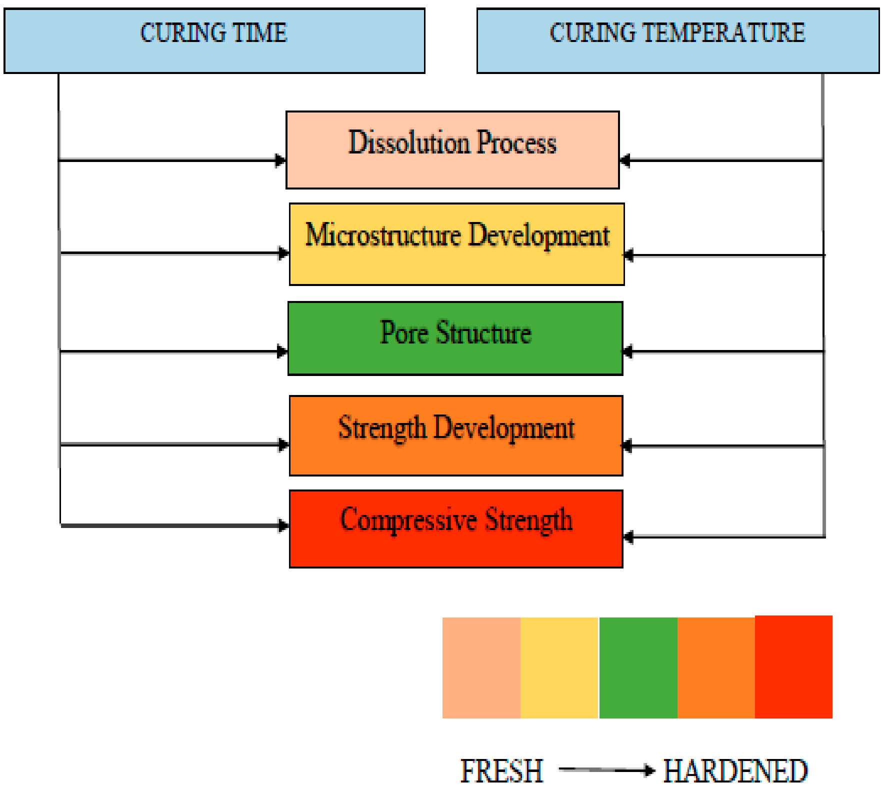

Figure 31. Fresh and hardened properties considered while determining curing conditions.

Table 9. Pros and cons of different parameters considered for GPC.

Parameters	Advantage	Disadvantage	Remarks
Activator Molarity	Increase in molarity increase the compressive and tensile strength.	Higher molarity of activator can cause the shrinkage cracks and affects the strength and durability properties	Most crucial parameter in preparing GPC mixture. In mix design, it is important to determine the optimum amount of activator molarity for effective strength development. Moreover, the type of activator and its different molarities used impacts differently on the microstructural properties of GPC.
Activator/binder ratio	Increase in activator/binder ratio results in workable mixture of GPC	Higher content of activator/binder ratio decreases the compressive strength	The optimum amount of activator/binder ratio in any GPC mixture depends on the type of precursor and activator used.
Silicate/hydroxide ratio	Increase in silicate/hydroxide content provides a workable GPC mixture along with an increase in compressive and tensile strength.	-Increase in Silicate/hydroxide ratio greater than 1 will result in porous microstructure [167] and effect compressive strength and durability,	The optimum amount of silicate/hydroxide ratio in GPC mixture depends on the type of precursor used. The precursor containing higher amount of silica and alumina requires less amount of silicate/hydroxide ratio while preparing GPC mixture and vice versa.
Silica/Alumina ratio	Important parameter considered for high strength GPC. Higher the silica/alumina ratio, higher will be the strength development due to increase in Si-O-Si bonds and decrease in Si-O-Al bonds [168].	-	The silica/alumina ratio in GPC mixture depends on precursor type and activator composition and content.
Curing temperature	Higher curing temperature results in greater early age strength development	Greater curing temperature also results in lower later age strength	Curing temperature used for GPC depends on the composition of precursor and reactants in geopolymeric process.

6. Geopolymer OPC Concrete

When aluminosilicates partially replace the cement, the water firstly reacts with aluminosilicate; however, further reaction stops due to the formation of the protective film coating of Ca+ ions. This film breaks if a high pH value is supplied by hydrated cement products, i.e., $Ca(OH)_2$. The aluminosilicate due to its pozzolanic property then forms secondary CSH by reacting with $Ca(OH)_2$. Hence, three reaction components—hydration of cement, hydration of aluminosilicate, and the pozzolanic reaction of aluminosilicate—are formed when aluminosilicate is partially replaced with cement in the geopolymerization process [2].

Mehta and Siddique [111], studied the effect of GPC containing OPC as a partial replacement of fly ash. They reported that GPC, with the inclusion of OPC, showed improved compressive strength when compared to fly ash-based GPC. The addition of OPC in GPC densified the microstructure of geopolymer paste due to the presence of hydration and poly-condensation products. Hence, it is deduced that the porosity, water absorption, sorptivity, and chloride penetration of GPC improved when compared to GPC not containing OPC [9,111]. The improved microstructure of GPC with or without OPC can be seen in SEM (Figure 32). Figure 32b showed a more compact and dense microstructure when compared to Figure 32a [9].

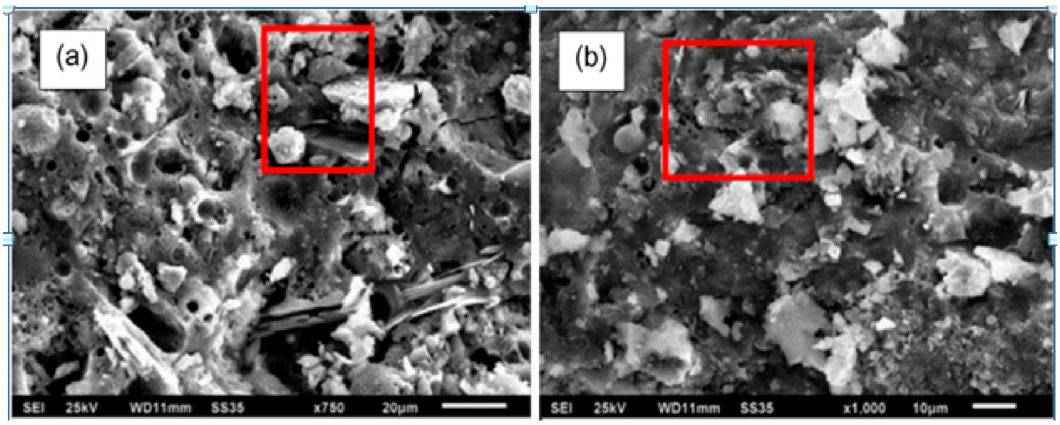

Figure 32. SEM images of GPC [9]. (**a**) Without OPC; (**b**) with OPC.

In addition, the setting time and workability of GPC are also affected by the addition of OPC. Nath et al. [53] investigated the setting time of GPC, which has been significantly reduced with 5% inclusion of OPC of total binder along with a slight reduction in workability. Consequently, the microstructure has been improved with higher compressive strength at 28 days due to the presence of a substantial portion of calcium-rich aluminosilicate gel. The effect of the OPC content on the setting time and compressive strength of geopolymer OPC concrete is shown in Figure 33.

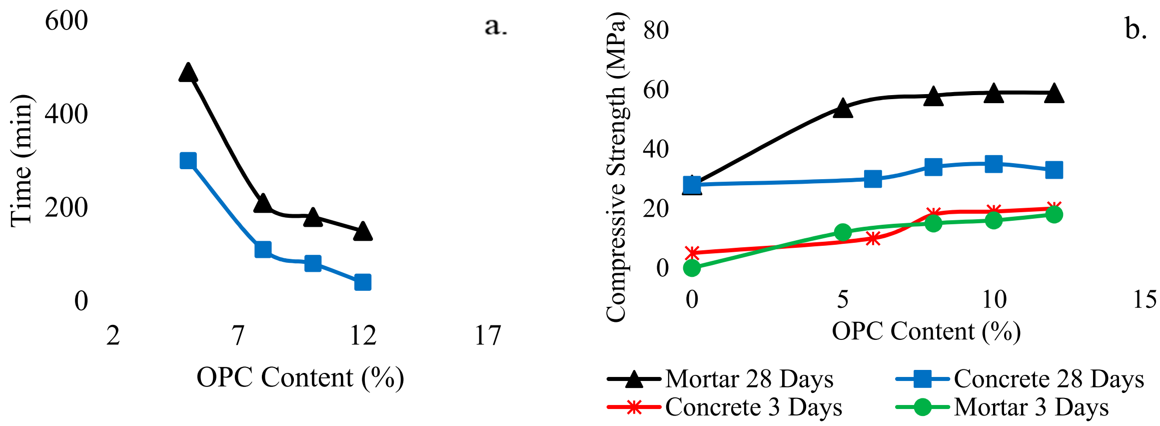

Figure 33. Effect on (**a**) setting time with addition of OPC; (**b**) compressive strength with addition of OPC, modified from [53], Elsevier, 2015.

Pangdaeng et al. [169] found that the properties of high calcium FA-based geopolymer have been improved by OPC usage. The increase in early and later age strength resulted due to the presence of both CSH and C-AS-H gel in the geopolymeric structure [169,170]. Nath et al. [53] studied the effect of FA-based GPC with 10% and 50% OPC replacement. With the help of SEM, they concluded that the GPC with 50% replacement exhibited more enrichment of C-AS-H, as compared to GPC with 10% OPC replacement, along with few partially reacted or unreacted FA and OPC particles. Hence, it is concluded that GPC containing OPC as partial replacement exhibits better mechanical and microstructural properties due to the presence of C-AS-H gel in geopolymeric reaction.

7. Reinforced GPC

The reinforced GPC is an important structural component to be studied and analyzed for its use in the construction industry. Different experimental investigations determined that the reinforced GPC, when compared to reinforced OPC concrete, possesses better mechanical and durable properties [7,171,172]. In reinforced GPC, the mechanical and structural properties depend significantly on the bond strength between the concrete and reinforcement because it is an essential property in the design of structural elements. From previous studies [172,173], it was found that the determination of bond strength of reinforced GPC mainly depends on factors like concrete strength, bar diameter, cover/bar diameter ratio, splice length, embedded length, and steel fiber reinforcement. Furthermore, other characteristics like type of binder, activator/binder ratio, silicate/hydroxide ratio, water/binder ratio, molarity and concentration of activator, and the curing conditions are considered for determining the bond strength [174–176]. Castel and Foster [174] reported that GPC possesses better performance than OPC concrete, with a 10% rise in bond strength of GPC. It was concluded that the bond strength of FA-based GPC depends on the bar type (smooth or ribbed) and curing conditions (time and temperature). Chang et al. [177] compared bond strength of reinforced GPC beams with ACI 318-02 and AS 3600 codes. It was reported that the experimental values of ratios are comparable with modeled values. Chang et al. [177] proposed the best fit experimental values of bond strength from Equations (7) and (8) proposed by Mo et al. [178].

$$\sigma = f_c\,[2.07 + 0.2 \times (c/\varphi) + 4.15 \times (\varphi/l_d)] \tag{7}$$

$$\sigma = 2.12 \times (f_c)^{0.5} \tag{8}$$

where,

σ = bond strength of GPC,

f_c = compressive strength of GPC,

c = concrete cover,

φ = bar diameter,

l_d = developmental length.

The research trend of reinforced GPC has been practically applied to structural elements like beams, columns, slabs, and walls. Several researchers [179,180] have found that reinforced GPC beams showed similar mechanical performance when compared to reinforced OPC concrete. It has also been reported that there is no disadvantageous effect of using reinforced GPC as the structural member in the construction industry [173]. The performance of reinforced GPC beam is considerably enhanced by the incorporation of steel fibers [181]. Chang et al. [177] analyzed the performance of bonding of lap-splices and shear behavior of GPC. It was found that the techniques used to predict the shear behavior of conventional OPC concrete can be applied to reinforced GPC. Furthermore, the code provisions and different analytical models applied for calculation and prediction of normal OPC concrete can be sued for reinforced GPC beams. Likewise, the code provisions of AS 3600 for determining the flexural behavior of OPC beams could be used for GPC beams [179]. Nonetheless, more research efforts are required to develop more desirable, realistic, and cost-effective design codes [172]. It has been reported that the load deflection, crack patterns, crack width, flexural stiffness, ultimate load, and failure mode of the reinforced GPC beams are similar to the OPC concrete beams [182,183]. Dattatreya et al. [182] reported that the total number of flexural cracks and their developed spacing was found the same for both types of beams. Likewise, the ultimate load and mid-span deflection of both reinforced GPC and OPC concrete was reported. It was found that the mechanical properties of reinforced GPC are comparable with that of OPC concrete [184]. In contrast, Yost et al. [185] reported brittle failure of GPC during the crushing test when compared to OPC concrete. In addition, when reinforced GPC beam was subjected to corrosive sodium chloride solution, it exhibited more flexural degradation than normal concrete [186]. When GPC is used in columns; its behavior depends on the eccentricity of loads, ratios of reinforcement, additional steel fibers, and compressive strength along with bond strength. Sumajouw et al. [187] found that the loading capacity of reinforced GPC columns increased when the eccentricity of loading was reduced. In addition, with high reinforcement ratio and concrete strength and lower load eccentricity, the reinforced GPC columns exhibit brittle failure. Similarly, while increasing strength and longitudinal reinforcement and decreasing load eccentricity, the loading capacity of the column increased [179]. However, to further improve the ductility and load-carrying capacity of reinforced GPC columns, the use of steel fibers and confinement was recommended [188,189]. In addition to beams and columns, the structural member includes reinforced structure GPC slab panels. Rajendran and Soundarapandian [190] performed flexural test on GPC and reinforced concrete slabs. It was found that GPC reinforced slab has a higher ultimate load, yield load, and cracking load with more micro-cracks and deflection when compared to the normal reinforced concrete. However, the number of cracks in the GPC slab were more, but their average crack width and spacing were less than conventional concrete, which might be due to improved microstructure of GPC.

In addition to the beams, columns, and slabs, one of the most important structural members to be considered are GPC wall panels. It was found from previous researches [173,191] that GPC walls when compared to normal OPC walls, exhibit more deflection and softening behavior under axial loading. Thus, it behaved more in a ductile manner. This ductility was due to the presence of a higher amount of finer aluminosilicate particles in the GPC mix [191]. This study also proposed equation 9 for finding the ultimate strength of GPC walls.

$$P_u = 0.585\,[f_c Lt + (f_y - f_c)\,A_{sc}]\,[1 + (h/40\,t) - (h/30\,t)^2]\,[1 - (h/18\,L)] \tag{9}$$

where,

P_u= ultimate load,
L= length of wall,
t = thickness of wall,
f_y = steel reinforcement strength,
A_{sc} = steel reinforcement area,
H = height of wall.

8. Application of GPC and Geopolymer Concrete Mortar (GCM)

GPC is gaining acceptance in actual field applications like precast members, bridge deck, boat ramp, retaining walls, road construction, and other structural members. In the year 2013, GPC was practically used for the first time in the multi-storey construction of a building as the precast GPC beams at the University of Queensland's global change institute [192]. Furthermore, a comparison of OC and GPC is provided in Table 10. It can be found easily that GPC can be used as replacement of OPC concrete. Figure 34 shows the application of GPC in prefabricated bridges. In addition, geopolymer material is gaining application in the form of a protective layer of concrete structures and road surfaces for long-lasting applications [193].

GPC is most commonly known for durable and acid-resistant applications; therefore, it is most suitable for marine structures. GPC durability is due to its resistance to freeze–thaw cycles, sulphate and chloride attack, fire, heat, and efflorescence [194]. For anti-corrosion and durable property of GPC in marine structures, the microstructure and chemical composition play an important role, which in turn, are mainly influenced by curing conditions, alkali solutions, and addition of superplasticizers [195,196]. Further, the GPC provides efficient and sustainable construction of marine structures due to the stability of amorphous aluminosilicate gel in GPC [197]. This stable structure leads to a dense and compact microstructure of GPC that prevent penetration and other chemical attacks of sea water on structures [198]. Likewise, Fan et al. [199] reported that GPM containing metakaolin as an aluminosilicate efficiently performs when exposed to different aggressive environments. Furthermore, the performance of GPC in the case of water-based structures is more effective against sulphate attack than any other acid attack [200].

GPC and GPM have also been used for repair and retrofitting applications because it prevents deterioration of reinforcement in structural members by sea water and de-icing compounds [201]. The geopolymer mix has been used as a bonding fiber material for structural members like bridges and newly constructed buildings in Japan [202]. Further, it is used in seismic prone and hurricane areas to strengthen the structures and prevent them from damage. [203]. It has been found that the repair resistance of GPC is more when compared to cement and other commercial repair materials [204]. Several researchers [205,206] have reported that the abrasion resistance of GPC can be significantly improved by the addition of steel slag.

GPC is the best alternative option for OPC concrete because it promotes sustainable development and provides a cleaner environment by utilizing industrial and agricultural waste and through immobilization of heavy metallic materials [207,208]. For example, GPC has been proposed as an excellent immobilization material for poisonous heavy metals [209]. This property of GPC is due to the complex and dense microstructure and low permeability property [7]. In the complex microstructure of GPC, the heavy metals can be utilized chemically by accumulated anions present in the matrix in order to balance the charge. Further, these heavy metals can be mobilized physically by their contact with voids and pores of the matrix of GPC [210]. However, it was reported that the metakaolin- and kaolin-based GPCs do not possess the immobilization property of heavy metals due to the presence of excessive leaching [211].

Table 10. Comparison between OPC concrete and GPC.

Properties	OPC Concrete	GPC	Remarks
Setting time	Slower	Faster	Generally GPC has faster rate of setting than ordinary concrete but the setting time also depends on factors like aluminosilicate source and activators
Compressive Strength	Lower	Higher	Compressive strength of GPC depends on number on factors such as aluminosilicate source, precursor reactivity, activator type and curing conditions. Further, early age strength of GPC is greater than normal concrete
Tensile Strength	Lower	Higher	Tensile strength usually higher than OPC concrete. Moreover, tensile strength of GPC exhibits similar behavior to compressive strength and depends on the same factors on which compressive strength depends
Water Absorption	Slightly lower	Moderate	Water absorption depends on internal pore structure of GPC
Shrinkage	Lower	Moderate	Shrinkage cracks in GPC mainly depends on the curing condition.
Porosity	Lower	Moderate	Porosity depends on internal geopolymeric structure of GPC.
Acid Attack	Lower resistance	Higher resistance	GPC have higher durability in terms of acid attacks than OPC concrete due to the presence of alumino-silicate products
Freeze and thaw cycling	More susceptible	Less susceptible	GPC have higher physical and chemical resistance against aggressive environment
Durability	Lower	Higher	GPC has higher durability than OPC concrete because of the chemical alumina and silicate products
Fire Resistance	Limited	Typically higher	GPC can withstand heat without age degradation when compared to OPC concrete
Insulating property	Limited	Higher	Usually have higher insulation but depends on type of precursor and activator along with curing conditions
CO2 Emission	High	Low	GPC has lower global warming potential than ordinary concrete
Age Degradation	High	Low	During heating OPC concrete has extreme age degradation and carbonation when compared to GPC

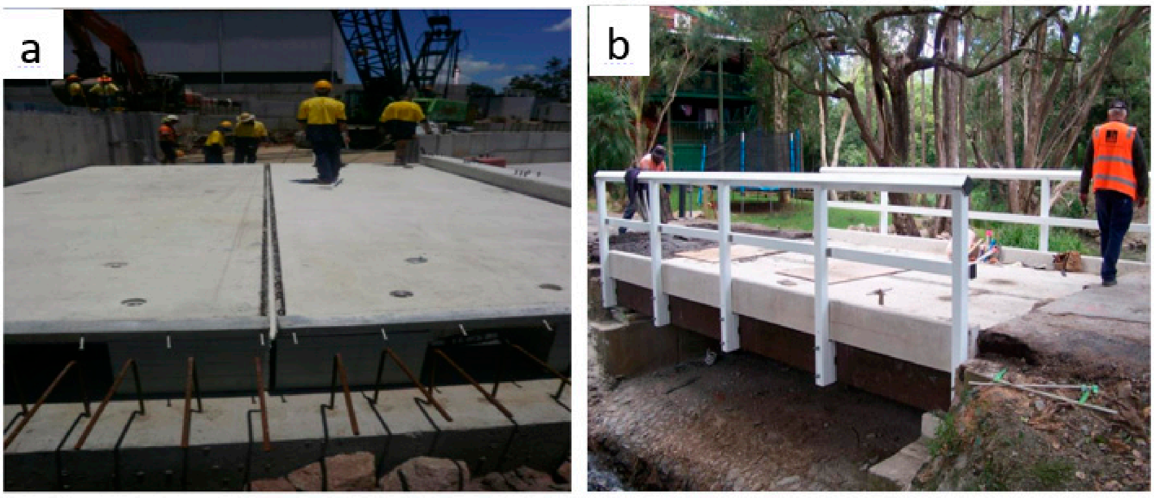

Figure 34. Application of GPC. (**a**) Prefabricated bridge, (**b**) deck bridge [192].

GPC can also be used in cooling systems. For example, the aluminosilicates generated from industrial and agricultural wastes in GPC employ in the applications of the evaporative cooling systems. The compressive strength of these geopolymers was not high as compared to other GPC, but was within the acceptable range for evaporative cooling applications [212].

Finally, GPC has been found to be efficient fire-resistant material when compared to conventional concrete. The fly ash-based GPC exhibits stability when exposed to elevated temperatures [213]. Likewise, it was reported that GPC increased its strength when exposed to elevated temperatures and hence has a superior fire resistance than conventional concrete that loses approximately all of its strength when exposed to the temperature of 800 °C [214,215].

9. Recent Advances in GPC

GPC is gaining acceptance in the construction industry because of its better mechanical properties and eco-efficiency than normal concrete. Due to its eminent performance, researchers are performing and analyzing different experimentations and techniques to promote the sustainable development. However, recently researchers are focusing on some new advances in GPC like 3D printing using GPC, nanomaterial-based GPC, self-compacting GPC, life cycle assessment (LCA), and GWP calculations. Some of the topical developments are discussed below.

9.1. GWP Calculation and Assessment

GWP is the best tool to assess the global warming impact of different gases. Generally, it allows the comparison of emission of any gas with CO_2 emission over a specified time interval. These days, GWP of GPC is a hot topic as it justifies that GPC has less potential to produce global warming than ordinary concrete. It has been reported by Intergovernmental Panel on Climate Change (IPCC) that GPCs containing different binders have substantially less impact of global warming production than OPC concrete [216]. Salas et al. [217] found that the GWP can reduced up to 64% when compared to ordinary concrete due to the environmental sustainable use of NaOH obtained from local solar salt. In Colombia, life cycle assessment (LCA) of natural volcanic pozzolan with 30% slag-based GPC was studied [218]. It was concluded that GPC has 44.7% GWP less than ordinary concrete with the same compressive strength. Ng et al. [219] evaluated the effect of GPC on global warming production and durability characteristics by using practical applications of bridge and retaining wall. The structures made with GPC and reactive powder concrete exhibit less GWP along with more durability characteristics and design life when compared to structures made with OPC concrete. Although GPC has less impact on global warming, it also has some other environmental impacts such as fresh water ecotoxicity, marine toxicity, abiotic depletion, and eutrophication. These impacts, in turn, are influenced by the type of binder and activator selection.

Researchers [217,220] made comparison between different binders to assess which aluminosilicate has environmental impact. The environmental impact depends on the internal chemical composition of binder and is influenced by the amount of silicate. For example, the binder that requires high amount of sodium silicate has higher impact of GWP [216,221]. Heath et al. [216] found that FA and GGBFS has lower CO_2 production and GWP than MK as MK requires more amount of silicates as an activator. However, Abbas et al. [221] reported that GPC having 30% MK as a binder has high mechanical strength along with low GWP compared to ordinary concrete. The comparison of binders of GPC along with OPC concrete with respect to environmental impact is presented in Figure 35.

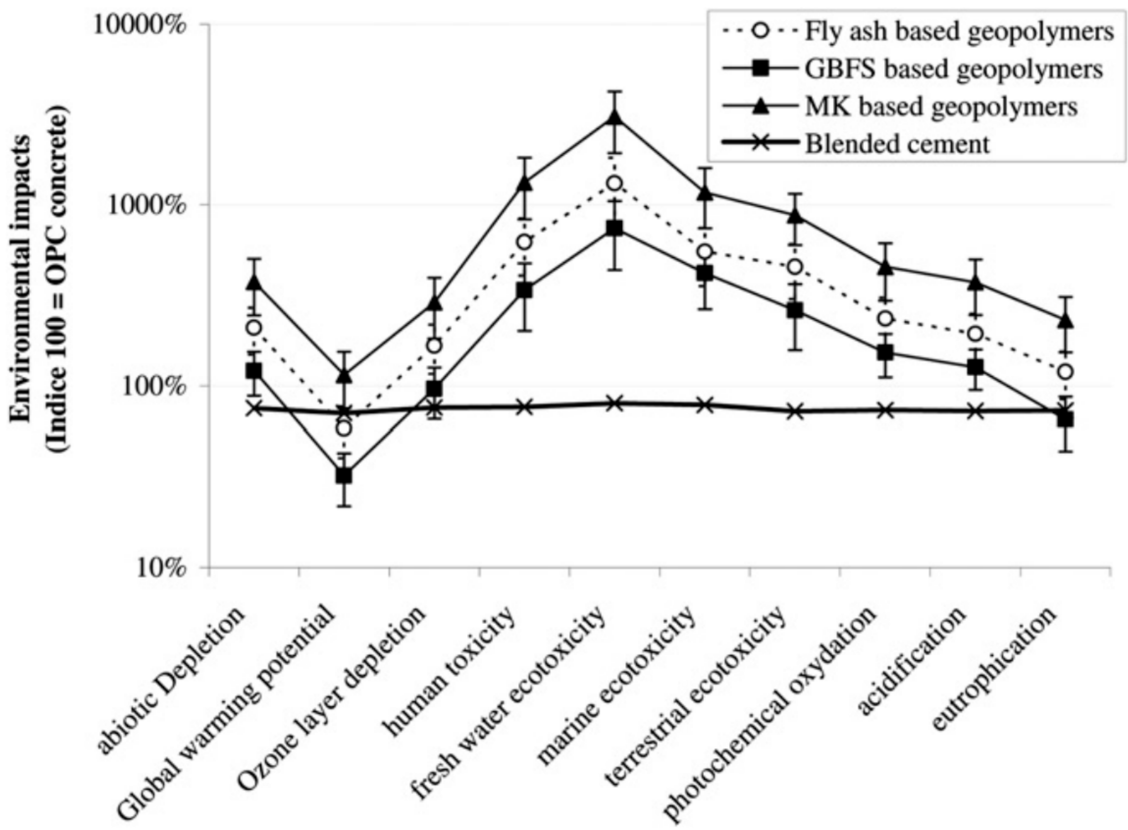

Figure 35. Comparison of different GPC containing different binders and OPC concrete [220].

The calculation of GWP of different types of GPC depends on the various types of techniques and methods involved in different studies. Louise et al. [222] studied the CO_2 emission of GPC by considering all the activities involved in production of GPC from raw material selection to manufacturing including transportation and other energy procedures. It was revealed that GPC has only 9% of CO_2 emission less than ordinary concrete. The steps involved in the calculation of CO_2 emission of GPC and alkaline activator are presented in Figures 36 and 37, respectively.

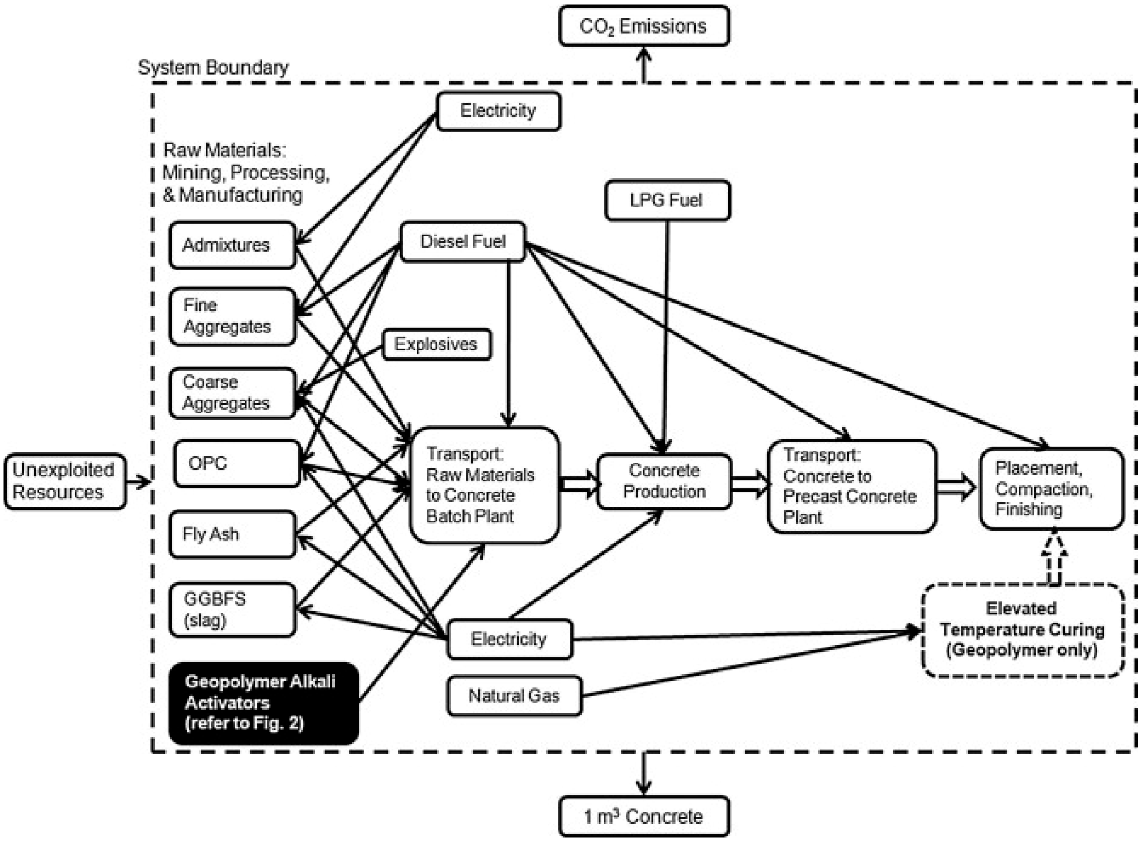

Figure 36. CO_2 emission resulting from GPC [222].

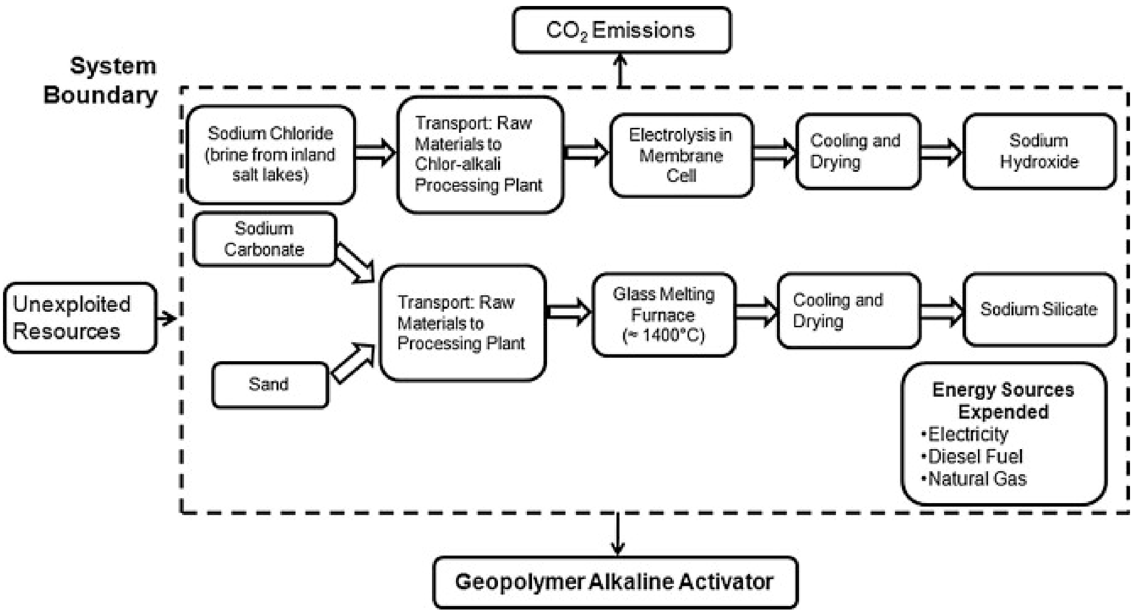

Figure 37. CO_2 emission resulting from alkaline activator [222].

Hence, it is concluded that the GPC containing any binder has less impact on global warming production than ordinary concrete. However, there exist some other environmental impacts of GPC like marine ecotoxicity, abiotic depletion, eutrophication, or acidification, as presented in Figure 38, which should be considered.

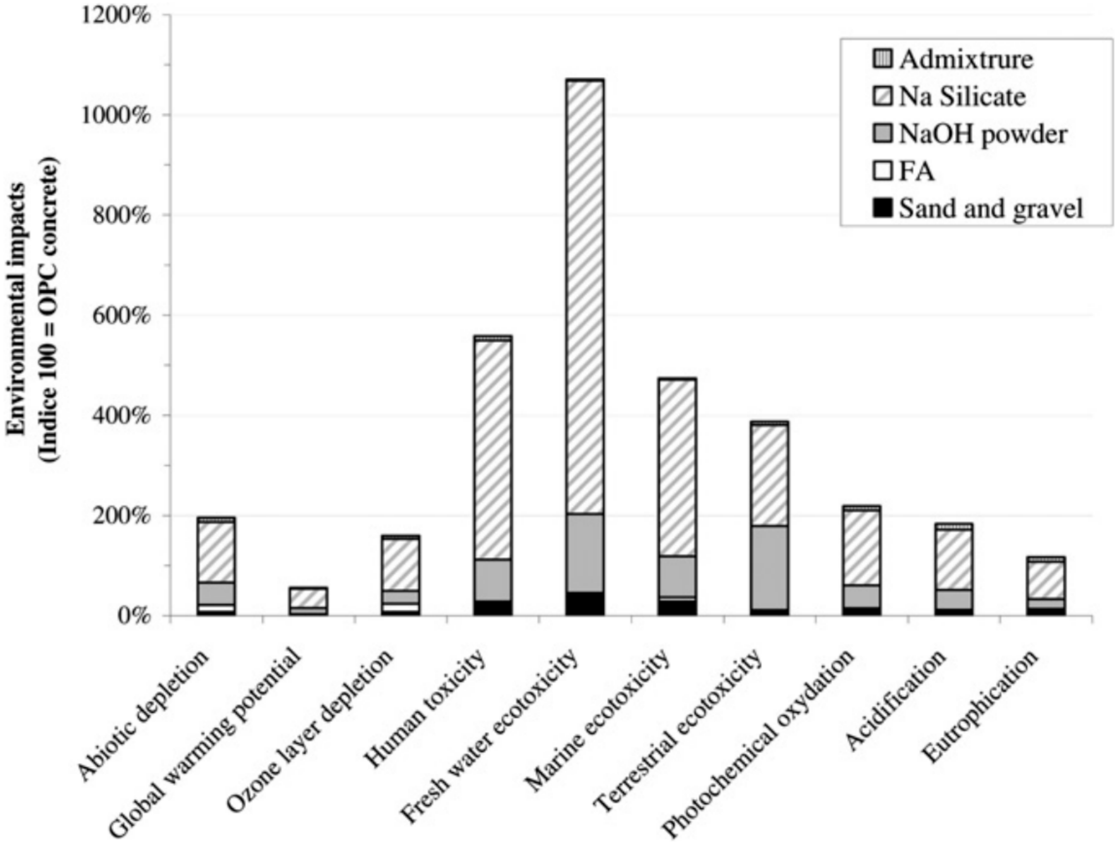

Figure 38. Comparison of GPC and OPC concrete with respect to environmental impacts [220].

9.2. 3D Printing Using Geopolymer

3D printing is gaining wide applications in different fields like aerospace, automotive manufacturing, and in the construction industry due to its sustainable development. In the construction industry, 3D printing is considered environment friendly due to designing freedom, automation, less waste generation, reduced raw material consumption [223], and labor cost, while GPC reduces carbon footprints as discussed earlier. Combining both the sustainable solutions is an innovative idea for construction industry and can help in environmental management and technology development.

Different studies were conducted by researchers to determine the fresh and hardened properties and mix design proportions of different types of geopolymers in 3D applications. The fresh properties of geopolymer containing FA, slag, and silica fume as a binder were investigated and the effect of activator percentage and water/binder ratios were assessed [224]. The study revealed that the better mechanical properties with compressive strength of 50MPa at 21 days achieved at water/solid ratio of 0.33 along with 8% activator percentage. Likewise, the effect of addition of different superplasticizers on mechanical, rheological, and microstructural properties of GPC were assessed under ambient curing condition [225]. It was reported that with inclusion of slag in FA-based GPC improved the microstructure and early age strength without significant improvement in rheology. However, addition of silica fume improved both yield stress and viscosity of GPC that was due to its particle shape and surface area.

Hence, changing activator or aluminosilicate type and content or effect of addition of superplasticizer, etc., can influence the GPC mixture designs due to presence of unique geopolymerization reactions involved. Further, the selection of appropriate 3D printing technique is crucial step in concrete printing technology. For different field or lab scale applications, different types of 3D printers are available with their advantages and limitation and selection of any printable technology depends on application and usage.

9.3. Graphene-Based GPC

Geopolymers are not only environmental ecofriendly but also improve mechanical properties when compared to other binding materials [135,226,227]. GPC containing binders like FA or GGBFS exhibit better mechanical and microstructural properties due to their chemical composition. However, some of the binders such as clay minerals or other agricultural wastes have not much influenced the mechanical properties of GPC due to their porous microstructure. Moreover, this porous microstructure can cause brittleness, shrinkage, and cracking that in turn effects the structural properties. Therefore, some mineral admixtures or external agents are added to improve their microstructural, mechanical, and durability properties. One of the modifiers to improve the properties of GPC is graphene.

Graphene, derived from graphite, is a single layer carbon atom in a two dimensional honeycomb structure [228]. It has excellent mechanical, optical, electrical, catalytical, and biological properties [229–231]. In structural applications, a graphene-based product called graphene oxide is most commonly used nanomaterial that greatly influence the microstructural properties of cement-based material. The incorporation of this nanomaterial make the microstructure dense, reduces nano-cracks, brittleness that directly impacts the durability properties of GPC [232]. Zhu et al. [233] found that inclusion of graphene oxide in slag-based GPC performed better in terms of mechanical properties with 20% increases in flexural strength. The optimum percentage of graphene oxide was found to be 0.01% by weight of slag. Ranjbar et al. [234] investigated the effect of inclusion of graphene nanoflake on FA-based GPC and found that with the addition of 1% graphene nanoflake, both the compressive and flexural strength increased by 2.16 and 1.44 times, respectively. However, it was found that the additional amount of graphene and NaOH content in GPC reduces the bending strength as presented in Figures 39 and 40, respectively [235]. Hence, it is important to determine the optimum amount of graphene in GPC in order to achieve desirable properties.

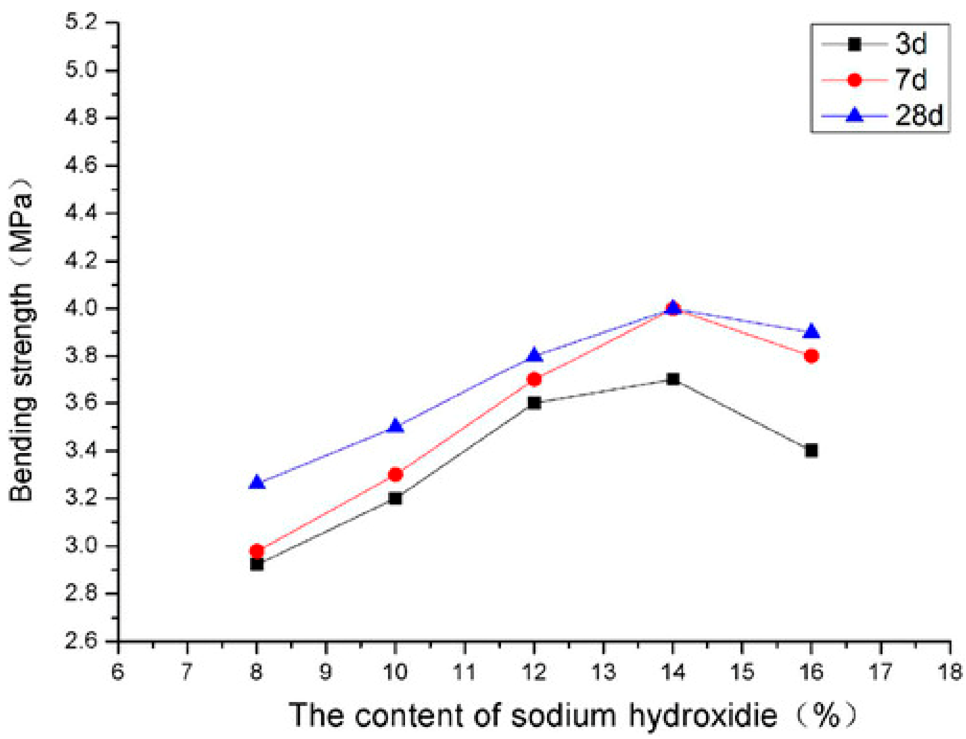

Figure 39. Effect of NaOH on bending strength [235].

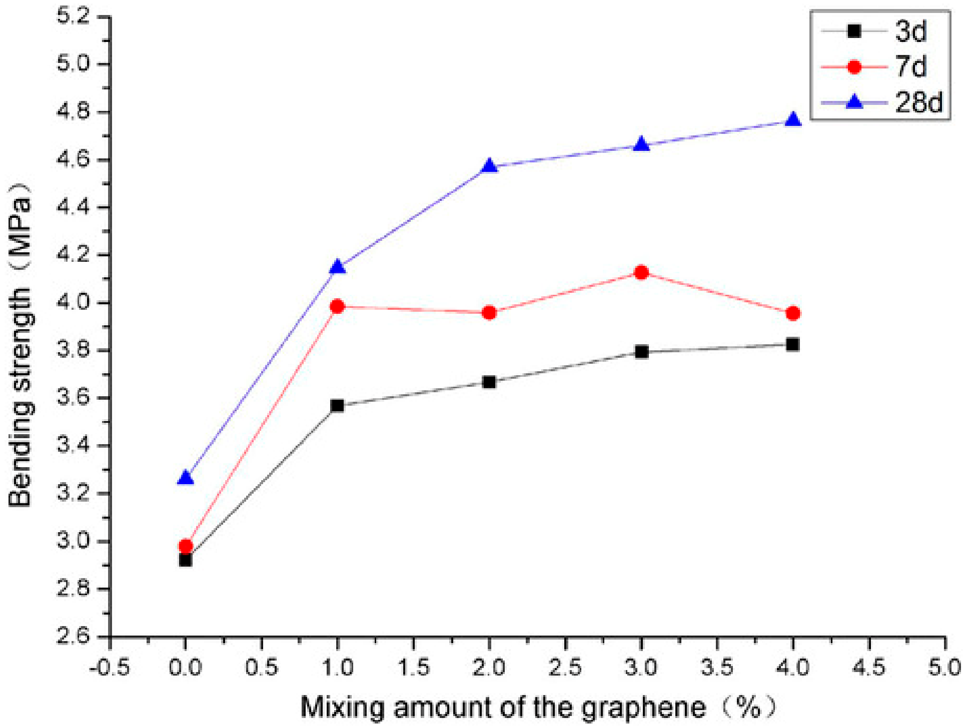

Figure 40. Effect of graphene amount on bending strength [235].

The addition of graphene oxide in geopolymers for the application of 3D printing is popular amongst scientific community. However, with inclusion of graphene, there exists some negative impacts on properties of geopolymers such as reduction in fluidity and workability of GPC. Lui et al. [232] stated that these properties can be improved by the addition of superplasticizers or silica fume. It was concluded that with inclusion of graphene oxide in GPC, the durability, rheological, and mechanical properties were improved making it possible for geopolymers to be used in 3D printing applications [236].

10. Conclusions and Recommendations

This review article covered the detailed discussion of GPC based on past research and investigations. The main conclusions are as follows:

- GPC can be recognized as an eco-friendly construction material with better mechanical and durable properties. It is considered to be an appropriate replacement of OPC concrete, which would be possible with an efficient supply of agricultural and industrial waste products.
- Researchers assessed the performance of common aluminosilicates like FA, GGBFS, PFOA, MK, HCWA, silica fume, and RHA or their combinations. However, most of the research was carried out on FA-based geopolymer mortar and concrete since it gave the better mechanical properties compared to other aluminosilicates-based geopolymers due to better physical and chemical characteristics. The most widely used activators in GPC are NaOH and Na_2SiO_3 or their combination. Several factors such as the concentration, amount, molarity, and reactivity play a vital role in the development of the geopolymerization reaction. In order to achieve better mechanical and durability properties, it is essential to find the optimum activator dosage in the geopolymer blend. Moreover, it was found that the soluble silicates exhibit a fast geopolymerization reaction compared to activators containing hydroxides.
- GPC mechanical, durable, and microstructural properties are further dependent on mix design proportion. While determining the mix design, all factors that are responsible to develop better mechanical properties should be considered like activator to binder ratio, silicates to hydroxide

ratio, binder content, activator concentration and molarity, aggregate type and grading, dosage of superplasticizer, water to binder and binder to sand ratio.

- Inclusion of OPC in GPC creates both geopolymerization and C-S-H products that make a compact and dense microstructure. Hence, compressive strength, durability, and microstructural behavior improved along with the reduction in shrinkage, porosity, and water absorption.
- Previous investigations were carried out to evaluate the mechanical properties and durability characteristics based on different factors like NaOH/Na_2SiO_3 ratio, NaOH/slag ratio, activator/binder ratio, the combination of different activators, curing conditions, curing temperature, curing duration, elevated temperature, molarity of activators, different binders ratio, aggregate type, the addition of nanoparticles, reinforcement ratio, and effect of adding different additives, nanoparticles, recycled aggregate, and steel fibers to find their optimum ratios and amounts.
- Recent advances in GPC such as 3D printing and fiber-based GPC require further in-depth investigations. GWP calculation and LCA techniques provide the way to analyze the sustainable growths. However, further investigations based on different types of aluminosilicates and activators are required.
- Experimental investigations are recommended on standard mix design procedure, newly compatible aluminosilicates and activators, microstructure, brittle behavior, efflorescence and shrinkage phenomenon, cost-effectiveness, practicality of easily handled and field-applicable strength compatible GPC to be used in the construction industry.

Author Contributions: S.K.U.R., L.I. and S.A.M. conceived and designed the idea; S.K.U.R. and M.K.K. analyzed the data; M.F.J. contributed reagents/materials/analysis tools; S.K.U.R., L.I., S.A.M., and M.F.J. wrote the original draft of paper, L.I., S.K.U.R., S.A.M., M.K.K., and M.F.J. revised the draft of paper. All authors have read and agreed to the published version of the manuscript.

Funding: This research was supported by Nazarbayev University Faculty development competitive research grants numbers 090118FD5316 and SEDS2021006.

Acknowledgments: The authors are thankful to the editor and reviewers who provide valuable suggestion to improve this manuscript.

Conflicts of Interest: The authors declare no conflict of interest.

Abbreviations

Alkali activated Fly ash-slag (AFS); Activator to Binder ratio (A/B); Alkali activated materials (AAM); Bagasse Ash (BA); Carbon dioxide (CO_2); Calcium Silicate Hydrate (CSH); Fly Ash (FA); Fly Ash-Silica fume (FAS); Fly Ash-Silica fume-furnace slag (FASS); Geopolymer concrete (GPC); Geopolymer mortar (GPM); Global warming potential (GWP); Ground granulated blast furnace slag (GGBFS); Micro-Encapsulated phase change materials (MPCM); Nano Silica (NS); Ordinary Portland Cement (OPC); Palm Oil fuel ash (POFA); Potassium Hydroxide (KOH); Potassium Silicate (K_2SiO_3); Rice husk ash (RHA/RA); Silica Fume (SF); Self compacting geopolymer concrete (SCGC); Sodium Silicate (Na_2SiO_3); Sodium Hydroxide (NaOH); Wheat straw ash (WSA); X-ray fluorescence (XRF).

References

1. Zhang, Z.; Provis, J.L.; Reid, A.; Wang, H. Geopolymer foam concrete: An emerging material for sustainable construction. *Constr. Build. Mater.* **2014**, *56*, 113–127. [CrossRef]
2. Aliabdo, A.A.; Elmoaty, A.E.M.A.; Emam, M.A. Factors affecting the mechanical properties of alkali activated ground granulated blast furnace slag concrete. *Constr. Build. Mater.* **2019**, *197*, 339–355. [CrossRef]
3. Rashad, A.M. A comprehensive overview about the influence of different additives on the properties of alkali-activated slag–A guide for civil engineer. *Constr. Build. Mater.* **2013**, *47*, 29–55. [CrossRef]
4. Bhikshma, V.; Koti, R.M.; Srinivas, R.T. An experimental investigation on properties of geopolymer concrete (no cement concrete). *Asian J. Civ. Eng. (Build. Hous.)* **2012**, *13*, 841–853.
5. Mccaffrey, R. Climate change and the cement industry. *Glob. Cem. Lime Mag. (Environ. Spec. Issue)* **2002**, *15*, 19.

6. WMO. Greenhouse Gas. Bulletin: The State of the Greenhouse Gases in the Atmosphere Based on Global Observations through 2018. 2019, Volume 15. Available online: https://library.wmo.int/doc_num.php?explnum_id=10100 (accessed on 26 October 2020).
7. Hassan, A.; Arif, M.; Shariq, M. Use of geopolymer concrete for a cleaner and sustainable environment—A review of mechanical properties and microstructure. *J. Clean. Prod.* **2019**, *223*, 704–728. [CrossRef]
8. Kumar, H.; Prasad, R.; Srivastava, A.; Vashista, M.; Khan, M. Utilisation of industrial waste (Fly ash) in synthesis of copper based surface composite through friction stir processing route for wear applications. *J. Clean. Prod.* **2018**, *196*, 460–468. [CrossRef]
9. Ma, C.-K.; Awang, A.Z.; Omar, W. Structural and material performance of geopolymer concrete: A review. *Constr. Build. Mater.* **2018**, *186*, 90–102. [CrossRef]
10. Zhang, P.; Zheng, Y.; Wang, K.; Zhang, J. A review on properties of fresh and hardened geopolymer mortar. *Compos. Part. B Eng.* **2018**, *152*, 79–95. [CrossRef]
11. Ng, C.; Alengaram, U.J.; Wong, L.S.; Mo, K.H.; Jumaat, M.Z.; Ramesh, S. A review on microstructural study and compressive strength of geopolymer mortar, paste and concrete. *Constr. Build. Mater.* **2018**, *186*, 550–576. [CrossRef]
12. Zhang, P.; Gao, Z.; Wang, J.; Guo, J.; Hu, S.; Ling, Y. Properties of fresh and hardened fly ash/slag based geopolymer concrete: A review. *J. Clean. Prod.* **2020**, *270*, 122389. [CrossRef]
13. Jindal, B.B. Investigations on the properties of geopolymer mortar and concrete with mineral admixtures: A review. *Constr. Build. Mater.* **2019**, *227*, 116644. [CrossRef]
14. Reddy, M.S.; Dinakar, P.; Rao, B.H. A review of the influence of source material's oxide composition on the compressive strength of geopolymer concrete. *Microporous Mesoporous Mater.* **2016**, *234*, 12–23. [CrossRef]
15. Al Bakri, M.M.; Mohammed, H.; Kamarudin, H.; Niza, I.K.; Zarina, Y. Review on fly ash-based geopolymer concrete without portland cement. *J. Eng. Technol. Res.* **2011**, *3*, 1–4.
16. Prabu, B.; Shalini, A.; Kumar, J. Rice husk ash based geopolymer concrete-a review. *Chem. Sci. Rev. Lett.* **2014**, *3*, 288–294.
17. Jindal, B.B. Feasibility study of ambient cured geopolymer concrete–A review. *Adv. Concr. Constr.* **2018**, *6*, 387.
18. Li, N.; Shi, C.; Zhang, Z.; Wang, H.; Liu, Y. A review on mixture design methods for geopolymer concrete. *Compos. Part. B Eng.* **2019**, *178*, 107490. [CrossRef]
19. Institute, G. Why Alkali-activated-materials AAM are not Geopolymers. 2017. Available online: https://www.geopolymer.org/library/technical-papers/25-why-alkali-activated-materials-aam-are-not-geopolymers/ (accessed on 26 October 2020).
20. Luukkonen, T.; Abdollahnejad, Z.; Yliniemi, J.; Kinnunen, P.; Illikainen, M. One-part alkali-activated materials: A review. *Cem. Concr. Res.* **2018**, *103*, 21–34. [CrossRef]
21. Duxson, P.; Fernández-Jiménez, A.; Provis, J.L.; Lukey, G.C.; Palomo, A.; van Deventer, J.S. Geopolymer technology: The current state of the art. *J. Mater. Sci.* **2007**, *42*, 2917–2933. [CrossRef]
22. Busari, A.A.; Akinmusuru, J.O.; Dahunsi, B.I. Review of sustainability in self-compacting concrete: The use of waste and mineral additives as supplementary cementitious materials and aggregates. *Port. Electrochim. Acta* **2018**, *36*, 147–162. [CrossRef]
23. Xu, H.; Van Deventer, J. The geopolymerisation of alumino-silicate minerals. *Int. J. Miner. Process.* **2000**, *59*, 247–266. [CrossRef]
24. Güllü, H.; Cevik, A.; Al-Ezzi, K.M.; Gülsan, M.E. On the rheology of using geopolymer for grouting: A comparative study with cement-based grout included fly ash and cold bonded fly ash. *Constr. Build. Mater.* **2019**, *196*, 594–610. [CrossRef]
25. Allahverdi, A.; Kani, E.N.; Yazdanipour, M. Effects of blast-furnace slag on natural pozzolan-based geopolymer cement. *Ceram.-Silikáty* **2011**, *55*, 68–78.
26. Kani, E.N.; Allahverdi, A.; Provis, J.L. Efflorescence control in geopolymer binders based on natural pozzolan. *Cem. Concr. Compos.* **2012**, *34*, 25–33. [CrossRef]
27. Brew, D.; MacKenzie, K. Geopolymer synthesis using silica fume and sodium aluminate. *J. Mater. Sci.* **2007**, *42*, 3990–3993. [CrossRef]
28. Khale, D.; Chaudhary, R. Mechanism of geopolymerization and factors influencing its development: A review. *J. Mater. Sci.* **2007**, *42*, 729–746. [CrossRef]

29. Payá, J.; Monzó, J.; Borrachero, M.; Tashima, M. Reuse of aluminosilicate industrial waste materials in the production of alkali-activated concrete binders. In *Handbook of Alkali-Activated Cements, Mortars and Concretes*; Elsevier: Amsterdam, The Netherlands, 2015; pp. 487–518.
30. Zain, H.; Abdullah, M.M.A.B.; Hussin, K.; Ariffin, N.; Bayuaji, R. Review on various types of geopolymer materials with the environmental impact assessment. In *MATEC Web of Conferences*; EDP Sciences: Les Ulis, France, 2017; p. 01021. [CrossRef]
31. Fernández-Jiménez, A.; Palomo, A. Characterisation of fly ashes. Potential reactivity as alkaline cements☆. *Fuel* **2003**, *82*, 2259–2265. [CrossRef]
32. Wattimena, O.K.; Antoni Hardjito, D. A review on the effect of fly ash characteristics and their variations on the synthesis of fly ash based geopolymer. In *AIP Conference Proceedings*; AIP Publishing: New York, NY, USA, 2017; p. 020041. [CrossRef]
33. Aughenbaugh, K.; Williamson, T.; Juenger, M. Critical evaluation of strength prediction methods for alkali-activated fly ash. *Mater. Struct.* **2015**, *48*, 607–620. [CrossRef]
34. Kamhangrittirong, P.; Suwanvitaya, P.; Chindaprasirt, P. Synthesis and properties of High Calcium fly ash based geopolymer for concrete applications. In Proceedings of the 36th Conference on Our World in Concrete & Structures, Singapore, 14–16 August 2011; p. 9.
35. Arioz, O.; Bzeni, D.K.; Zangy, R.R.; Arioz, E. Properties of slag-based geopolymer pervious concrete for ambient curing condition. *MS&E* **2020**, *737*, 012068.
36. Awoyera, P.; Adesina, A. A critical review on application of alkali activated slag as a sustainable composite binder. *Case Stud. Constr. Mater.* **2019**, *11*, e00268. [CrossRef]
37. Brykov, A.; Korneev, V. Production and usage of powdered alkali metal silicate hydrates. *Metallurgist* **2008**, *52*, 648–652. [CrossRef]
38. Nath, P.; Sarker, P.K. Effect of GGBFS on setting, workability and early strength properties of fly ash geopolymer concrete cured in ambient condition. *Constr. Build. Mater.* **2014**, *66*, 163–171. [CrossRef]
39. Xie, J.; Wang, J.; Rao, R.; Wang, C.; Fang, C. Effects of combined usage of GGBS and fly ash on workability and mechanical properties of alkali activated geopolymer concrete with recycled aggregate. *Compos. Part. B Eng.* **2019**, *164*, 179–190. [CrossRef]
40. Ryu, G.S.; Lee, Y.B.; Koh, K.T.; Chung, Y.S. The mechanical properties of fly ash-based geopolymer concrete with alkaline activators. *Constr. Build. Mater.* **2013**, *47*, 409–418. [CrossRef]
41. Juenger, M.C.G.; Jennings, H.M. Effects of high alkalinity on cement pastes. *Mater. J.* **2001**, *98*, 251–255.
42. Sant, G.; Kumar, A.; Patapy, C.; Le Saout, G.; Scrivener, K. The influence of sodium and potassium hydroxide on volume changes in cementitious materials. *Cem. Concr. Res.* **2012**, *42*, 1447–1455. [CrossRef]
43. Phoo-ngernkham, T.; Hanjitsuwan, S.; Damrongwiriyanupap, N.; Chindaprasirt, P. Effect of sodium hydroxide and sodium silicate solutions on strengths of alkali activated high calcium fly ash containing Portland cement. *KSCE J. Civ. Eng.* **2017**, *21*, 2202–2210. [CrossRef]
44. Patankar, S.V.; Jamkar, S.S.; Ghugal, Y.M. Geopolymer concrete-a best solution to cement concrete in hot climate. *J. Emerg. Technol. Innov. Res.* **2019**, *6*, 271–276.
45. Ravichandran, G.; Sivaraja, M.; Jegan, M.; Harihanandh, M.; Krishnaraja, A. Performance of glass fiber reinforced geopolymer concrete under varying temperature effect. *Technology* **2018**, *9*, 1316–1323.
46. Mehta, A.; Siddique, R. Sustainable geopolymer concrete using ground granulated blast furnace slag and rice husk ash: Strength and permeability properties. *J. Clean. Prod.* **2018**, *205*, 49–57. [CrossRef]
47. Özcan, A.; Karakoç, M.B. The resistance of blast furnace slag-and ferrochrome slag-based geopolymer concrete against acid attack. *Int. J. Civ. Eng.* **2019**, *17*, 1571–1583. [CrossRef]
48. Wongsa, A.; Sata, V.; Nuaklong, P.; Chindaprasirt, P. Use of crushed clay brick and pumice aggregates in lightweight geopolymer concrete. *Constr. Build. Mater.* **2018**, *188*, 1025–1034. [CrossRef]
49. Risdanareni, P.; Ekaputri, J.J. The influence of alkali activator concentration to mechanical properties of geopolymer concrete with trass as a filler. In *Materials Science Forum*; Trans Tech Publications Ltd.: Zürich, Switzerland, 2015; Volume 803, pp. 125–134.
50. Memon, F.A.; Nuruddin, M.F.; Demie, S.; Shafiq, N. Effect of curing conditions on strength of fly ash-based self-compacting geopolymer concrete. *Int. J. Civ. Environ. Eng.* **2011**, *3*, 183–186.
51. Chindaprasirt, P.; Chareerat, T.; Sirivivatnanon, V. Workability and strength of coarse high calcium fly ash geopolymer. *Cem. Concr. Compos.* **2007**, *29*, 224–229. [CrossRef]

52. Umniati, B.S.; Risdanareni, P.; Zein, F.T.Z. Workability enhancement of geopolymer concrete through the use of retarder. In *AIP Conference Proceedings*; AIP Publishing: New York, NY, USA, 2017; p. 020033. [CrossRef]
53. Nath, P.; Sarker, P.K. Use of OPC to improve setting and early strength properties of low calcium fly ash geopolymer concrete cured at room temperature. *Cem. Concr. Compos.* **2015**, *55*, 205–214. [CrossRef]
54. Kumar, S.; Kumar, R. Mechanical activation of fly ash: Effect on reaction, structure and properties of resulting geopolymer. *Ceram. Int.* **2011**, *37*, 533–541. [CrossRef]
55. Deb, P.S.; Nath, P.; Sarker, P.K. The effects of ground granulated blast-furnace slag blending with fly ash and activator content on the workability and strength properties of geopolymer concrete cured at ambient temperature. *Mater. Des. (1980–2015)* **2014**, *62*, 32–39. [CrossRef]
56. Islam, A.; Alengaram, U.J.; Jumaat, M.Z.; Bashar, I.I. The development of compressive strength of ground granulated blast furnace slag-palm oil fuel ash-fly ash based geopolymer mortar. *Mater. Des. (1980–2015)* **2014**, *56*, 833–841. [CrossRef]
57. Živica, V. Effects of type and dosage of alkaline activator and temperature on the properties of alkali-activated slag mixtures. *Constr. Build. Mater.* **2007**, *21*, 1463–1469. [CrossRef]
58. Kong, D.L.; Sanjayan, J.G. Effect of elevated temperatures on geopolymer paste, mortar and concrete. *Cem. Concr. Compos.* **2010**, *40*, 334–339. [CrossRef]
59. Zhang, Z.; Provis, J.L.; Ma, X.; Reid, A.; Wang, H. Efflorescence and subflorescence induced microstructural and mechanical evolution in fly ash-based geopolymers. *Cem. Concr. Compos.* **2018**, *92*, 165–177. [CrossRef]
60. Goriparthi, M.R.; Td, G.R. Effect of fly ash and GGBS combination on mechanical and durability properties of GPC. *Adv. Concr. Constr.* **2017**, *5*, 313.
61. Koushkbaghi, M.; Alipour, P.; Tahmouresi, B.; Mohseni, E.; Saradar, A.; Sarker, P.K. Influence of different monomer ratios and recycled concrete aggregate on mechanical properties and durability of geopolymer concretes. *Constr. Build. Mater.* **2019**, *205*, 519–528. [CrossRef]
62. Pimraksa, K.; Chindaprasirt, P.; Rungchet, A.; Sagoe-Crentsil, K.; Sato, T. Lightweight geopolymer made of highly porous siliceous materials with various Na2O/Al2O3 and SiO2/Al2O3 ratios. *Mater. Sci. Eng. A* **2011**, *528*, 6616–6623. [CrossRef]
63. Panias, D.; Giannopoulou, I.P.; Perraki, T. Effect of synthesis parameters on the mechanical properties of fly ash-based geopolymers. *Colloids Surf. A Physicochem. Eng. Asp.* **2007**, *301*, 246–254. [CrossRef]
64. Ravikumar, D.; Neithalath, N. Effects of activator characteristics on the reaction product formation in slag binders activated using alkali silicate powder and NaOH. *Cem. Concr. Compos.* **2012**, *34*, 809–818. [CrossRef]
65. Kumar, S.; Kumar, R.; Mehrotra, S. Influence of granulated blast furnace slag on the reaction, structure and properties of fly ash based geopolymer. *J. Mater. Sci.* **2010**, *45*, 607–615. [CrossRef]
66. Reddy, M.S.; Dinakar, P.; Rao, B.H. Mix design development of fly ash and ground granulated blast furnace slag based geopolymer concrete. *J. Build. Eng.* **2018**, *20*, 712–722. [CrossRef]
67. Patankar, S.V.; Ghugal, Y.M.; Jamkar, S.S. Effect of concentration of sodium hydroxide and degree of heat curing on fly ash-based geopolymer mortar. *Indian J. Mater. Sci.* **2014**, *2014*, 938789. [CrossRef]
68. Patil, A.A.; Chore, H.; Dodeb, P. Effect of curing condition on strength of geopolymer concrete. *Adv. Concr. Constr.* **2014**, *2*, 29–37. [CrossRef]
69. Ferdous, M.; Kayali, O.; Khennane, A. A detailed procedure of mix design for fly ash based geopolymer concrete. In Proceedings of the Fourth Asia-Pacific Conference on FRP in Structures (APFIS 2013), Melbourne, Australia, 11–13 December 2013; pp. 11–13.
70. Abdullah, M.; Hussin, K.; Bnhussain, M.; Ismail, K.; Ibrahim, W. Mechanism and chemical reaction of fly ash geopolymer cement—A review. *Int. J. Pure Appl. Sci. Technol.* **2011**, *6*, 35–44.
71. Gunasekara, M.; Law, D.; Setunge, S. Effect of composition of fly ash on compressive strength of fly ash based geopolymer mortar. In Proceedings of the 23rd Australasian Conference on the Mechanics of Structures and Materials (ACMSM23), Byron Bay, Australia, 9–12 December 2014.
72. Duxson, P.; Mallicoat, S.W.; Lukey, G.C.; Kriven, W.M.; van Deventer, J.S. The effect of alkali and Si/Al ratio on the development of mechanical properties of metakaolin-based geopolymers. *Colloids Surf. A Physicochem. Eng. Asp.* **2007**, *292*, 8–20. [CrossRef]
73. Pavithra, P.; Srinivasula Reddy, M.; Dinakar, P.; Hanumantha Rao, B.; Satpathy, B.; Mohanty, A. Effect of the Na2SiO3/NaOH ratio and NaOH molarity on the synthesis of fly ash-based geopolymer mortar. *Geo-Chicago* **2016**, 336–344. [CrossRef]

74. Mallikarjuna Rao, G.; Gunneswara Rao, T. A quantitative method of approach in designing the mix proportions of fly ash and GGBS-based geopolymer concrete. *Aust. J. Civ. Eng.* **2018**, *16*, 53–63. [CrossRef]
75. Azarsa, P.; Gupta, R. Durability and leach-ability evaluation of K-based geopolymer concrete in real environmental conditions. *Case Stud. Constr. Mater.* **2020**, *30*, e00366.
76. Hadi, M.N.; Farhan, N.A.; Sheikh, M.N. Design of geopolymer concrete with GGBFS at ambient curing condition using Taguchi method. *Constr. Build. Mater.* **2017**, *140*, 424–431. [CrossRef]
77. Anuradha, R.; Sreevidya, V.; Venkatasubramani, R.; Rangan, B.V. Modified guidelines for geopolymer concrete mix design using Indian standard. *Asian J. Civ. Eng.* **2012**, *13*, 357–368.
78. Ogheneochuko, D.; Orie, O. Optimization of superplasticized concrete using Taguchi approach: A case study of hydroplast 200. *Niger. J. Technol.* **2018**, *37*, 611–618. [CrossRef]
79. Olivia, M.; Nikraz, H. Properties of fly ash geopolymer concrete designed by Taguchi method. *Mater. Des. (1980–2015)* **2012**, *36*, 191–198. [CrossRef]
80. Junaid, M.T.; Kayali, O.; Khennane, A.; Black, J. A mix design procedure for low calcium alkali activated fly ash-based concretes. *Constr. Build. Mater.* **2015**, *79*, 301–310. [CrossRef]
81. Lokuge, W.; Wilson, A.; Gunasekara, C.; Law, D.W.; Setunge, S. Design of fly ash geopolymer concrete mix proportions using multivariate adaptive regression spline model. *Constr. Build. Mater.* **2018**, *166*, 472–481. [CrossRef]
82. ACI 211.4R-93, A. *Guide for Selecting Proportions for HighStrength Concrete with Portland Cement and Fly Ash*; American Concrete Institute: Farmington Hills, MI, USA, 1993.
83. Phoo-Ngernkham, T.; Phiangphimai, C.; Damrongwiriyanupap, N.; Hanjitsuwan, S.; Thumrongvut, J.; Chindaprasirt, P. A mix design procedure for alkali-activated high-calcium fly ash concrete cured at ambient temperature. *Adv. Mater. Sci. Eng.* **2018**, *2018*. [CrossRef]
84. Kim, Y.Y.; Lee, B.-J.; Saraswathy, V.; Kwon, S.-J. Strength and durability performance of alkali-activated rice husk ash geopolymer mortar. *Sci. World J.* **2014**, *2014*. [CrossRef] [PubMed]
85. Zhang, J.; Li, G.; Yang, X.; Ren, S.; Song, Z. Study on a high strength ternary blend containing calcium sulfoaluminate cement/calcium aluminate cement/ordinary Portland cement. *Constr. Build. Mater.* **2018**, *191*, 544–553. [CrossRef]
86. Cheah, C.B.; Tan, L.E.; Ramli, M. The engineering properties and microstructure of sodium carbonate activated fly ash/slag blended mortars with silica fume. *Compos. Part. B Eng.* **2019**, *160*, 558–572. [CrossRef]
87. Bellum, R.R.; Nerella, R.; Madduru, S.R.C.; Indukuri, C.S.R. Mix design and mechanical properties of fly ash and GGBFS-synthesized alkali-activated concrete (AAC). *Infrastructures* **2019**, *4*, 20. [CrossRef]
88. Jithendra, C.; Elavenil, S. Role of superplasticizer on GGBS based geopolymer concrete under ambient curing. *Mater. Today Proc.* **2019**, *18*, 148–154. [CrossRef]
89. Davidovits, J. Geopolymers: Inorganic polymeric new materials. *J. Therm. Anal. Calorim.* **1991**, *37*, 1633–1656. [CrossRef]
90. De Silva, P.; Sagoe-Crenstil, K.; Sirivivatnanon, V. Kinetics of geopolymerization: Role of Al2O3 and SiO2. *Cem. Concr. Res.* **2007**, *37*, 512–518. [CrossRef]
91. Komnitsas, K.A. Potential of geopolymer technology towards green buildings and sustainable cities. *Procedia Eng.* **2011**, *21*, 1023–1032. [CrossRef]
92. Glukhovsky, A. Stability of nonlinear chain-type systems used to model cascaded energy transfer processes. *Atmos. Ocean. Phys.* **1975**, *11*, 491.
93. McCormick, A.; Bell, A.; Radke, C. Multinuclear NMR investigation of the formation of aluminosilicate anions. *J. Phys. Chem.* **1989**, *93*, 1741–1744. [CrossRef]
94. Palomo, A.; Fernández-Jiménez, A. Alkaline activation, procedure for transforming fly ash into new materials. Part I: Applications. In Proceedings of the World of Coal Ash (WOCA) Conference, Denver, CO, USA, 9–12 May 2011; pp. 1–14.
95. Mehta, A.; Siddique, R. An overview of geopolymers derived from industrial by-products. *Constr. Build. Mater.* **2016**, *127*, 183–198. [CrossRef]
96. Hajimohammadi, A.; Provis, J.L.; Van Deventer, J.S. Effect of alumina release rate on the mechanism of geopolymer gel formation. *Chem. Mater.* **2010**, *22*, 5199–5208. [CrossRef]
97. Poojidha, M.; Nirmalkumar, K. Review paper on reaction of alkaline solution in GEO-polymer concrete. *Int. J. Recent Innov. Trends Comput. Commun.* **2016**, *4*, 223–227.
98. Davidovits, J. High-alkali cements for 21st century concretes. *Spec. Publ.* **1994**, *144*, 383–398.

99. Silva, S.; Kithalawa Arachchi, J.; Wijewardena, C.; Nanayakkara, S. Development of fly ash based geopolymer concrete. In Proceedings of the Annual Session 2012, Honolulu, HI, USA, 4–8 May 2012.
100. Temuujin, J.v.; Van Riessen, A.; Williams, R. Influence of calcium compounds on the mechanical properties of fly ash geopolymer pastes. *J. Hazard. Mater.* **2009**, *167*, 82–88. [CrossRef] [PubMed]
101. Cheah, C.B.; Samsudin, M.H.; Ramli, M.; Part, W.K.; Tan, L.E. The use of high calcium wood ash in the preparation of ground granulated blast furnace slag and pulverized fly ash geopolymers: A complete microstructural and mechanical characterization. *J. Clean. Prod.* **2017**, *156*, 114–123. [CrossRef]
102. Nath, P.; Sarker, P.K.; Rangan, V.B. Early age properties of low-calcium fly ash geopolymer concrete suitable for ambient curing. *Procedia Eng.* **2015**, *125*, 601–607. [CrossRef]
103. Their, J.M.; Özakça, M. Developing geopolymer concrete by using cold-bonded fly ash aggregate, nano-silica, and steel fiber. *Constr. Build. Mater.* **2018**, *180*, 12–22. [CrossRef]
104. Krishnan, L.; Karthikeyan, S.; Nathiya, S.; Suganya, K. Geopolymer concrete an eco-friendly construction material. *Magnesium* **2014**, *1*, 1.
105. Jumrat, S.; Chatveera, B.; Rattanadecho, P. Dielectric properties and temperature profile of fly ash-based geopolymer mortar. *Int. Commun. Heat Mass Transf.* **2011**, *38*, 242–248.
106. Shadnia, R.; Zhang, L.; Li, P. Experimental study of geopolymer mortar with incorporated PCM. *Constr. Build. Mater.* **2015**, *84*, 95–102. [CrossRef]
107. Mehta, A.; Siddique, R.; Singh, B.P.; Aggoun, S.; Łagód, G.; Barnat-Hunek, D. Influence of various parameters on strength and absorption properties of fly ash based geopolymer concrete designed by Taguchi method. *Constr. Build. Mater.* **2017**, *150*, 817–824. [CrossRef]
108. Malkawi, A.B.; Nuruddin, M.F.; Fauzi, A.; Almattarneh, H.; Mohammed, B.S. Effects of alkaline solution on properties of the HCFA geopolymer mortars. *Procedia Eng.* **2016**, *148*, 710–717. [CrossRef]
109. Huseien, G.F.; Mirza, J.; Ismail, M.; Hussin, M.W. Influence of different curing temperatures and alkali activators on properties of GBFS geopolymer mortars containing fly ash and palm-oil fuel ash. *Constr. Build. Mater.* **2016**, *125*, 1229–1240. [CrossRef]
110. Laskar, M.S.; Talukdar, S. Development of ultrafine slag-based geopolymer mortar for use as repairing mortar. *J. Mater. Civ. Eng.* **2016**, *29*, 04016292. [CrossRef]
111. Mehta, A.; Siddique, R. Properties of low-calcium fly ash based geopolymer concrete incorporating OPC as partial replacement of fly ash. *Constr. Build. Mater.* **2017**, *150*, 792–807.
112. Rangan, B.V.; Hardjito, D.; Wallah, S.E.; Sumajouw, D.M. Studies on fly ash-based geopolymer concrete. In Proceedings of the World Congress Geopolymer, Saint Quentin, France, 29 June–1 July 2005; pp. 133–137.
113. Sathonsaowaphak, A.; Chindaprasirt, P.; Pimraksa, K. Workability and strength of lignite bottom ash geopolymer mortar. *J. Hazard. Mater.* **2009**, *168*, 44–50.
114. Al-Majidi, M.H.; Lampropoulos, A.; Cundy, A.; Meikle, S. Development of geopolymer mortar under ambient temperature for in situ applications. *Constr. Build. Mater.* **2016**, *120*, 198–211.
115. Deb, P.S.; Sarker, P.K.; Barbhuiya, S. Sorptivity and acid resistance of ambient-cured geopolymer mortars containing nano-silica. *Cem. Concr. Compos.* **2016**, *72*, 235–245. [CrossRef]
116. Elyamany, H.E.; Elmoaty, A.E.M.A.; Elshaboury, A.M. Setting time and 7-day strength of geopolymer mortar with various binders. *Constr. Build. Mater.* **2018**, *187*, 974–983. [CrossRef]
117. Karakoç, M.B.; Türkmen, İ.; Maraş, M.M.; Kantarci, F.; Demirboğa, R.; Toprak, M.U. Mechanical properties and setting time of ferrochrome slag based geopolymer paste and mortar. *Constr. Build. Mater.* **2014**, *72*, 283–292. [CrossRef]
118. Temuujin, J.; Williams, R.; Van Riessen, A.v. Effect of mechanical activation of fly ash on the properties of geopolymer cured at ambient temperature. *J. Mater. Process. Technol.* **2009**, *209*, 5276–5280. [CrossRef]
119. Rao, G.M.; Rao, T.G. Final setting time and compressive strength of fly ash and GGBS-based geopolymer paste and mortar. *Arab. J. Sci. Eng.* **2015**, *40*, 3067–3074.
120. Phoo-ngernkham, T.; Sata, V.; Hanjitsuwan, S.; Ridtirud, C.; Hatanaka, S.; Chindaprasirt, P. Compressive strength, bending and fracture characteristics of high calcium fly ash geopolymer mortar containing portland cement cured at ambient temperature. *Arab. J. Sci. Eng.* **2016**, *41*, 1263–1271. [CrossRef]
121. Satria, J.; Sugiarto, A.; Hardjito, D. Effect of variability of fly ash obtained from the same source on the characteristics of geopolymer. In *MATEC Web of Conferences*; EDP Sciences: Les Ulis, France, 2017; p. 01026.

122. Pilehvar, S.; Cao, V.D.; Szczotok, A.M.; Carmona, M.; Valentini, L.; Lanzón, M.; Pamies, R.; Kjøniksen, A.-L. Physical and mechanical properties of fly ash and slag geopolymer concrete containing different types of micro-encapsulated phase change materials. *Constr. Build. Mater.* **2018**, *173*, 28–39.
123. Bilal, H.; Yaqub, M.; Rehman, S.K.U.; Abid, M.; Alyousef, R.; Alabduljabbar, H.; Aslam, F. Performance of Foundry Sand Concrete under Ambient and Elevated Temperatures. *Materials* **2019**, *12*, 2645. [CrossRef]
124. Zhang, H.Y.; Kodur, V.; Wu, B.; Cao, L.; Wang, F. Thermal behavior and mechanical properties of geopolymer mortar after exposure to elevated temperatures. *Constr. Build. Mater.* **2016**, *109*, 17–24.
125. Singh, B.; Rahman, M.; Paswan, R.; Bhattacharyya, S. Effect of activator concentration on the strength, ITZ and drying shrinkage of fly ash/slag geopolymer concrete. *Constr. Build. Mater.* **2016**, *118*, 171–179.
126. Shekhovtsova, J.; Kearsley, E.P.; Kovtun, M. Effect of activator dosage, water-to-binder-solids ratio, temperature and duration of elevated temperature curing on the compressive strength of alkali-activated fly ash cement pastes. *J. South. Afr. Inst. Civ. Eng.* **2014**, *56*, 44–52.
127. Chi, M.; Huang, R. Binding mechanism and properties of alkali-activated fly ash/slag mortars. *Constr. Build. Mater.* **2013**, *40*, 291–298. [CrossRef]
128. Zhang, H.; Li, L.; Sarker, P.K.; Long, T.; Shi, X.; Wang, Q.; Cai, G. Investigating various factors affecting the long-term compressive strength of heat-cured fly ash geopolymer concrete and the use of orthogonal experimental design method. *Int. J. Concr. Struct. Mater.* **2019**, *13*, 1–18. [CrossRef]
129. Mo, B.-H.; Zhu, H.; Cui, X.-M.; He, Y.; Gong, S.-Y. Effect of curing temperature on geopolymerization of metakaolin-based geopolymers. *Appl. Clay Sci.* **2014**, *99*, 144–148. [CrossRef]
130. Assi, L.N.; Deaver, E.E.; Ziehl, P. Effect of source and particle size distribution on the mechanical and microstructural properties of fly Ash-Based geopolymer concrete. *Constr. Build. Mater.* **2018**, *167*, 372–380. [CrossRef]
131. Ranjbar, N.; Mehrali, M.; Behnia, A.; Alengaram, U.J.; Jumaat, M.Z. Compressive strength and microstructural analysis of fly ash/palm oil fuel ash based geopolymer mortar. *Mater. Des.* **2014**, *59*, 532–539. [CrossRef]
132. Arellano-Aguilar, R.; Burciaga-Díaz, O.; Gorokhovsky, A.; Escalante-García, J.I. Geopolymer mortars based on a low grade metakaolin: Effects of the chemical composition, temperature and aggregate: Binder ratio. *Constr. Build. Mater.* **2014**, *50*, 642–648. [CrossRef]
133. Kotwal, A.R.; Kim, Y.J.; Hu, J.; Sriraman, V. Characterization and early age physical properties of ambient cured geopolymer mortar based on class C fly ash. *Int. J. Concr. Struct. Mater.* **2015**, *9*, 35–43. [CrossRef]
134. Ishwarya, G.; Singh, B.; Deshwal, S.; Bhattacharyya, S. Effect of sodium carbonate/sodium silicate activator on the rheology, geopolymerization and strength of fly ash/slag geopolymer pastes. *Cem. Concr. Compos.* **2019**, *97*, 226–238.
135. Vora, P.R.; Dave, U.V. Parametric studies on compressive strength of geopolymer concrete. *Procedia Eng.* **2013**, *51*, 210–219. [CrossRef]
136. Adak, D.; Sarkar, M.; Maiti, M.; Tamang, A.; Mandal, S.; Chattopadhyay, B. Anti-microbial efficiency of nano silver–silica modified geopolymer mortar for eco-friendly green construction technology. *RSC Adv.* **2015**, *5*, 64037–64045. [CrossRef]
137. ASTM C496/C496M-17. *Standard Test. Method for Splitting Tensile Strength of Cylindrical Concrete Specimens*; American Society for Testing and Materials: West Conshohocken, PA, USA, 2017.
138. ASTM C78/C78M-18. *Standard Test. Method for Flexural Strength of Concrete (Using Simple Beam with Third-Point Loading)*; American Society for Testing and Materials: West Conshohocken, PA, USA, 2018.
139. Ramujee, K.; PothaRaju, M. Mechanical properties of geopolymer concrete composites. *Mater. Today Proc.* **2017**, *4*, 2937–2945. [CrossRef]
140. Adak, D.; Sarkar, M.; Mandal, S. Effect of nano-silica on strength and durability of fly ash based geopolymer mortar. *Constr. Build. Mater.* **2014**, *70*, 453–459. [CrossRef]
141. Lee, B.; Kim, G.; Kim, R.; Cho, B.; Lee, S.; Chon, C.-M. Strength development properties of geopolymer paste and mortar with respect to amorphous Si/Al ratio of fly ash. *Constr. Build. Mater.* **2017**, *151*, 512–519. [CrossRef]
142. ASTM C469/C469M-14. *Standard Test. Method for Static Modulus of Elasticity and Poisson's Ratio of Concrete in Compression*; American Society for Testing and Materials: West Conshohocken, PA, USA, 2014.
143. Noushini, A.; Aslani, F.; Castel, A.; Gilbert, R.I.; Uy, B.; Foster, S. Compressive stress-strain model for low-calcium fly ash-based geopolymer and heat-cured Portland cement concrete. *Cem. Concr. Compos.* **2016**, *73*, 136–146. [CrossRef]

144. Hardjito, D.; Rangan, B.V. *Development and Properties of Low-Calcium fly Ash-Based Geopolymer Concrete*; Research Report GC1; Curtin University of Technology: Perth, Australia, 2005.
145. Farooq, F.; Rahman, S.K.U.; Akbar, A.; Khushnood, R.A.; Javed, M.F.; alyousef, R.; alabduljabbar, H.; aslam, F. A comparative study on performance evaluation of hybrid GNPs/CNTs in conventional and self-compacting mortar. *Alex. Eng. J.* **2020**, *59*, 369–379. [CrossRef]
146. Hung, T.V.; Tien, N.D.; van Dong, D. Experimental study on section curvature and ductility of reinforced geopolymer concrete beams. *Sci. J. Transp.* **2017**, *8*, 3–11.
147. Haq, E.U.; Padmanabhan, S.K.; Zubair, M.; Ali, L.; Licciulli, A. Intumescence behaviour of bottom ash based geopolymer mortar through microwave irradiation—As affected by alkali activation. *Constr. Build. Mater.* **2016**, *126*, 951–956. [CrossRef]
148. Ban, C.C.; Ken, P.W.; Ramli, M. Mechanical and durability performance of novel self-activating geopolymer mortars. *Procedia Eng.* **2017**, *171*, 564–571. [CrossRef]
149. Matalkah, F.; Salem, T.; Shaafaey, M.; Soroushian, P. Drying shrinkage of alkali activated binders cured at room temperature. *Constr. Build. Mater.* **2019**, *201*, 563–570. [CrossRef]
150. Lee, N.; Jang, J.G.; Lee, H.-K. Shrinkage characteristics of alkali-activated fly ash/slag paste and mortar at early ages. *Cem. Concr. Compos.* **2014**, *53*, 239–248. [CrossRef]
151. Hojati, M.; Radlińska, A. Shrinkage and strength development of alkali-activated fly ash-slag binary cements. *Constr. Build. Mater.* **2017**, *150*, 808–816. [CrossRef]
152. Sumesh, M.; Alengaram, U.J.; Jumaat, M.Z.; Mo, K.H.; Alnahhal, M.F. Incorporation of nano-materials in cement composite and geopolymer based paste and mortar–A review. *Constr. Build. Mater.* **2017**, *148*, 62–84. [CrossRef]
153. Gunasekara, C.; Law, D.W.; Setunge, S. Long term permeation properties of different fly ash geopolymer concretes. *Constr. Build. Mater.* **2016**, *124*, 352–362. [CrossRef]
154. Rehman, S.K.U.; Imtiaz, L.; Aslam, F.; Khan, M.K.; Haseeb, M.; Javed, M.F.; Alyousef, R.; Alabduljabbar, H. Experimental investigation of NaOH and KOH mixture in SCBA-based geopolymer cement composite. *Materials* **2020**, *13*, 3437. [CrossRef]
155. Vignesh, P.; Vivek, K. An experimental investigation on strength parameters of flyash based geopolymer concrete with GGBS. *Int. Res. J. Eng. Technol.* **2015**, *2*, 135–142.
156. Luhar, S.; Khandelwal, U. Durability studies of flyash based geopolymer concrete. *Int. J. Eng. Res. Appl.* **2015**, *5*, 17–32.
157. Deepak, A.L.; Lakshmi, T.V. Durability properties of geopolymer concrete with flyash and metakaolin. *Int. J. Sci. Technol. Res.* **2020**, *9*, 256–260.
158. Kurtoglu, A.E.; Alzeebaree, R.; Aljumaili, O.; Nis, A.; Gulsan, M.E.; Humur, G.; Cevik, A. Mechanical and durability properties of fly ash and slag based geopolymer concrete. *Adv. Concr. Constr.* **2018**, *6*, 345.
159. Venkatesan, R.P.; Pazhani, K. Strength and durability properties of geopolymer concrete made with ground granulated blast furnace slag and black rice husk ash. *KSCE J. Civ. Eng.* **2016**, *20*, 2384–2391. [CrossRef]
160. Shaikh, F.U.A. Mechanical and durability properties of fly ash geopolymer concrete containing recycled coarse aggregates. *Int. J. Sustain. Built Environ.* **2016**, *5*, 277–287. [CrossRef]
161. Albitar, M.; Ali, M.M.; Visintin, P.; Drechsler, M. Durability evaluation of geopolymer and conventional concretes. *Constr. Build. Mater.* **2017**, *136*, 374–385. [CrossRef]
162. Palomo, A.; Grutzeck, M.; Blanco, M. Alkali-activated fly ashes: A cement for the future. *Cem. Concr. Compos.* **1999**, *29*, 1323–1329. [CrossRef]
163. Satpute, S.M.S.; Hake, S. Investigation of alkaline activators for fly-ash based geopolymer concrete. *Int. J. Adv. Res. Innov. Ideas Educ.* **2016**, *2*, 2395–4396.
164. Hardjito, D.; Cheak, C.C.; Ing, C.H.L. Strength and setting times of low calcium fly ash-based geopolymer mortar. *Mod. Appl. Sci.* **2008**, *2*, 3–11. [CrossRef]
165. Vijai, K.; Kumutha, R.; Vishnuram, B. Effect of types of curing on strength of geopolymer concrete. *Int. J. Phys. Sci.* **2010**, *5*, 1419–1423.
166. Xie, T.; Ozbakkaloglu, T. Behavior of low-calcium fly and bottom ash-based geopolymer concrete cured at ambient temperature. *Ceram. Int.* **2015**, *41*, 5945–5958. [CrossRef]
167. Morsy, M.; Alsayed, S.; Al-Salloum, Y.; Almusallam, T. Effect of sodium silicate to sodium hydroxide ratios on strength and microstructure of fly ash geopolymer binder. *Arab. J. Sci. Eng.* **2014**, *39*, 4333–4339. [CrossRef]

168. Kim, E. Understanding Effects of Silicon/Aluminum Ratio and Calcium Hydroxide on Chemical Composition, Nanostructure and Compressive Strength for Metakaolin Geopolymers. ME Thesis, University of Illinois at Urbana-Champaign, Champaign, IL, USA, 2012.
169. Pangdaeng, S.; Phoo-ngernkham, T.; Sata, V.; Chindaprasirt, P. Influence of curing conditions on properties of high calcium fly ash geopolymer containing Portland cement as additive. *Mater. Des.* **2014**, *53*, 269–274. [CrossRef]
170. Suwan, T.; Fan, M. Influence of OPC replacement and manufacturing procedures on the properties of self-cured geopolymer. *Constr. Build. Mater.* **2014**, *73*, 551–561. [CrossRef]
171. Javed, M.F.; Sulong, N.H.R.; Memon, S.A.; Rehman, S.K.U.; Khan, N.B. FE modelling of the flexural behaviour of square and rectangular steel tubes filled with normal and high strength concrete. *Thin-Walled Struct.* **2017**, *119*, 470–481. [CrossRef]
172. Mo, K.H.; Alengaram, U.J.; Jumaat, M.Z. Structural performance of reinforced geopolymer concrete members: A review. *Constr. Build. Mater.* **2016**, *120*, 251–264. [CrossRef]
173. Hassan, A.; Arif, M.; Shariq, M. A review of properties and behaviour of reinforced geopolymer concrete structural elements—A clean technology option for sustainable development. *J. Clean. Prod.* **2020**, *245*, 118762. [CrossRef]
174. Castel, A.; Foster, S.J. Bond strength between blended slag and Class F fly ash geopolymer concrete with steel reinforcement. *Cem. Concr. Res.* **2015**, *72*, 48–53. [CrossRef]
175. Sofi, M.; Van Deventer, J.; Mendis, P.; Lukey, G. Bond performance of reinforcing bars in inorganic polymer concrete (IPC). *J. Mater. Sci.* **2007**, *42*, 3107–3116. [CrossRef]
176. Maranan, G.; Manalo, A.; Karunasena, K.; Benmokrane, B. Bond stress-slip behavior: Case of GFRP bars in geopolymer concrete. *J. Mater. Civ. Eng.* **2014**, *27*, 04014116. [CrossRef]
177. Chang, E.H.; Sarker, P.; Lloyd, N.; Rangan, B.V. Bond behaviour of reinforced fly ash-based geopolymer concrete beams. In Proceedings of the 24th Biennial Conference of the Concrete Institute Australia, Sydney, Australia, 8–11 September 2019.
178. Mo, K.H.; Yeap, K.W.; Alengaram, U.J.; Jumaat, M.Z.; Bashar, I.I. Bond strength evaluation of palm oil fuel ash-based geopolymer normal weight and lightweight concretes with steel reinforcement. *J. Adhes. Sci. Technol.* **2018**, *32*, 19–35. [CrossRef]
179. Sumajouw, M.; Rangan, B.V. *Low-Calcium Fly Ash-Based Geopolymer Concrete: Reinforced Beams and Columns*; Research report GC3; Curtin University of Technology: Perth, Australia, 2006.
180. Sumajouw, D.; Hadrjito, D.; Wallah, S.; Rangan, B. Flexural behaviour of reinforced fly ash-based geopolymer concrete beams. In Proceedings of the Concrete 05, CIA 22nd Biennial Conference, Melbourne, Australia, 17–19 October 2005.
181. Ng, T.S.; Amin, A.; Foster, S.J. The behaviour of steel-fibre-reinforced geopolymer concrete beams in shear. *Mag. Concr. Res.* **2013**, *65*, 308–318. [CrossRef]
182. Dattatreya, J.; Rajamane, N.; Sabitha, D.; Ambily, P.; Nataraja, M. Flexural behaviour of reinforced Geopolymer concrete beams. *Int. J. Civ. Struct. Eng.* **2011**, *2*, 138.
183. Kumaravel, S.; Thirugnanasambandam, S. Flexural behaviour of reinforced low calcium fly ash based geopolymer concrete beam. *Glob. J. Res. Eng.* **2013**, *13*. Available online: https://www.engineeringresearch.org/index.php/GJRE/article/view/938 (accessed on 26 October 2020).
184. Jeyasehar, C.A.; Saravanan, G.; Salahuddin, M.; Thirugnanasambandam, S. Development of Fly Ash Based Geopolymer Precast Concrete Elements. *Asian J. Civ. Eng. (BHRC)* **2013**, *14*, 605–615.
185. Yost, J.R.; Radlińska, A.; Ernst, S.; Salera, M.; Martignetti, N.J. Structural behavior of alkali activated fly ash concrete. Part 2: Structural testing and experimental findings. *Mater. Struct.* **2013**, *46*, 449–462. [CrossRef]
186. Yodsudjai, W. Application of fly ash-based geopolymer for structural member and repair materials. In *Advances in Science and Technology*; Trans Tech Publications Ltd.: Zürich, Switzerland, 2014; pp. 74–83.
187. Sumajouw, D.; Hardjito, D.; Wallah, S.; Rangan, B. Fly ash-based geopolymer concrete: Study of slender reinforced columns. *J. Mater. Sci.* **2007**, *42*, 3124–3130. [CrossRef]
188. Ganesan, N.; Abraham, R.; Deepa Raj, S.; Namitha, K. Effect of fibres on the strength and behaviour of GPC columns. *Mag. Concr. Res.* **2015**, *68*, 99–106. [CrossRef]
189. Nagan, S.; Karthiyaini, S. A study on load carrying capacity of fly ash based polymer concrete columns strengthened using double layer GFRP wrapping. *Adv. Mater. Sci. Eng.* **2014**, *2014*. [CrossRef]

190. Rajendran, M.; Soundarapandian, N. An experimental investigation on the flexural behavior of geopolymer ferrocement slabs. *J. Eng. Technol.* **2013**, *3*. [CrossRef]
191. Ganesan, N.; Indira, P.; Santhakumar, A. Prediction of ultimate strength of reinforced geopolymer concrete wall panels in one-way action. *Constr. Build. Mater.* **2013**, *48*, 91–97.
192. Aldred, J.; Day, J. Is geopolymer concrete a suitable alternative to traditional concrete. In Proceedings of the 37th Conference on Our World in Concrete & Structures, Singapore, 29–31 August 2012; pp. 29–31.
193. Bołtryk, M.; Granatyr, K.; Stankiewicz, N. Ecological aspects in the application of geopolymer composites on road surfaces. *Ekon. Środowisko* **2019**. [CrossRef]
194. Zhuang, X.Y.; Chen, L.; Komarneni, S.; Zhou, C.H.; Tong, D.S.; Yang, H.M.; Yu, W.H.; Wang, H. Fly ash-based geopolymer: Clean production, properties and applications. *J. Clean. Prod.* **2016**, *125*, 253–267.
195. Duan, P.; Shui, Z.; Chen, W.; Shen, C. Enhancing microstructure and durability of concrete from ground granulated blast furnace slag and metakaolin as cement replacement materials. *J. Mater. Res. Technol.* **2013**, *2*, 52–59.
196. Topçu, İ.B.; Toprak, M.U.; Uygunoğlu, T. Durability and microstructure characteristics of alkali activated coal bottom ash geopolymer cement. *J. Clean. Prod.* **2014**, *81*, 211–217. [CrossRef]
197. Ismail, I.; Bernal, S.A.; Provis, J.L.; Hamdan, S.; van Deventer, J.S. Microstructural changes in alkali activated fly ash/slag geopolymers with sulfate exposure. *Mater. Struct.* **2013**, *46*, 361–373. [CrossRef]
198. Hassan, A.; Arif, M.; Shariq, M. Influence of microstructure of geopolymer concrete on its mechanical properties—A review. In *Advances in Sustainable Construction Materials and Geotechnical Engineering*; Springer: Berlin/Heidelberg, Germany, 2020; pp. 119–129.
199. Fan, F.; Liu, Z.; Xu, G.; Peng, H.; Cai, C. Mechanical and thermal properties of fly ash based geopolymers. *Constr. Build. Mater.* **2018**, *160*, 66–81. [CrossRef]
200. Niveditha, M.; Koniki, S. Effect of Durability properties on Geopolymer concrete—A review. In *E3S Web of Conferences*; EDP Sciences: Les Ulis, France, 2020; p. 01092.
201. Fernandez, I.; Herrador, M.F.; Marí, A.R.; Bairán, J.M. Structural effects of steel reinforcement corrosion on statically indeterminate reinforced concrete members. *Mater. Struct.* **2016**, *49*, 4959–4973. [CrossRef]
202. Ichimiya, K.; Hatanaka, S.; Atarashi, D.; Minoru, K. Technical Committee on Application of Geopolymer Technology to Construction Field. Japan Concrete Institute, Committee Report: JCI-TC155A; 2017. Available online: https://www.jci-net.or.jp/j/jci/study/tcr/tcr2017/TC155A.pdf (accessed on 26 October 2020).
203. Balaguru, P.; Kurtz, S.; Rudolph, J. *Geopolymer for Repair and Rehabilitation of Reinforced Concrete Beams*; Geopolymer Institute: St Quentin, France, 1997; Volume 5.
204. Jiang, C.; Wang, A.; Bao, X.; Ni, T.; Ling, J. A review on geopolymer in potential coating application: Materials, preparation and basic properties. *J. Build. Eng.* **2020**, *32*, 101734. [CrossRef]
205. Zailani, W.; Abdullah, M.; Razak, R.; Zainol, M.; Tahir, M. Bond strength mechanism of fly ash based geopolymer mortars: A review. *MS&E* **2017**, *267*, 012008.
206. Hussin, M.; Bhutta, M.; Azreen, M.; Ramadhansyah, P.; Mirza, J. Performance of blended ash geopolymer concrete at elevated temperatures. *Mater. Struct.* **2015**, *48*, 709–720. [CrossRef]
207. Ahmmad, R.; Alengaram, U.J.; Jumaat, M.Z.; Sulong, N.R.; Yusuf, M.O.; Rehman, M.A. Feasibility study on the use of high volume palm oil clinker waste in environmental friendly lightweight concrete. *Constr. Build. Mater.* **2017**, *135*, 94–103. [CrossRef]
208. Nayaka, R.R.; Alengaram, U.J.; Jumaat, M.Z.; Yusoff, S.B.; Alnahhal, M.F. High volume cement replacement by environmental friendly industrial by-product palm oil clinker powder in cement–lime masonry mortar. *J. Clean. Prod.* **2018**, *190*, 272–284. [CrossRef]
209. Van Jaarsveld, J.; Van Deventer, J.; Lorenzen, L. The potential use of geopolymeric materials to immobilise toxic metals: Part I. Theory and applications. *Miner. Eng.* **1997**, *10*, 659–669. [CrossRef]
210. Fernández-Jiménez, A.; Puertas, F. Alkali-activated slag cements: Kinetic studies. *Cem. Concr. Res.* **1997**, *27*, 359–368. [CrossRef]
211. Luna, Y.; Querol, X.; Antenucci, D.; Jdid, E.-A.; Fernández, C.; Vale, J. Immobilization of a metallurgical waste using fly ash-based geopolymers. In Proceedings of the 2007 World of Coal Ash, Covington, KY, USA, 7–10 May 2007.
212. Emdadi, Z.; Asim, N.; Amin, M.; Yarmo, A.M.; Maleki, A.; Azizi, M.; Sopian, K. Development of green geopolymer using agricultural and industrial waste materials with high water absorbency. *Appl. Sci.* **2017**, *7*, 514. [CrossRef]

213. Hung, T.D.; Louda, P.; Kroisová, D.; Bortnovsky, O.; Xiem, N.T. New generation of geopolymer composite for fire-resistance. In *Advances in Composite Materials-Analysis of Natural and Man-Made Materials*; IntechOpen: London, UK, 2011.
214. Abdulkareem, O.A.; Al Bakri, A.M.; Kamarudin, H.; Nizar, I.K.; Ala'eddin, A.S. Effects of elevated temperatures on the thermal behavior and mechanical performance of fly ash geopolymer paste, mortar and lightweight concrete. *Constr. Build. Mater.* **2014**, *50*, 377–387. [CrossRef]
215. Zhang, H.-Y.; Kodur, V.; Cao, L.; Qi, S.-L. Fiber reinforced geopolymers for fire resistance applications. *Procedia Eng.* **2014**, *71*, 153–158. [CrossRef]
216. Heath, A.; Paine, K.; McManus, M. Minimising the global warming potential of clay based geopolymers. *J. Clean. Prod.* **2014**, *78*, 75–83. [CrossRef]
217. Salas, D.A.; Ramirez, A.D.; Ulloa, N.; Baykara, H.; Boero, A.J. Life cycle assessment of geopolymer concrete. *Constr. Build. Mater.* **2018**, *190*, 170–177. [CrossRef]
218. Robayo-Salazar, R.; Mejía-Arcila, J.; de Gutiérrez, R.M.; Martínez, E. Life cycle assessment (LCA) of an alkali-activated binary concrete based on natural volcanic pozzolan: A comparative analysis to OPC concrete. *Constr. Build. Mater.* **2018**, *176*, 103–111. [CrossRef]
219. Ng, T.S.; Voo, Y.L.; Foster, S.J. Sustainability with ultra-high performance and geopolymer concrete construction. In *Innovative Materials and Techniques in Concrete Construction*; Springer: Berlin/Heidelberg, Germany, 2012; pp. 81–100.
220. Habert, G.; De Lacaillerie, J.D.E.; Roussel, N. An environmental evaluation of geopolymer based concrete production: Reviewing current research trends. *J. Clean. Prod.* **2011**, *19*, 1229–1238. [CrossRef]
221. Abbas, R.; Khereby, M.A.; Ghorab, H.Y.; Elkhoshkhany, N. Preparation of geopolymer concrete using Egyptian kaolin clay and the study of its environmental effects and economic cost. *Clean Technol. Environ. Policy* **2020**, *22*, 1–19. [CrossRef]
222. Turner, L.K.; Collins, F.G. Carbon dioxide equivalent (CO2-e) emissions: A comparison between geopolymer and OPC cement concrete. *Constr. Build. Mater.* **2013**, *43*, 125–130. [CrossRef]
223. Wu, P.; Wang, J.; Wang, X. A critical review of the use of 3-D printing in the construction industry. *Autom. Constr.* **2016**, *68*, 21–31.
224. Kashani, A.; Ngo, T. Optimisation of mixture properties for 3D printing of geopolymer concrete. In Proceedings of the International Symposium on Automation and Robotics in Construction, Berlin, Germany, 20–25 July 2018; pp. 1–8.
225. Panda, B.; Unluer, C.; Tan, M.J. Investigation of the rheology and strength of geopolymer mixtures for extrusion-based 3D printing. *Cem. Concr. Compos.* **2018**, *94*, 307–314.
226. Rehman, S.K.U.; Ibrahim, Z.; Memon, S.A.; Jameel, M. Nondestructive test methods for concrete bridges: A review. *Constr. Build. Mater.* **2016**, *107*, 58–86.
227. Rehman, S.K.U.; Ibrahim, Z.; Memon, S.A.; Javed, M.F.; Khushnood, R.A. A sustainable graphene based cement composite. *Sustainability* **2017**, *9*, 1229.
228. Nazar, S.; Yang, J.; Thomas, B.S.; Azim, I.; Ur Rehman, S.K. Rheological properties of cementitious composites with and without nano-materials: A comprehensive review. *J. Clean. Prod.* **2020**, *272*, 122701. [CrossRef]
229. Rehman, S.K.U.; Ibrahim, Z.; Memon, S.A.; Aunkor, M.; Hossain, T.; Javed, M.F.; Mehmood, K.; Shah, S.M.A. Influence of Graphene Nanosheets on Rheology, Microstructure, Strength Development and Self-Sensing Properties of Cement Based Composites. *Sustainability* **2018**, *10*, 822.
230. Rehman, S.K.U.; Ibrahim, Z.; Jameel, M.; Memon, S.A.; Javed, M.F.; Aslam, M.; Mehmood, K.; Nazar, S. Assessment of Rheological and Piezoresistive Properties of Graphene based Cement Composites. *Int. J. Concr. Struct. Mater.* **2018**, *12*, 64. [CrossRef]
231. Farooq, F.; Akbar, A.; Khushnood, R.A.; Muhammad, W.L.; Rehman, S.K.; Javed, M.F. Experimental Investigation of Hybrid Carbon Nanotubes and Graphite Nanoplatelets on Rheology, Shrinkage, Mechanical, and Microstructure of SCCM. *Materials* **2020**, *13*, 230. [CrossRef]
232. Rehman, S.K.U.; Kumarova, S.; Memon, S.A.; Javed, M.F.; Jameel, M. A Review of Microscale, Rheological, Mechanical, Thermoelectrical and Piezoresistive Properties of Graphene Based Cement Composite. *Nanomaterials* **2020**, *10*, 102076. [CrossRef]
233. Zhu, X.H.; Kang, X.J.; Yang, K.; Yang, C.H. Effect of graphene oxide on the mechanical properties and the formation of layered double hydroxides (LDHs) in alkali-activated slag cement. *Constr. Build. Mater.* **2017**, *132*, 290–295. [CrossRef]

234. Ranjbar, N.; Mehrali, M.; Mehrali, M.; Alengaram, U.J.; Jumaat, M.Z. Graphene nanoplatelet-fly ash based geopolymer composites. *Cem. Concr. Res.* **2015**, *76*, 222–231. [CrossRef]
235. Zhang, G.; Lu, J. Experimental research on the mechanical properties of graphene geopolymer. *AIP Adv.* **2018**, *8*, 065209. [CrossRef]
236. Zhong, J.; Zhou, G.-X.; He, P.-G.; Yang, Z.-H.; Jia, D.-C. 3D printing strong and conductive geo-polymer nanocomposite structures modified by graphene oxide. *Carbon* **2017**, *117*, 421–426.